The influence of micro- and nano- sisal fibres on the morphology and properties of different polymers

by

ESSA ESMAIL MOHAMMAD AHMAD (M.Sc.)

Submitted in accordance with the requirements for the degree of

DOCTOR OF PHILOSOPHY (Ph.D.) IN POLYMER SCIENCE

Department of Chemistry

Faculty of Natural and Agricultural Sciences

at the

UNIVERSITY OF THE FREE STATE (QWAQWA CAMPUS)

SUPERVISOR: PROF AS LUYT

December 2011

Declaration

We, the undersigned, hereby declare that the research in this thesis is Mr. Ahmad's own original work, which has not partly or fully been submitted to any other University in order to obtain a degree.

Mr. E.E.M. Ahmad	Prof. A.S. Luyt

Dedication

To my late parents Esmail Mohamed and Ayesha Elbasheer. Special dedication to my mother who has recently passed away (September 2011). My dreams were to see your face shining with happiness and satisfaction when you welcome your son back home as you used to do every time when I visit. This Ph.D. is for you. I love all of you forever.

To my sister Amena. I really do not feel that the words will express my appreciation for all sacrifices you have made for the life and education of your brothers. I love you.

To my brothers and sisters Mohamed, Fatima, Bakheita, Abdurahman, Abduallah, and Mossa. Thank you for your love and support. You are my world. I love you all.

To my nephews and nieces. You are so special to me and life is so enjoyable around you.

To my uncles and aunts. Special dedication to my uncle Abduallah Elbasheer. Thank you for your help, support, and kindness.

Abstract

In this study, three types of polyethylene, low-density (LDPE), linear low-density (LLDPE), and high-density (HDPE) polyethylene, were used as polymer matrices to prepare sisal fibre reinforced polyethylene composites containing 10-30 wt% fibre. The untreated and the dicumyl peroxide (DCP) treated composites were prepared by melt mixing, followed by hot melt pressing. The influence of the DCP treatment, the polyethylene molecular characteristics, and the sisal fibre loadings on the morphology and on the thermal, mechanical, and dynamic mechanical properties of the composites was investigated. The gel contents of the composites varied significantly depending on the polyethylene molecular characteristics. The LLDPE composites had the highest gel content values followed by LDPE and then HDPE, for which the gel content did not change significantly. These results strongly suggested the presence of grafting of the polyethylene chains onto the sisal fibre surfaces combined with crosslinking between the polymer chains. The morphologies of the cryofractured surfaces and the xylene-extracted samples further confirmed the presence of the grafting, particularly in the case of the treated LLDPE and LDPE composites. The SEM micrographs of the treated LLDPE and LDPE composites showed better interfacial adhesion between the polymers and the sisal fibres. For HDPE composites, however, such interfacial bonding was not observed from the SEM micrographs. The SEM images of all the untreated polyethylene composites showed poor interfacial interactions. TGA analyses showed that the treatment did significantly affect the thermal stabilities of the composites, and all the untreated and the treated samples were thermally less stable than the neat polymer matrices. The DSC results demonstrated that the crystallization and melting behaviour of all the untreated polyethylene composites remained unaffected. However, both the DCP treatment and the sisal fibre loadings to some extent influenced the crystallization and melting behaviour of the LLDPE composites, whereas those of the LDPE composites were only slightly affected. The treated HDPE composites, however, did not show significant changes in their crystallization and melting behaviour. The elongation at break for all the treated and the untreated polyethylene composites showed similar trends and the treatment did not bring about any differences. Compared to the untreated composites, the tensile strength and the Young's modulus of the treated LLDPE and LDPE composites were remarkably higher, whereas the Young's modulus of the treated HDPE composites was observably lower and no significant effect on the tensile strength was noticed. The storage modulus of the LLDPE and

LDPE composites showed good correlation with the tensile testing results. The tan δ curves showed a slight increase in the glass transition temperatures for the treated composites. The storage modulus of the treated HDPE composites remarkably decreased, and the tan δ curves did not show the β-relaxation as in the case of the other two polymers.

The effect of the incorporation of sisal whickers on the properties of poly(lactic acid) was also investigated in this study. Untreated and the MA/DCP and DCP treated PLA nanocomposites, with sisal whiskers loadings of 2 and 6 wt%, were prepared by melt mixing and hot melt pressing. The dispersion of the whiskers in the PLA matrix as well as the thermal and viscoelastic properties of the nanocomposites were determined using TEM, DSC, TGA, and DMA. The dispersion of the whiskers was found to be similar, whether the samples were treated or not. The presence and the amount of whiskers in the untreated nanocomposites slightly decreased the calculated percent crystallinity, but the T_m, T_c and T_g remained fairly constant compared to neat PLA. The type of treatment was also found to influence the crystallization and melting behaviour of the nanocomposites. The TGA results showed that neither the sisal whiskers loading nor the treatment had a significant effect on the thermal stabilities of the nanocomposites. The incorporation of the whiskers remarkably reduced the intensity of the glass transition in the tan δ curve, and all the nanocomposites showed higher storage modulus values compared to the neat PLA. The type of treatment did not really influence the stiffness of the samples.

Entirely bio-based nanocomposites of PFA and sisal whiskers were prepared by an *in situ* polymerization method. The effect of increased sisal whiskers loadings (1 and 2 wt%) on the thermal and the dynamic mechanical properties of the nanocomposites were studied. No significant changes in the thermal stabilities of the nanocomposites could be seen. The storage moduli of the nanocomposites were significantly increased by the presence and the amount of sisal whiskers, and the intensity of the glass transition relaxation in the tan δ curve observably decreased and slightly shifted to lower temperatures.

TABLE OF CONTENTS

LIST OF TABLES

LIST OF FIGURES

LIST OF SYMBOLS AND ABBREVIATIONS

AFM	Atomic force microscopy
ATR-FTIR	Attenuated total reflectance-Fourier transform infrared
BPO	Benzoyl peroxide
CNs	Cellulose nano-whiskers
DCP	Dicumyl peroxide
DMA	Dynamic mechanical analysis
DMAc/LiCl	N,N-Dimethyl formamide/lithium chloride
DP	Degree of polymerization
DSC	Differential scanning calorimetry
E’	Storage modulus
E”	Loss modulus
FA	Furfuryl alcohol
FTIR	Fourier transform infrared
HDPE	High-density polyethylene
$KMnO_4$	Potassium permanganate
LDPE	Low-density polyethylene
LLDPE	Linear low-density polyethylene
MA	Maleic anhydride
MAPE	Maleic anhydride grafted polyethylene
MAPP	Maleic anhydride-grafted polypropylene
MDPE	Medium density polyethylene
MFC	Microfibrillated cellulose
MFI	Melt flow index
PALF	Pineapple leaf fibre
PCL	Poly(ε-caprolactone)
PE	Polyethylene
PFA	Poly(furfuryl alcohol)
PLA	Poly(lactic acid)
PMMA	Poly(methyl methacrylate)
POM	Polarized optical microscopy
PPy	Polypyrrole

SANS	Small angle neutron scattering
SEM	Scanning electron microscopy
T_c	Crystallization temperature
TEM	Transmission electron microscopy
T_g	Glass transition temperature
TGA	Thermogravimetric analysis
T_m	Melting temperature
UHMWPE	Ultra high molecular weight polyethylene
ULDPE	Ultra low-density polyethylene
UV	Ultraviolet
WF	Wood fibre
ΔH_c	Enthalpy of crystallization
ΔH_m^{calc}	Calculated melting enthalpy
ΔH_m^{obs}	Observed melting enthalpy
ΔH_m	Melting enthalpy
X_c	Percent crystallinity

Chapter 1

Introduction

1.1 Natural fibres reinforced thermoplastic composites

Over the past few decades, synthetic fibres such as aramid, carbon, and glass, reinforced composite materials have dominated the aerospace, leisure, automotive, construction, and sporting industries due to better performance. Among these fibres, glass fibres are the most widely used reinforcement due to their good balance of mechanical properties and low cost [1-3]. However, glass fibre reinforced composite materials have very serious drawbacks. The production of glass fibres is an energy intensive process, which depends mainly on fossil fuels; besides, they are abrasive to processing equipment, bear potential health risks to production workers, and they have a severe environmental impact in terms of pollutant emissions. Furthermore, glass fibre reinforced composites are non-biodegradable, non-renewable, and non-recyclable, a fact that reflects in both economical and ecological concerns [4-6].

In recent years, increasing worldwide environmental awareness together with a decline of petroleum resources have incited material scientists and engineers to look for alternative materials that are more sustainable, renewable, low cost, and environmentally friendly. Therefore, over the past decade, natural fibres as reinforcing materials in polymer matrix composites have received increasing attention as potential candidates to substitute the synthetic reinforcing materials (e.g. glass fibres) because of their unique properties [6-15]. Compared to synthetic reinforcing materials, natural fibres have many advantages such as low density and cost, wide availability, low energy consumption, biodegradability, recyclability and renewability [6-8,16-19].

Among the various natural fibres, sisal fibre is of particular interest. It is a hard fibre extracted from the leaves of the sisal plant (*Agava sisalana*), which has a short renewing time, wide availability, ease of cultivation and low cost, associated with excellent physical and mechanical characteristics [7,13,20-24]. The chemical constituents of sisal fibre are

cellulose, hemicellulose, lignin, pectin, waxes, water-soluble substances, and moisture. These components vary in percentage from one source to another, depending on growth conditions (climate, location, soil characteristics, weather circumstances), as well as the plant age and the extraction processes of the fibres [7,13,23].

Thermoplastic matrices offer many advantages over their thermosets counterparts, which give them wide application in composite technology. They can be easily processed through heating, shaping and cooling. Moreover, they have an unlimited storage life at room temperature, higher strain to failure, ease of handling, the possibility of recycling, and very low toxicity, which make them of better choice when the environmental issues are concerned [3]. Polyethylene (PE) offers many characteristics which make them one of the most widely used synthetic polymers used as matrix for fibre composites. They have excellent value (cost and performance), chemical inertness, good electrical resistance, relatively modest physical properties, ease of processing, recyclability, and adequate mechanical properties. In addition, their properties can be improved *via* blending and composite technologies. Polyethylene comes in various forms, differing in chain structure, crystallinity, and density. These are high-density polyethylene (HDPE), low-density polyethylene (LDPE), linear low-density polyethylene (LLDPE), ultra low-density polyethylene (ULDPE), and ultra high molecular weight polyethylene (UHMWPE) [25,26].

Natural fibres reinforced thermoplastic composites offer several advantages over their synthetic fibre counterparts such as low density, improved acoustic properties, favourable processing properties, low cost, good performance/weight ratio, as well as the possibility of recycling after use [7,27,28]. Therefore, natural fibre reinforced thermoplastic composites have found many application in a number of industrial sectors. In the automotive industry they are used as exterior and interior components (like front and rear door liners, boot liners, seat backs, etc). These components are mainly made from polypropylene reinforced with fibres like jute, flax, hemp, Kenaf, and wood [27,29-31]. Natural fibre composites are also used in structural parts such as roofing for low cost housing, pipes, and sandwich plates [32-36].

Despite the promise of natural fibres as alternative reinforcing materials, there are still some drawbacks. Besides their high moisture absorption, low microbial resistance, relatively high

variability in diameter and length, and low thermal stability, natural fibres are incompatible with hydrophobic polymers due to their polar and hydrophilic nature. This incompatibility leads to weak interfacial adhesion as well as to non-uniform dispersion within the matrix during compounding. Because of this weak interface, a decrease in the mechanical properties with the incorporation of natural fibres is one of the inherent problems [7,8,11]. To overcome this, several strategies have been tested to enhance the adhesion between the lignocellulosic fillers and the polymer matrix. These strategies generally involve modifications of the fibre and/or the matrix by physical or chemical methods. Chemical modification such as acetylation, mercerization, cyanoethylation, peroxide treatments, graft copolymerization (methylmethacrylate, acrylamide, and acrylonitrile) as well as various coupling agents (silane, isocyanate and titanate based compounds), has been studied extensively and reviewed by many researchers [9,37-39]. Among all these treatments, organic peroxides have shown a better compatibilization effect in polyethylene based natural fibre and wood flour composites associated with easy processability, as has been reported by some researchers [40-46]. The most important conclusion from these studies is that organic peroxides are very effective as compatibilizers by generating better interfacial adhesion. Moreover, in almost all of these studies grafting of PE onto natural fibres surfaces were proposed as a reason for the enhancement in composite properties after peroxide treatment. However, the evidence of grafting, which has been reported by these researchers, does not seem to be convincing, and therefore a more detailed study with additional evidence is necessary.

1.2 Cellulose nanofibres reinforced poly(lactic acid) nanocomposites

Plant fibres, that are also known as cellulosic fibres, lignocellulosic fibres, as well as biofibres, are made up of cellulose as a major component with other constituents like lignin, hemicellulose, pectin, waxes, water-soluble substances, and moisture [7,8,11]. Cellulose is one of the most ubiquitous and abundant renewable polymers on the planet. It is obtainable from both plants and non-plants sources. Cotton, ramie, hemp, sisal, jute and wood fibres are examples of fibres obtained from plants, whereas bacterial cellulose (*Acetobacter xylinum*), green algae, and tunicate cellulose are obtained from non-plant sources. Cellulose is a high-molecular weight linear homopolymer constituted of repeating β-D-glucopyranosyl units joined by (1→4) glycosidic linkages in a variety of arrangements. It is characterized by its hydrophilicity, chirality, degradability, and unique reactivities, which is a direct result of its

molecular structure. Cellulose has a hierarchical structure, which forms *via* cellulose chains that aggregate into a repeated crystalline structure to form microfibrils in the plant cell wall, which in turn aggregate into larger macroscopic fibres. The microfibrils are composed of bundles of nanofibres (nanowhiskers, microfibrillated cellulose), which have a diameter in the nanometer range and lengths that can reach several tens of microns, depending on their origin and the method of extraction. Microfibrilated cellulose is extracted through the fibrillation of pulp fibres by a mechanical treatment, which consists of refining and high-pressure homogenization to obtain a nano-order unit web-like network structure. On the other hand, nano-whiskers are extracted *via* acid hydrolysis, which followed treatments like mercerization and bleaching to remove other natural fibre constituents such as lignin and hemicelluloses.

Cellulose nanofibres have great potential to be used as reinforcement due to their high surface area and good mechanical properties combined with low weight, biodegradability, and renewability. The axial Young's modulus of cellulose has been measured to be 134 GPa [47-50]. Many studies have been performed on the extraction of cellulose nanofibres from various sources and on utilizing them as reinforcing materials in composite manufacturing. Both natural and synthetic polymers were explored as matrices. Natural polymers such as starch [51], poly(hydroxy alkanoate) [52], and poly(caprolactone) [53] reinforced with cellulose whiskers were reported in the literature. Polypropylene [54], poly(oxyethylene) [55], and poly(vinyl chloride) [56] were used as synthetic polymer matrices.

Biodegradable/biobased polymers are a new generation of polymeric materials that are derived from renewable resources. They can be found naturally, synthesized from renewable bio-derived monomers, or produced by the microorganisms. Recently, due to environmental and ecological factors, biobased polymers have found increasing attention as potential alternatives to currently dominating petroleum based polymers [57-59]. Poly(lactic acid) (PLA) is one of the oldest and most promising biodegradable polymers. It is an aliphatic polyester derived from lactic acid made from renewable resources, such as corn starch or sugar cane. The physical, thermal, and mechanical properties of PLA are very dependent on the molecular weight, molecular weight distribution, and composition [60-62].

Despite their excellent reinforcing capabilities, cellulose nanofibres reinforced hydrophobic polymers, like poly(lactic acid), have not been studied extensively due to poor dispersion/compatibility, which results in deterioration of the mechanical properties of the resulting composites. Therefore, the incorporation of cellulose fibres as reinforcing materials has so far been largely limited to aqueous or polar systems. To overcome these problems, various methods such as surfactant coating and graft copolymerization have been examined to enhance the compatibility of cellulose fibres with and their dispersion in non-polar polymer matrices [54,63,64].

1.3 Cellulose nanofibres reinforced poly(furfuryl alcohol) nanocomposites

Poly(furfuryl alcohol) (PFA) is a common typical thermosetting resin that can be synthesized from furfuryl alcohol (FA) obtained from renewable saccharidic resources. The monomer FA has a high solubility in water and many organic solvents and it can be easily polymerized by heating or under acidic catalysis to produce polyfurfuryl alcohol [65]. Owing to its unique physical and chemical properties, PFA is widely used for many applications, such as adsorbents [66], membranes [67], negative photoresists [65], and precursors for fabrication of different nanostructured carbon and nanocomposites [68].

Natural fibre reinforced PFA can provide composite materials that are entirely based on renewable components and that are completely environmentally friendly. Only two papers could be found on natural fibre reinforced PFA [69,70].

1.4 Research objectives

The first objective of this research was to find convincing evidence for peroxide initiated grafting between the sisal fibre and the polyethylene matrices, as well as to investigate the influence of the polyethylene molecular characteristics on the grafting efficiency. Three types of polyethylene were used as polymer matrices. These are high-density polyethylene (HDPE), linear low-density polyethylene (LLDPE), and low-density polyethylene (LDPE). The composites were prepared by melt mixing, and DCP was added shortly before the end of mixing, after which the composites were hot pressed. Enhancement of the interfacial bonding *via* grafting of PE into the sisal fibre surfaces, together with crosslinking of the PE chains, are

suggested by many studies as a direct result of peroxide treatment. Polyethylene molecular characteristics such as chain structures, amount of unsaturation, and molecular weight are expected to influence the ability of the polymer to undergo grafting/crosslinking processes. Different characterization techniques were carried out to achieve a better understanding and get more evidence about possible grafting and crosslinking in this study.

The second objective was to study the effect of the grafting efficiency of the polyethylene matrix on the thermal and mechanical properties of their sisal fibre reinforced composites. Untreated and DCP treated composites with different fibre loadings as well as neat and DCP treated polyethylene matrices were prepared and characterized.

The third objective was to investigate the effect of the incorporation of nano-sized sisal fibres on the properties of poly(lactic acid) (PLA) and poly(furfuryl alcohol) (PFA), as well as to examine the effect of addition of MA/DCP and DCP on the properties of the resultant PLA nanocomposites. Nano-sized natural fibres have a high aspect ratios and a Young's modulus that is comparable to that of aramid fibres, so it is expected to impart excellent reinforcement to the PLA and PFA matrices. This type of bio-based nanocomposites has greater potential than other types of nanocomposites that are not derived from a bio-origin, because the bio-resource can be both sustainable and environmentally friendly. The resulting nanocomposites are expected to have improved thermal stability, toughness, and barrier properties. Untreated and maleic anhydride (MA)/dicumyl peroxide (DCP) and DCP treated PLA nanocomposites were prepared by melt mixing, followed by hot melt pressing. Freeze-drying of the aqueous suspensions of the sisal whiskers together with premixing of the powdered PLA and the dried whiskers, as well as the treatments of the nanocomposites with MA/DCP and with DCP, were all expected to positively influence both the dispersion of the whiskers in PLA and the interfacial bonding. The morphologies as well as the thermal and the dynamic mechanical properties of the nanocomposites were investigated.

PFA nanocomposites were prepared *via in situ* polymerization of FA in the presence of the sisal whiskers. Citric acid was used as a catalyst for the polymerization of furfuryl alcohol (FA), and this is in agreement with current tendency towards using raw materials from renewable resources. To the best of our knowledge, the dynamic mechanical properties of these bio-based nanocomposites have not been studied before, and in this study these

properties were investigated. We also investigated the effects of the incorporation of nano-sized sisal fibres on the thermal degradation behaviour of the nanocomposite.

1.5 Thesis organization

This thesis contains seven chapters. There is not an 'Experimental' chapter, because all the details about the materials and methods used in this study are given in Chapters 3 to 6, that are in the form of publications.

Chapter 1: Introduction

Chapter 2: Literature review

Chapter 3: Effects of organic peroxide and polymer chain structure on morphology and thermal properties of sisal fibre reinforced polyethylene composites (paper accepted for publication in *Composites Part A*)

Chapter 4: Effects of organic peroxide and polymer chain structure on mechanical and dynamic mechanical properties of sisal fibre reinforced polyethylene composites (paper accepted for publication in *Journal of Applied Polymer Science*)

Chapter 5: Morphology, thermal and dynamic mechanical properties of poly(lactic acid)/sisal whiskers nanocomposites (submitted for publication in *Polymer Composites)*

Chapter 6: Thermal and dynamic mechanical properties of biobased poly(furfuryl alcohol)/sisal whiskers nanocomposites (submitted for publication in *Composites Science and Technology)*

Chapter 7: Conclusions

1.6 References

1. F.C. Campbell. Manufacturing Processes for Advanced Composites. Elsevier Ltd, Oxford, UK (2004) p.40-61.
2. S.T. Peters. Handbook of Composites, 2nd edition. Chapman and Hall, London (1998) p.131-169.

3. P.K. Mallick. Fiber-Reinforced Composites: Materials, Manufacturing, and Design, 2nd edition. Marcel Dekker Inc, New York (1993) p.6-25 (Chapter 1), p.3-30 (Chapter 2).
4. S.V. Joshi, L.T. Drzal, A.K. Mohanty, S. Arora. Are natural fibre composites environmentally superior to glass fibre reinforced composites? Composites: Part A 2004; 35:371-375.
DOI: 10.1016/j.compositesa.2003.09.016
5. T. Corbière-Nicollier, B.G. Laban, L. Lundquist, Y. Leterrier, J.A.E. Månson, O. Jolliet. Life cycle assessment of biofibres replacing glass fibres as reinforcement in plastics. Resources, Conservation, and Recycling 2001; 33:267-287.
DOI: 10.1016/S0921-3449(01)00089-1
6. P. Wambua, J. Ivens, I. Verpoest. Natural fibres: can they replace glass in fibre reinforced plastics? Composites Science and Technology 2003; 63:1259-1264.
DOI: 10.1016/S0266-3538(03)00096-4
7. A.K. Bledzki, J. Gassan. Composites reinforced with cellulose based fibres. Progress in Polymer Science 1999; 24:221-274.
DOI: 10.1016/S0079-6700(98)00018-5
8. A.K. Mohanty, M. Mishra, G. Hinrichsen. Biofibres, biodegradable polymers and biocomposites: An overview. Macromolecular Materials and Engineering 2000; 276/277:1-24.
DOI: 10.1002/(SICI)1439-2054(20000301)276
9. S. Kalia, B.S. Kaith, I. Kaur. Pretreatment of natural fibres and their application as reinforcing material in polymer composites – a review. Polymer Engineering & Science 2009; 49:1253-1272.
DOI: 10.1002/pen.21328
10. G. Bogoeva-Gaceva, M. Avella, M. Malinconico, A. Buzarovska, A. Grozdanov, G. Gentile, M.E. Errico. Natural fibre eco-composites. Polymer Composites 2007; 28:98-107.
DOI: 10.1002/pc.20270
11. J.M. John, S. Thomas. Biofibres and biocomposites. Carbohydrate Polymers 2008; 71:343-364.
DOI: 10.1016/j.carbpol.2007.05.040
12. N.D. Saheb, P.J. Jog. Natural fibre polymer composites: A review. Advances in Polymer Technology 1999; 18:351-363.

DOI: 10.1002/(SICI)1098-2329(199924)18

13. Y. Li, Y-M. Mai, L. Ye. Sisal fibre and its composites: A review of recent developments. Composites Science and Technology 2000; 60:2037-2055.
DOI: 10.1016/S0266-3538(00)00101-9
14. G. Jayamol, M.S. Sreekala, S. Thomas. A review on interface modification and characterization of natural fibre reinforced plastic composites. Polymer Engineering and Science 2001; 41:1471-1485.
DOI: 10.1002/pen.10846
15. P.A. Fowler, J.M. Hughes, R.M. Elias. Biocomposites: Technology, environmental credentials, and market forces. Journal of the Science of Food and Agriculture 2006; 86:1781-1789.
DOI: 10.1002/jsfa.2558
16. S.M. Huda, T.L. Drzal, M. Misra, K.A. Mohanty, K. Williams, F.D. Mielewski. Study on biocomposites from recycled newspaper fibre and poly(lactic acid). Industrial & Engineering Chemistry Research 2005; 44:5593-5601.
DOI: 10.1021/ie0488849
17. T. Nishino, I. Matsuda, K. Hiro. All-cellulose composites. Macromolecules 2004; 37:7683-7687.
DOI: 10.1021/ma049300h
18. D. Puglia, A. Tomassucci, M.J. Kenny. Processing, properties and stability of biodegradable composites based on Mater-Bi® and cellulose fibres. Polymers for Advanced Technologies 2003; 14:749-756.
DOI: 10.1002/pat.390
19. E. Chiellini, P. Cinelli, F. Chiellini, S.H. Imam. Environmentally degradable bio-based polymeric blends and composites. Macromolecular Bioscience 2004; 4:218-231.
DOI: 10.1002/mabi.200300126
20. F.A. Silva, N. Chawla, R.D. Toledo Filho. Tensile behavior of high performance natural (sisal) fibres. Composites Science and Technology 2008; 68:3438-3443.
DOI: 10.1016/j.composcitech.2008.10.001
21. S.S. Munawar, K. Umemura, S. Kawai, Characterization of the morphological, physical, and mechanical properties of seven nonwood plant fibre bundles. Journal of Wood Science 2007; 53:108-113.
DOI: 10.1007/s10086-006-0836-x

22. P.S. Mukherjee, K.G. Satyanarayana. Structure and properties of some vegetable fibres – Part1: Sisal fibre. Journal of Materials Science 1984; 19:3925-3934.
DOI: 10.1007/BF00980755
23. S. Mishra, A.K. Mohanty, L.T. Drzal, M. Misra, G. Hinrichsen. A review on pineapple leaf fibres, sisal fibres and their biocomposites. Macromolecular Materials and Engineering 2004; 289:955-974.
DOI: 10.1002/mame.200400132
24. K.G. Satyanarayana, J.L. Guimarães, F. Wypych. Studies on lignocellulosic fibres of Brazil. Part 1: Source, production, morphology, properties and applications. Composites: Part A 2007; 38:1694-1709.
DOI: 10.1016/j.compositesa.2007.02.006
25. A.J. Peacock. Handbook of Polyethylene: Structures, Properties, and Applications. Marcel Dekker Inc., New York (2000) p.123-238.
26. D. Nwabunma. Overview of Polyolefin Composites. In: D. Nwabunma, T .Kyu (Eds.). Polyolefin Composites. John Wiley& Sons Inc., USA (2008) p.3-8.
27. A.K. Bledzki, O. Faruk, V.E. Sperber. Cars from biofibres. Macromolecular Materials and Engineering 2006; 291:449-457.
DOI: 10.1002/mame.200600113
28. M. Zampaloni, F. Pourboghrat, S.A. Yankovich, B.N. Rodgers, J. Moore, L.T. Drzal, A.K. Mohanty, M. Misra. Kenaf natural fiber reinforced polypropylene composites: A discussion on manufacturing problems and solutions. Composites: Part A 2007; 38:1569-1580.
DOI: 10.1016/j.compositesa.2007.01.001
29. C. Alves, P.M.C. Ferrão, A.J. Silva, L.G. Reis, M. Freitas, L.B. Rodrigues, D.E. Alives. Ecodesign of automotive components making use of natural fibre composites. Journal of Cleaner Production 2010; 18:313-327.
DOI: 10.1018/j.jclepro.2009.10.022
30. M. Pervaiz, M.M. Sain. Sheet-molded polyolefin natural fibre composites for automotive applications. Macromolecular Materials and Engineering 2003; 288:553-557.
DOI: 10.1002/mame.200350002
31. R. Zah, R. Hischier, A.L. Leão, I. Braun. Curauá fibres in automobile industry: A sustainability assessment. Journal of Cleaner Production 2007; 15:1032-1040.

DOI: 10.1016/j.jclepro.2006.05.036

32. U. Riedel, J. Nickel. Natural fibre-reinforced biopolymers as construction materials – New discoveries. Die Angewandte Makromolekulare Chemie 1999; 272:34-40.
DOI: 10.1002/(SICI)1522-9505(19991201)

33. M.A. Dweib, B. Hu, A. O'Donnell, W.H. Shenton, P.R. Wool. All natural composites sandwich beams for structural applications. Composite Structures 2004; 63:147-157.
DOI: 10.1016/S0263-8223(03)00143-0

34. R. Burgueño, M.J. Quagliata, A.K. Mohanty, G. Metha, L.T. Drzal, M. Misra. Load-bearing natural fibre composite cellular beams and panels. Composites: Part A 2004; 35:645-656.
DOI: 10.1016/j.compositesa.2004.02.012

35. V.K. Mathur. Composite material from local resources. Construction and Building Materials. 2006; 20:470-477.
DOI: 10.1016/j.conbuildmat.2005.01.031

36. W.D. Brouwer. Natural fiber composites in structural components: Alternative application for sisal? (2000) http://www.fao.org/docrep/004/Y1873E/y1873e0a.htm

37. M.J. John, R.D. Anandjiwala. Recent developments in chemical modification and characterization of natural fiber-reinforced composites. Polymer Composites 2008; 29:187-207.
DOI: 10.1002/pc.20461

38. X. Li, L.G. Tabil, S. Panigrahi. Chemical treatment of natural fiber for use in natural fiber-reinforced composites: A review. Journal of Polymers and the Environment 2007; 15:25-33.
DOI: 10.1007/s10924-006-0042-3

39. J. George, M.S. Sreekala, S. Thomas. A review on interface modification and characterization of natural fiber reinforced plastic composites. Polymer Engineering and Science 2001; 41:1471-1485.
DOI: 10.1002/pen.10846

40. K. Joseph, S. Thomas, C. Pavithran. Effect of chemical treatment on the tensile properties of short sisal fibre-reinforced polyethylene composites. Polymer 1996; 37:5139-5149.
DOI: 10.1016/0032-3861(96)00144-9

41. M.A. Mokoena, V. Djoković, A.S. Luyt. Composites of linear low-density polyethylene and short sisal fibres: The effects of peroxide treatment. Journal of Materials Science 2004; 39, 3403-3412.
DOI: 10.1023/B:JMSC.0000026943.47803.0b

42. M.E. Malunka, A.S. Luyt, H. Krump. Preparation and characterization of EVA-sisal fibre composites. Journal of Applied Polymer Science 2006; 100:1607-1617.
DOI: 10.1002/app.23650

43. A.S. Luyt, M.E. Malunka. Composites of low-density polyethylene and short sisal fibres: The effect of wax addition and peroxide treatment on thermal properties. Thermochimica Acta 2005; 426:101-107.
DOI: 10.1016/j.tca.2004.07.010

44. J. George, S.S. Bhagawan, S. Thomas. Thermogravimetric and dynamic mechanical thermal analysis of pineapple fibre reinforced polyethylene composites. Journal of Thermal Analysis 1996; 47:1121-1140.
DOI: 10.1007/BF01979452

45. I. Janigová, F. Lednický, Z. Nógellová, B.V. Kokta, I. Chodák. The effect of crosslinking on properties of low-density polyethylene filled with organic filler. Macromolecular Symposia 2001; 169:149-158.
DOI: 10.1016/j.eurpolymj.2006.05.024

46. M. Mičušík, M. Omastová, Z. Nógellová, P. Fedorko, K. Olejníková, M. Trchová, I. Chodák. Effect of crosslinking on the properties of composites based on LDPE and conducting organic filler. European Polymer Journal 2006; 42:2379-2388.
DOI: 10.1016/j.europolymj.2006.05.024

47. D. Klemm, B. Heublein, H-P. Fink, A. Bohn. Cellulose: Fascinating biopolymers and sustainable raw material. Angewandte Chemie International Edition 2005; 44:3358-3393.
DOI: 10.1002/anie.200460587

48. S.J. Eichhorn, A. Dufresne, M. Aranguren, N.E. Marcovich, J.R. Capadona, S.J. Rowan, C. Weder, W. Thielemans, M. Roman, S. Renneckar, W. Gindl, S. Veigel, J. Keckes, H. Yano, K. Abe, M. Nogi, A.N. Nakagaito, A. Mangalam, J. Simonsen, A.S. Benight, A. Bismarck, L.A. Berglund, T. Peijs. Review: Current international research into cellulose nanofibres and nanocomposites. Journal of Materials Science 2010; 45:1-33.

DOI: 10.1007/s10853-009-3874-0

49. W.G. Glasser. Cellulose and associated heteropolysaccharides. In: B. Fraser-Reid, K. Tatsuta, J. Thiem (Eds.). Glycoscience. Springer-Verlag, Berlin (2008) p.1473-1512. DOI: 10.1007/978-3-540-30429-6_36
50. S. Kamel. Nanotechnology and its application in lignocellulosic composites, a mini review. Express Polymer Letters 2007; 1:546-575. DOI: 10.3144/expresspolymlett.2007.78
51. M.N. Anglés, A. Dufresne. Plasticized starch/tunicin whiskers nanocomposite materials. 2. Mechanical behavior. Macromolecules 2001; 34:2921-2931. DOI: 10.1021/ma001555h
52. D. Dubief, E. Samain, A. Dufresne. Polysacchride microcrystals reinforced amorphous poly(β-hydroxyoctanoate) nanocomposites. Macromolecules 1999; 32:5765-5771. DOI: 10.1021/ma990274a
53. A. Morin, A. Dufresne. Nanocomposites of chitin whiskers from *Riftia Tubes* and poly(caprolactone). Macromolecules 2002; 35:2190-2199. DOI: 10.1021/ma011493a
54. N. Ljungberg, C. Bonini, F. Bortolussi, C. Boisson, L. Heux, J.Y. Cavaill. New nanocomposite materials reinforced with cellulose whiskers in atactic polypropylene: Effect of surface and dispersion characteristics. Biomacromolecules 2005; 6:2732-2739. DOI: 10.1021/bm050222v
55. M.A.S. Azizi Samir, F. Alloin, J-Y. Sanchez, A. Dufresne. Cellulose nanocrystals reinforced poly(oxyethylene). Polymer 2004; 45:4149-4157. DOI: 10.1016/j.polymer.2004.03.094
56. L. Chazeau, J.Y. Cavaillé, G. Canova, R. Dendievel, B. Boutheria. Viscoelastic properties of plasticized PVC reinforced with cellulose whiskers. Journal of Applied Polymer Science 1999; 71:1797-1808. DOI: 10.1002/(SICI)1097-4628(19990314)
57. W. Amass, A. Amass, B. Tighe. A review of biodegradable polymers: Uses, current developments in the synthesis and characterization of biodegradable polyesters, blends of biodegradable polymers and recent advances in biodegradation studies. Polymer International 1998; 47:89-144. DOI: 10.1002/(SICI)1097-0126(1998100)

58. K.G. Satyanarayana, G.G.C. Arizaga, F. Wypych. Biodegradable composites based on lignocellulosic fibres – An overview. Progress in Polymer Science 2009; 34:982-1021. DOI: 10.1016/j.progpolymsci.2008.12.002
59. J.M. John, S. Thomas. Biofibres and biocomposites: Review. Carbohydrate Polymers 2008; 71:343-364. DOI: 10.1016/j.carbpol.2007.05.040
60. X. Pang, X. Zhuang, Z. Tang, X. Chen. Polylactic acid (PLA): Research, development and industrialization. Biotechnology Journal 2010; 5:1125-1136. DOI: 10.1002/biot.201000135
61. Y. Cheng, S. Deng, P. Chen, R. Ruan. Polylactic acid (PLA) synthesis and modifications: A review. Frontiers of Chemistry in China 2009; 4:259-264. DOI: 10.1007/s11458-009-0092-x
62. R.M. Rasal. A.V. Janorkar, D.E. Hirt. Poly(lactic acid) modifications. Progress in Polymer Science 2010; 35:338-356. DOI: 10.1016/j.progpolymsci.2009.12.003
63. B. Wang, M. Sain. Isolation of nanofibers from soybean source and their reinforcing capability on synthetic polymers. Composites Science and Technology 2007; 67:2521-2527. DOI: 10.1016/j.compscitech.2006.12.015
64. D. Bondeson, K. Oksman. Dispersion and characteristics of surfactant modified cellulose whiskers nanocomposites. Composite Interfaces 2007; 14:617-630. DOI: 10.1163/156855407782106519
65. M. Sthel, J. Rieumont, R. Martinez. Testing of a furfuryl alcohol as a negative photoresist. Polymer Testing 1999; 18:47-50. DOI: 10.1018/S0142-9418(98)00006-3
66. A. Francesc, F.A. Estever-Turrillas, M. Pérez-Cabero, T.de la C. García, S. Zahedi, A. Pastor, R. Martínez. Poly(furfuryl alcohol) composite as adsorbent of polychlorinated biphenyls and pyrethroid in insecticides. Polymer Testing 2007; 26:587-594. DOI: 10.1016/j.polymertesting.2007.02.006
67. J. Liu, H. Wang, S. Cheng, K-Y. Chan. Nafion-polyfurfuryl alcohol nanocomposite membranes with low methanol permeation. Chemical Communications 2004; 728-729. DOI: 10.1039/b315742c

68. H. Wang, J. Yao. Use of poly(furfuryl alcohol) in the fabrication of nanostructured carbons and nanocomposites. Industrial & Engineering Chemistry Research 2006; 45:6393-6404.
DOI: 10.1021/ie0602660

69. L. Pranger, R. Tannenbaum. Biobased nanocomposites prepared by in situ polymerization of furfuryl alcohol with cellulose whiskers or montmorillonite clay. Macromolecules 2008; 41:8682-8687.
DOI: 10.1021/ma8020213

70. L. Pranger, G.A. Nunnery, R. Tannenbaum. Mechanism of the nanoparticle-catalyzed polymerization of furfuryl alcohol and the thermal and mechanical properties of the resulting nanocomposites. Composites: Part B (In press).
DOI: 10.1016/j.compositesb.2011.08.010

Chapter 2

Literature review

2.1 Natural fibres: Source and classification

Natural fibres are raw materials directly obtainable from animal, vegetable, or mineral sources. The use of natural fibres, both plant and animals, to meet our needs played a significant role throughout history. Natural fibres were the basis for producing clothes, paper, tools, and building materials. Plant fibres are a composite material designed by nature. Based on the part of the plant from which they are obtained, plant fibres are classified as bast (or stem) fibres, leaf fibres, and seed fibres. The fibres are rigid, crystalline cellulose microfibril-reinforced amorphous lignin and/or hemicellulose matrices. Recently, because of the declining of the fossil fuels, the continuously rising high crude oil prices in combination with increasing environmental consciousness, more attention have been given to the use of renewable, recyclable, and environmentally friendly materials. Plant or vegetables fibres are a renewable raw material and their availability is more or less unlimited. Over the last few years, a number of researchers have been involved in investigating the use of natural fibres as load bearing constituents in composite materials. This growing interest in plant fibres is mainly due to their unique characteristics. They are cheap, non-abrasive, have low density, are widely available, low energy consumption, biodegradable, recyclable and renewable [1-3].

2.2 Properties of natural fibres

The performance of a given fibre used in a given application depends among other factors on the chemical composition and physical properties of the fibre. In order to understand the properties of fibre-reinforced composites it is important to know these properties of the fibres.

2.2.1 Chemical composition of natural fibres

Natural fibres, that are also known as biofibres, lignocellulosic fibres, cellulosic fibres or plant fibres can be considered as naturally occurring composites consisting mainly of cellulose fibrils embedded in a lignin matrix. The main constituents of the biofibres are cellulose, hemicellulose, and lignin with other constituents like pectins, waxes, water-soluble substances, and moisture [3-5]. However, it is important to mention that the chemical composition of lignocellulosic fibres depends on various factors such as species, variety, type of soil used, weather conditions, part from which the fibres are extracted, and age of the plants. [6-8].

2.2.1.1 Cellulose

Cellulose is regarded as the most important skeletal component in plants; it is an almost inexhaustible polymeric raw material with fascinating structure and properties. It is ubiquitous in wood and plant fibres like sisal, cotton, ramie, hemp, and jute. In addition to these, there are non-plant sources of cellulose such as bacterial cellulose (*Acetobacter xylinum*), algae (such as *Valonia ventricosa*), as well as tunicate cellulose, which is produced by sea creatures (e.g. *Microcosmus fulcatus*). Cellulose is a high molecular weight carbohydrate polymer generated from repeating β-D-glucopyranose molecules that are covalently linked through acetal functions between the equatorial OH group of C4 and the C1 carbon atom (β-1,4-glucan). As a result, cellulose is an extensive, linear-chain polymer with a large number of hydroxy groups present in the thermodynamically preferred $^4C_1$ conformation. Although the chemical structure of cellulose from different natural fibres is the same, the degree of polymerization (DP) varies. The mechanical properties of a fibre are significantly related to the DP. Cellulose is characterized by its hydrophilicity, chirality, degradability, and unique reactivities, which is a direct result of its molecular structure. This structure is also the basis for extensive hydrogen bond networks, which give cellulose a multitude of crystalline fibre structures and morphologies. Cellulose crystallinity manifests itself through the existence of distinctive X-ray diffraction patterns. These patterns allow the determination of the overall dimensions of unit cells, which reflect the molecular arrangement of cellulose chains in the crystal. The crystal structure of the native cellulose (cellulose I) contains two coexisting phases: cellulose I_α (triclinic) and cellulose I_β

(monoclinic) in varying proportion depending on its origin. Apart from the thermodynamically less stable cellulose I, cellulose may also occur in other crystal structures (cellulose II, III_1, III_{11}, IV_1 and IV_{11}), of which cellulose II is the most stable structure. Cellulose is resistant to strong alkali but is easily hydrolyzed by acids to water-soluble sugars [1-3,9,10].

2.2.1.2 Hemicellulose

Hemicelluloses represent a class of noncellulosic polysaccharides that is associated with cellulose in plant cell. They are classified into five primary classes, xylans, glucomannans, arabinans, galactans, and glucans. With few exceptions, hemicelluloses consist of linear homo- or copolymers with variable degrees of branching (usually by single monosaccharidic branches) and with occasional (3-13 wt. %) replacement of OH groups by O-acetyl groups. Hemicellulose differs from cellulose in three aspects. Firstly, they contain several different sugar units whereas cellulose contains only 1,4-β-D-glucopyranose units. Secondly, they exhibit a considerable degree of chain branching containing pendant side groups giving rise to its non-crystalline nature, whereas cellulose is a linear polymer. Thirdly, the degree of polymerization of native cellulose is 10-100 times higher than that of hemicellulose. Mechanically, hemicelluloses contribute little to the stiffness and strength of fibres, as well as the individual cells, and they are very hydrophilic, soluble in alkali and easily hydrolyzed in acids [3,4,9,11].

2.2.1.3 Lignin

Lignin is a biochemical polymer, which functions as a structural support material in plants. During synthesis of plant cell walls, polysaccharides such as cellulose and hemicellulose are laid down first, and lignin fills the spaces between the polysaccharide fibres, cementing them together. Lignin is a high molecular weight phenolic compound with both aliphatic and aromatic constituents. It is totally amorphous and hydrophobic in nature and considered as the compound that gives rigidity to the plants. Although the exact structural formula of lignin has not been established, most of the functional groups and units, which make up the molecule, have been identified. Hydroxy, methoxy, and carbonyl groups have been identified. In addition, lignin has been found to contain five hydroxyl and five methoxyl groups per

building unit. It is believed that the structural units of a lignin molecule are derivatives of 4-hydroxy-3-methoxy phenypropane. Lignin is not hydrolyzed by acids, but it is soluble in hot alkali, readily oxidized, and easily condensable with phenol. The main difficulty in lignin chemistry is that no method has been established by which it is possible to isolate lignin in its native state from the fibre [4,5].

Xiao *et al*. [12] characterized the chemical, structural, and thermal properties of alkali soluble lignin and hemicellulose, and cellulose from maize stems, rye straw, and rice straw. The dewaxed fibres were treated with molar (1 M) sodium hydroxide (NaOH) solution at 30 ^{o}C for 30 hours. Different methods such as degraded methods (nitrobenzene and acid hydrolysis) and non-destructive techniques (ultraviolet, Fourier transform infrared, carbon-13 nuclear magnetic resonance spectroscopy, and gas permeation chromatography) were used to characterize the alkali soluble lignins and hemicelluloses and the residue (mainly cellulose). The results showed that the lignin soluble fractions were dominated by substantial amounts of non-condensed guaiacyl and syringyl units with fewer p-hydroxyphenyl units. In addition, thermal analysis showed that lignin is more thermally stable than both hemicellulose and cellulose, and therefore its structure is more stable.

2.2.1.4 Pectin

Pectins are a collective name for heteropolysaccharides, which consist essentially of polygalacturon acid. Pectin is soluble in water only after a partial neutralization with alkali or ammonium hydroxide [3].

2.2.1.5 Waxes

Waxes make up the part of the fibres which can be extracted with organic solutions. These waxy materials consist of different types of alcohols, which are insoluble in water as well as in several acids (palmitic acid, oleaginous acid, stearic acid) [3].

2.2.2 Structure, mechanical, and physical properties of natural fibres

A single fibre of all plant based natural fibres consists of several cells. The dimensions of individual cells in natural fibres are dependent on the species, maturity, and location of the fibres in the plant as well as on the fibre extraction conditions. These cells are formed out of crystalline microfibrils based on cellulose, which are connected to a complete layer, by amorphous lignin and hemicellulose. The diameter of these microfibrils ranges from 10 to 30 nm, and each microfibril is made up of 30-100 cellulose molecules in extended chain conformation. Every fibril has a complex, layered structure consisting of a thin primary wall that is the first layer deposited during cell growth encircling a secondary wall. The secondary wall is made up of three layers and the thick middle layer determines the mechanical properties of the fibre. The middle layer consists of a series of helically wound cellular microfibrils formed from long chain cellulose molecules. The angle between the fibre axis and the microfibrils is called the microfibrillar angle. The characteristic value for this parameter varies from one fibre to another. The spiral angle of the fibrils and the content of cellulose generally determines the mechanical properties of the cellulose based natural fibres [3-5,11].

Mukherjee *et al*. [13,14], Kulkarni *et al*. [15] and Satyanarayana *et al*. [16] studied the mechanical properties of sisal, pineapple, banana, as well as talipot and palmyrah fibres. Properties such as the initial modulus, ultimate tensile strength, and percentage elongation were evaluated as a function of fibre diameter, test length, and speed of testing. The results of these studies were interpreted in terms of the variation in structure characteristics of these fibres, namely chemical constituents, spiral angle, defect centre, and cell sizes. Generally, the tensile strength and Young's modulus of the fibres increase with increasing cellulose content. The microfibril angle determines the stiffness of the fibres. Plant fibres are more ductile if the microfibrils have a spiral orientation to the fibre axis. If the microfibrils are oriented parallel to the fibre axis, the fibre will be rigid, inflexible and have a high tensile strength.

Munawar *et al*. [17] characterized the morphological, physical, and mechanical properties of seven nonwood plant fibre bundles (abaca, pineapple, sansevieria, and sisal that are leaf fibres, whereas Kenaf and ramie are bast fibres and coconut a husk fibre). The results demonstrated that the ramie fibres had the highest density of 1.38 g cm^{-3} while sisal fibres

had the lowest density of 0.76 g cm^{-3}. In addition, the densities of the fibre bundles decreased with increasing diameter. The mechanical properties of the fibres confirmed that ramie fibre had the highest tensile strength (849 ± 108 MPa) and Young's modulus (28.4 ± 3.6 MPa), and again the values showed a decreasing trend with increasing diameter of fibre bundles. On the other hand, sisal fibre display the highest value of tensile strength (631 MPa), followed by ramie fibre (615 MPa). The higher values of the mechanical properties of ramie fibre compared to other fibres were related to its high cellulose content (69%-97%) combined with a higher molecular weight (10 000) and small spiral angle (7^{o}-12^{o}).

2.3 Sisal fibres

Sisal fibres are hard fibres extracted from the leaves of the sisal plant (*Agava sisalana*), which have short renewal times, wide availability, ease of cultivation and low cost, associated with excellent physical and mechanical characteristics. Brazil, Tanzania, and Kenya are the three main producing countries. A sisal plant produces about 200-250 leaves and each leaf contains 1000-1200 fibre bundles which is composed of 4% fibre, 0.75% cuticle, 8% dry matter and 87.25% water. It contains three types of fibres: mechanical, ribbon and xylem. The mechanical fibres are mostly extracted from the periphery of the leaf. They have a roughly thickened-horseshoe shape and seldom divide during the extraction processes. They are the most commercially useful of the sisal fibre. Ribbon fibres occur in association with the conducting tissues in the median line of the fibre. The related conducting tissue structure of the ribbon fibre gives them considerable mechanical strength. They are the longest fibres and compared to mechanical fibres they can be easily split longitudinally during processing. Xylem fibres have an irregular shape and occur opposite the ribbon fibres through the connection of vascular bundles. They are composed of thin-walled cells and are therefore easily broken up and lost during the extraction process [13,17,18-20].

2.3.1 Chemical composition of sisal fibres

The chemical composition of sisal fibres have been reported by many researchers [21-24]. Sydenstricker *et al*. [21] showed that sisal fibre contains 73% cellulose, 10% hemicellulose, 7.6% lignin, 6.2% extractives, and about 3.1% ash, whereas Megiatto *et al*. [22] found that sisal fibre contains 65% cellulose, 20% hemicellulose, 12% lignin, and 1% ash. Paiva and

Frollini [23] showed that the chemical composition of sisal is 64.3% cellulose, 27.4% hemicellulose, 13.2% lignin, 10.9% humidity, and 1.4% ash. Recently, Botaro *et al*. [24] reported that sisal fibre contains 64.5% cellulose, 17.5% hemicellulose, 9.4% lignin, 3.5% extractives, 9.0% humidity, and 0.9% ash by weight. This variation in chemical composition of sisal fibres can be attributed to the fact that the chemical composition of lignocellulosic fibres depends on various factors such as species, variety, type of soil used, weather conditions, part from which the fibres are extracted, and age of the plant. [7,8].

2.3.2 Structure and physical properties of sisal fibres

The microstructure of sisal fibre has been investigated by some researchers [13,17,25]. Mukherjee and Satyanarayana [13] investigated the transversal and longitudinal sections of sisal fibre using scanning electron microscopy (SEM). The results showed that sisal fibre is a multicellular fibre such as other vegetable fibres, having mainly compactly arranged sclerenchyma cells (strengthening cells). The cells have a diameter (d) of 25 μm and a mean length (l) of 2.5 mm with a (l/d) ratio of 100 for fibres of diameter 50 to 300 μm. The cell walls of sisal fibre appear to be thicker (8 to 25 μm) with varying lumen sizes of 8 to 12 μm. In another study, Martins *et al*. [25] examined the structure, morphology, and fracture surface of raw and chemically modified (mercerization and acetylation) sisal fibres using SEM. The SEM micrographs of the transversal sections of embedded fibres revealed that sisal fibre contains three types of fibres: mechanical, ribbon, and xylem. The transversal surface of the cryofractured samples was also investigated to evaluate the shape of the ultimate cells and the effects of the chemical treatments on the fibre bundle. The SEM micrographs of these cryofractured cross sectional views of sisal fibres demonstrated that a single sisal fibre is made of several elongated fibre cells. The multicellular structure of the fibre cells is characterized by a large lumen, the middle lamella, and the thickened walls. These cells are mainly polygonal in shape, and the lumen is round or has round corners. Extensive SEM observations of the fibres have shown that the lumen has different and well-defined shapes. The shapes of these ultimate cells of sisal fibres vary considerably; they range in length from 1.5 to 4.0 mm, the average length being about 3 mm. The width varies from 10 to 30 μm.

Munawar *et al*. [17], characterized the microstructure of seven non-wood plant fibre bundles (abaca, pineapple, sansevieria, sisal, coconut, kenaf, and ramie) using SEM. SEM images for

the cross section of each fibre indicated that all fibres except coconut exhibited noncircular shapes on the cross section of the fibre bundles. Moreover, ramie fibre showed the smallest bundle diameter, while sisal has the largest diameter. In general, cell wall thickness and lumen diameter of fibres varied in the range of 1-5 μm and 0.1-18 μm, respectively. All the cross-sectional shapes of single fibres provided were polygonal to round. The density, microfibrillar-spiral angle, as well as the diameter of sisal fibre have been evaluated and reported in the literature by many researchers [13,26-28]. Mukherjee and Satyanarayana [13] found that the density of sisal fibre is 1.45 g cm^{-3} and the diameter of the fibre is ranging from 100 to 300 μm. Martins *et al*. [26] reported that sisal fibre had a density of about 1.31 g cm^{-3}, and an average diameter of about 124 ± 26 μm, but Gañan *et al*. [27] indicated that the density of sisal fibre is 1.51 g cm^{-3}, and the diameter is about 0.18 mm. The microfibrillar spiral angle of sisal fibre was evaluated by Mishra *et al*. [28] to be 20°. The crystallinity index of sisal fibres was estimated and reported by Paiva and Frollini [23] and Botaro *et al*. [24] to be 57% and 76.8% respectively.

2.3.3 Mechanical properties of sisal fibres

The tensile properties (Young's modulus, ultimate tensile strength, and percentage elongation) of sisal fibres have been studied extensively and reported by many workers [13,17,26,27,29]. Mukherjee and Satyanarayana [13] measured the tensile properties (ultimate tensile strength (UTS), initial modulus (YM), average modulus (AM), and percent elongation at break) of sisal fibres as a function of fibre diameter, test length, and test speed. The result revealed that UTS, YM, AM and percent elongation lie in the range 530 to 630 MPa, 17 to 22 GPa, 9.8 to 16.5 GPa and 3.64 to 5.12% respectively for fibres of diameters ranging between 100 and 300 μm. No significant variation of mechanical properties with change in diameter of the fibres was observed. In another study, Munawar *et al*. [17] found that the sisal fibre has a tensile strength of 375 ± 38 MPa, specific tensile strength of 493 MPa, Young's modulus of 9.1 ± 0.8 GPa, specific Young's modulus of 12.1 GPa, and toughness of 10.7 ± 1.2 MPa. Martins *et al*. [26] determined the tensile properties of sisal fibres and reported the values of Young's modulus, ultimate tensile strength, and elongation at break to be 30 ± 13 GPa, 701 ± 306 MPa, and 3 ± 1% respectively, whereas Gañan *et al*. [27] showed that the tensile strength of sisal fibre is 434 MPa and their Young's modulus is 17.5 GPa. The tensile behaviour of sisal fibre collected from Madhya-Pradesh, India was

determined by Chand *et al*. [29] using an Instron testing machine at a speed of 0.02 m min^{-1}. The average ultimate tensile strength and modulus were reported to be 445 MPa and 10 GPa respectively.

2.3.4 Thermal properties of sisal fibres

The thermal properties of sisal fibres have been studied by a number of researchers using thermogravimetric analysis (TGA) and differential scanning calorimetry (DSC) [23,29-31]. The results of the weight loss of sisal fibres as a function of temperature for these studies can be summarized as follows: the first small change in weight up to 100 °C could be related to water loss associated with moisture present in the fibres. Then, between 100 and 200 °C, the fibre present thermal stability. Above 200 °C up to 300 °C, the weight loss was about 10%. From 300 °C up to 400 °C, the fibre displayed considerable mass loss (more than 70%) due to decomposition of both cellulose and hemicellulose. Further, above 400 °C, degradation of fibres can be attributed to the breakage of bonds of the lignin. Above 500 °C, only the ash was observed which is about 1%. Therefore, 200 °C can be considered as the maximum temperature up to which sisal fibres can be used since above this temperature, mass loss is high.

The DSC results for sisal fibres showed two peaks; the first peak is related to the cellulose decomposition occurring around 300 °C, which is in agreement with the mass loss observed in this range in TGA. The second peak, which is ranging between 400 and 500 °C, is attributed mainly to the break of the chemical bonds of the lignin in the fibre; this is again confirmed by TGA, which showed a mass loss in the same temperature interval.

2.4 Polyolefins: Characteristics and classifications

Polyolefins are synthetic polymers of olefinic monomers, which are based only on carbon and hydrogen, and which contain a double bond in the 1-position (C_nH_{2n}, $n \geq 2$), sometimes called α-olefins. They are the largest polymer family by volume of production and consumption. Polyolefins have enjoyed great success due to many application opportunities, relatively low cost, and a wide range of properties. They are recyclable and significant improvement in properties is available via blending and composite technologies.

Polyolefins may be classified based on their monomeric unit and chain structures as ethylene-based polyolefins (contain mostly ethylene units), polypropylene-based polyolefins (contain mostly propylene units), higher polyolefins (contain mostly higher olefin units), and polyolefin elastomers. Among the synthetic polymers, polyethylene and polypropylene are the largest tonnage synthetic polymers. These materials are relatively easy to manufacture, have a range of useful properties, and are low priced. It can be concluded that a given polyolefin may be a homopolymer, copolymer, or terpolymer depending on the number of monomers used in making the polyolefin, crystalline or amorphous depending on their chain conformation, configuration, and processing conditions [32,33].

2.4.1 Polyethylene

In its simplest form, a polyethylene molecule consists of a long backbone of an even number of covalently linked carbon atoms with a pair of hydrogen atoms attached to each carbon; chain ends are terminated by methyl groups. Polyethylenes comprise chains with a range of backbone lengths. Typically, the degree of polymerization is well in excess of 100 and can be as high as 250,000 or more, equating to molecular weights varying from 1400 to more than 3,500,000. Polyethylene molecules can be branched to various degrees and contain small amounts of unsaturations. There are many types of branches, ranging from simple alkyl groups to acid and ester functionalities. In the solid state, branches and other defects in the regular chain structure limit a sample's crystallinity level. Chains that have few defects have a higher degree of crystallinity and density than those that have many. The properties of polyethylene such as melting temperature, extent of crystallinity, modulus, and the mechanical behavior depend on many parameters like the method of manufacture, the addition of comonomers, as well as overall molecular weight. Polyethylene is manufactured by several major processes. These include high-pressure polymerization (free radical polymerization), Ziegler-Natta type catalyzed polymerization, metallocene polymerization, and metal oxide catalyzed polymerization. Polyethylene can be classified depending on their density, molecular weight, as well as the comonomer employed. Therefore, polyethylene comes in various forms differing in chain structures, crystallinity, and density levels [34,35]. Table 2.1 displays polymer acronyms, comonomers, and industrial names of selected polymers and copolymers of ethylene. In this study only LDPE, LLDPE, and HDPE were

utilized as polymer matrices to fabricate the composites with sisal fibres. Therefore, the methods of production as well as the properties of these polymers will be discussed.

2.4.1.1 Low density polyethylene (LDPE)

LDPE is produced only by free radical polymerization of ethylene initiated by organic peroxide or other reagents that readily decompose into free radicals. It is commercially available in a wide variety of molecular weights, molecular weight distributions, short and long chain branch contents, as well as density ranges (0.915-0.930 g cm^{-3}). LDPE has a good balance of mechanical and optical properties with easy processability and low cost. Some of the major applications of LDPE include blown film for bags and packaging, extrusion coatings for paper, metal, and glass, and injection moulding for can lids, toys, and pails [34-36].

Table 2.1 Polymer acronyms, comonomers, and industrial names of selected polymers and copolymers of ethylene

Polymer acronym	Comonomer	Industrial name
LDPE	None	Low density polyethylene
VLDPE	Butene-1	Very low density polyethylene
LLDPE	Butene-1	Linear low density polyethylene
LLDPE	Hexene-1	Linear low density polyethylene
LLDPE	Octene-1	Linear low density polyethylene
LLDPE	4-methyl-pentene-1	Linear low density polyethylene
EVA	Vinyl acetate	Ethylene vinyl acetate copolymer
EMA	Methacrylic acid	Ethylene Methacrylic acid copolymer
EVOH	Vinyl alcohol	Ethylene vinyl alcohol copolymer
HDPE	none	High density polyethylene
COC	norbornene	Cyclic olefin copolymer

2.4.1.2 Linear low-density polyethylene (LLDPE)

LLDPE is produced by copolymerization of ethylene with α-olefins using Ziegler-Natta, supported chromium or single site catalysts. The comonomers most frequently used

commercially are butane, hexane, and octene. LLDPE differs from LDPE principally through a lack of long-chain branching and a narrower molecular weight distribution. It is commercially available in a wide variety of melt indices and density ranges (0.915-0.930 g cm^{-3}). The properties of LLDPE are functions of molecular weight, molecular weight distribution, density, type, and amount of comonomer. Physical and mechanical properties also vary accordingly. It has a high impact strength, low brittleness temperature, good chemical resistance to acids and aqueous solvents, and good dielectric resistance. It also has good toughness, low cost, and very good thermal and stress-crack resistance. Some of the major applications of LLDPE include blown and cast films for bags, packaging, injection moulding, lamination, and wire and cable coatings [34,35,37].

2.4.1.3 High density polyethylene (HDPE)

HDPE is produced by polymerization of ethylene using Ziegler-Natta or supported chromium catalysts. It consists primarily of unbranched molecules with very few flaws to spoil its linearity. The density of HDPE is typically 0.94-0.97 g cm^{-3}). It has a high modulus, yield, and tensile properties compared to LLDPE and medium density polyethylene (MDPE). However, because it has higher crystallinity, HDPE cannot match the clarity of LDPE or LLDPE film. The most important applications of HDPE include extruded pipe for potable water and gas distribution, and blow molded packaging for household and industrial chemicals (bottles for bleach, shampoo, detergent, etc.) [34,35,38].

2.5 Polyolefin reinforced natural fibre composites

In recent years, the use of natural fibres as reinforcement in plastics has received considerable attention. Natural fibres have many advantages over their synthetic counterparts. They are cheap, widely available, renewable, recyclable, biodegradable, and have high specific strength. These properties are in agreement with the recent tendency and legislation towards using materials that are renewable and environmentally friendly. Therefore, many studies have been carried out on natural fibres reinforced polymer composites as alternative to synthetic reinforcing materials. However, there are some shortcomings of natural fibres, which affect their reinforcing capabilities. Natural fibres have a tendency to absorb moisture due to their hydrophilic nature, as well as forming aggregates during processing. In addition,

their thermal stability (start degrading above 200 ^{o}C) limits their utilization in certain polymer matrices. On top of that, owing to their hydrophilic nature, natural fibres are incompatible with hydrophobic polymers, which leads to weak interfacial bonding between the two components. Consequently, this will deteriorate the mechanical properties and the whole performance of the resulting composites [3-5]. Hence, modification of the fibre and/or the polymer is required to improve the compatibility and consequently the performance of the composites.

2.5.1 Modifications of the polymer-fibre interface

The quality of the fibre-matrix interface is significant for the application of natural fibres as reinforcing materials in polymer matrices. The properties of composites depend on those of the individual components and on their interfacial compatibility. A major disadvantage of cellulose fibres is their incompatibility with non-polar polymers due to their polar nature. Pretreatments of natural fibres can clean the fibre surface, chemically modify the surface, increase the surface roughness, and reduce the moisture absorption process. Modifications of the polymer matrix and the fibre during processing as well as the polymer matrix alone have also been reported to improve the interfacial bonding. The surface modifications of natural fibres include physical, physico-chemical, as well as chemical treatments. The physical treatments can be done *via* methods like solvent extraction, while physico-chemical treatments include use of corona and plasma discharges or laser, X-ray, and ultraviolet (UV) bombardment. Chemical treatments can be carried out *via* alkalization, bleaching, acetylation, etherification, benzoylation, peroxide treatment, and graft copolymerization. On the other hand, modifications of the polymer matrix consist of different methods like grafting of polar monomers, such as maleic anhydride, or generating some oxygen containing functional groups via oxidation by using plasma treatment and gamma radiation. The various strategies, which have been used to enhance the polymer-fibre interface, were reviewed by a number of researchers [39-43]. Among the various treatments, peroxide treatment of cellulose fibre as well as the addition of peroxide to the molten polymer-fibre mixture during processing, has attracted the attention of various researchers due to easy processability and the improvement in the mechanical properties.

Many studies [44-51] were concerned with the effectiveness of organic peroxides as compatibilizers in the cellulose fibres reinforced polymer composites. Both grafting and crosslinking induced by peroxide treatment were suggested for the observed improvement in the interfacial bonding as well as the overall properties of the composites. Joseph *et al* [44] suggested an expected mechanism of the peroxide initiated radical reaction between the polymer (LDPE) matrix and cellulose fibres (sisal fibres) as shown below:

$$RO—OR \longrightarrow 2RO^{\bullet}$$

$$RO^{\bullet} + PE—H \longrightarrow ROH + PE^{\bullet}$$

$$RO^{\bullet} + Cellulose—H \longrightarrow ROH + Cellulose^{\bullet}$$

$$PE^{\bullet} + Cellulose^{\bullet} \longrightarrow PE—Cellulose$$

They investigated the influence of different chemical treatments, such as sodium hydroxide, isocyanate, permanganate, and peroxide on the tensile properties of short sisal/LDPE composites (both unidirectional and random). Peroxide treatments were performed using both dicumyl peroxide (DCP) and benzoyl peroxide (BPO). The alkali treated sisal fibres were soaked in 6% solution DCP in acetone for 30 min, then the solution was decanted and the fibres were oven dried. The same method was repeated for BPO. The results showed that the different types of treatments have improved the tensile properties (tensile strength, modulus, and elongation at break) of the composites, but to varying degrees. Addition of small amounts of peroxide was reported to have observable enhancement in tensile properties, which was attributed to the peroxide induced grafting of PE onto sisal fibre surfaces. It was also reported that among the various treatments, peroxide imparted the maximum interfacial adhesion. Furthermore, it was found that DCP was more effective than BPO at all levels of peroxide addition. This was attributed to the difference in the relative rates of peroxide decomposition. DCP has a lower decomposition rate than BPO.

The effect of sisal fibres content together with different dicumyl peroxide (DCP) concentrations, on the thermal, mechanical, and viscoelastic properties of sisal fibre reinforced LLDPE composites were studied by Mokoena *et al*. [45]. The samples were prepared by mechanically mixing LLDPE, sisal fibres, and DCP (0, 1, and 3%) in a coffee

mill, after which they were melt pressed. Significant improvements in the tensile and viscoelastic properties after addition of 1% of DCP to the composites were reported. The results also showed an increase of up to 70% in the strength of the treated composites compared to the untreated ones with the same fibre load. DCP induced grafting between sisal fibre and LLDPE was suggested as an explanation of these effects.

Malunka *et al*. [46] examined the physical, morphological, and chemical interactions between ethylene vinyl acetate (EVA) and sisal fibres in sisal fibres reinforced EVA composites, which was prepared in the presence of DCP. Melt mixing in a Brabender Plastograph was used to prepare the DCP treated and untreated samples. The results of the Fourier transform infrared (FTIR) microscopy in combination with gel content, scanning electron microscopy (SEM), porosity, and surface energy measurements revealed strong evidence of grafting even in the absence of DCP.

The influence of sisal fibre content, DCP, as well as wax addition on the thermal properties of LDPE based sisal fibre composited was reported by Luyt and Malunka [47]. The composites were prepared by mechanically mixing LDPE, sisal fibres, and the corresponding amount of DCP (2%) and wax (0 and 5%) in a coffee mill, and then they were melting pressed. It was observed that the crystallinity of LDPE in the blend of LDPE and the wax increased, due to the presence of the wax. On the other hand, the DCP treated sisal/LDPE composites showed a substantial decrease in the crystallinity of LDPE and a further decrease with an increase in sisal content was also observed. However, the presence of the wax in DCP treated composites reduced the extent of the decrease in the LDPE crystallinity. These observations were attributed to both grafting of sisal-LDPE and epitaxial crystallization. TGA results proved that the presence of both wax and sisal reduced the thermal stability of LDPE in the absence of DCP.

George *et al*. [48] investigated the effect of fibre loading as well as fibre surface modifications on the thermal properties of pineapple leaf fibre (PALF) reinforced LDPE by means of thermogravimetric and dynamic thermal analysis. The fibre surface treatments were done using isocyanate, silane, and peroxide. BPO (1% by wt. of polymer) and DCP (0.5% by wt. of polymer) were added to the melt of polyethylene before being mixed with fibres. They found that the treated composites displayed better thermal and mechanical properties

compared to the untreated ones. They attributed this to the improved interfacial adhesion between the LDPE-PALF as the result of the treatments.

Janigová *et al*. [49] examined the effect of peroxide initiated crosslinking on the behaviour of LDPE reinforced wood flour composites. The composites were prepared through melt mixing of the LDPE with the filler and the peroxide. Significant increases in Young's modulus and tensile strength were observed, whereas the strain at break showed a modest increase. The fracture surfaces of the notched samples as well as the cryofractured samples were observed by SEM. Formation of direct covalent bonds between the fibre surfaces and the LDPE was suggested as the SEM results revealed strong evidence of this.

Kalaprasad *et al*. [50] investigated the influence of fibre length and chemical treatments on the tensile properties of hybrid sisal/glass fibres reinforced LDPE composites, which were prepared via solution mixing. Various treatments such as akali, acetic anhydride, stearic acid, potassium permanganate, maleic anhydride, silane, dicumyl peroxide (DCP), and benzoyl peroxide (BPO) were applied. BPO (0.2-1.8% by weight of the polymer) and DCP (0.2-1.6% by weight of the polymer) were added to the molten polymer at the time of mixing with the fibre. The results showed the maximum increase in tensile strength and modulus for the samples treated with BPO and DCP. Peroxide induced grafting of LDPE onto the fibres surfaces was proposed as the reason for the observed improvement in the composite properties.

The effect of crosslinking brought about by the addition of 1% (wt) of (2,5-dimethyl-2,5-diterbutyl peroxy)hexyne on the thermal, mechanical, and electrical properties of LDPE composites reinforced with Canadian grass modified by polypyrrole (PPy) was reported by Mičušík *et al*. [51]. The crosslinked samples were prepared by adding peroxide to the mixing chamber in half of the procedure time (10 min). They found that the tensile strength of the treated composites was enhanced in the whole range of fibre contents. On the other hand, Young's modulus of the treated composites was slightly lower than the untreated ones when the fibre content was less than 60%. The conductivity of the uncrosslinked composites, which contain 40 wt.% of the PPy treated fibres, was 10^{-14} S cm^{-1} while the conductivity of the crosslinked composites was five orders of magnitude lower than the conductivity of the

uncrosslinked ones. This was attributed to the decomposition of PPy after the reaction with peroxide during the crosslinking process.

2.5.2 Composite properties

2.5.2.1 Morphology of polyolefin/natural fibre composites

The interface between the fibre and the polymer matrix has generally been considered to determine the final properties of the composite. Improved interfacial adhesion usually leads to better fibre dispersion and transfer of stress from one phase to the other. As mentioned earlier, several methods have been reported for improving the interfacial compatibility between hydrophilic cellulosic fibres and hydrophobic polyolefins. The influence of these modification methods on the morphologies and interfacial properties of polyolefin reinforced natural fibre composites have been investigated by several researchers [44-46,49,50,52-61], and compared with their unmodified counterparts. Scanning electron microscopy (SEM) and Fourier transform infrared (FTIR) spectroscopy were frequently used techniques to examine the morphologies and the interfacial bonding between the fibre and the polymer in cellulosic fibres reinforced plastics. The findings of these studies demonstrated that the interfacial bonding between the fibre and the polymer improved when the fibre surfaces were treated with chemical or physical treatments [44,53,56,57,60], when only the polymer matrix was modified [58,59,61], or when both of them were modified [52,54,55]. The untreated composites, on the other hand, showed poor interfacial adhesion, as the existence of fibre pull-out from the matrix material during fracture was observed in the SEM images, and their surfaces remained practically clean. Moreover, the absence of any physical contact between the fibre and the matrix was also detected [44,52-61].

Joseph *et al*. [44] investigated the effect of chemical treatments of sisal fibres with alkali, isocyanate, permanganate, and peroxide on the interfacial adhesion of sisal-LDPE composites. The fracture surfaces of the treated and untreated composites were examined by SEM. All treated composites showed better adhesion between LDPE and sisal fibres compared to the untreated ones, where poor adhesion and pull-out of the fibres from the matrix were observed.

Martin *et al.* [52] examined the morphology of the surface functionalized sisal fibres and HDPE in sisal/HDPE composites. Dichlorosilane (DS) was used to modify both sisal fibres and HDPE on a radio-frequency plasma reactor. The composites were prepared from DS plasma-treated HDPE/untreated sisal (T/UN), and DS plasma-treated HDPE/DS plasma-treated sisal (T/T), as well as untreated HDPE/untreated sisal (UN/UN). SEM micrographs of the interfaces of the untreated composites indicated that the interaction between the fibres and the polymer was poor as fibre pull-out from HDPE was seen. Moreover, the fibres had smooth surface topographies and they were dislocated from the HDPE matrix. Conversely, the SEM micrographs of the treated composites (T/T and T/UN) showed that the sisal fibres were coated with HDPE, and the presence of fibrous interconnections between the two component surfaces was also observed. Because of these topographical features, the authors suggested that bonding developed between the HDPE and sisal fibre surfaces during the composite preparation processes.

Freire *et al*. [53] reported on the composites of low-density polyethylene (LDPE) with unmodified and fatty acids (hexanoic, dodecanoic, octadecanoic, and docosanoic acids) esterified cellulose fibres (industrial Eucalyptus globulus ECF (Elemental Chlorine Free) bleached kraft pulp). It was found that the surface acylation of cellulose fibres with fatty acids improved the interfacial adhesion with the matrix. SEM micrographs of unmodified composites showed fibre pull out from the matrix, with the fibres practically intact, as well as fibre aggregation. On the other hand, the treated composites displayed fibre breakage during fracture, in addition to the fibres being well dispersed in the polymer.

Viksne *et al*. [54] studied the influence of paraffin (PAR) on wood fibre (WF) dispersion in LDPE, HDPE, and recycled polyethylene, as well as on the morphology of WF-reinforced polyethylene composites. SEM images of the fracture surfaces of LDPE-WF, which were prepared without paraffin, demonstrated that the interfacial adhesion between the matrix and WF was poor, and large aggregates were observed. Alternatively, for paraffin containing LDPE-WF, no aggregates were detected, and the components were intimately mixed.

Fávaro *et al*. [55] investigated the influence of the chemical modification of the fibre and the polymer in the morphology of sisal fibre reinforced recycled high-density polyethylene. Sisal was first mercerized with NaOH solution and then acetylated by using acetic anhydride in an

acidic medium, whereas PE was oxidized with potassium permanganate ($KMnO_4$) solution. In the case of untreated composites, SEM images revealed fibre pull-out at the fracture and the absence of phase adherence. In contrast, the adhesion between the phases was improved, when the composites were prepared with one of the modified materials. In the case of the oxidized PE, the micrographs showed regions of no adherence and the mechanical properties of these samples did not improve. The authors attributed this to the increase in the hydrophilic character of the polymer surface, in combination with the increase in hydrophobic character of the sisal fibre surface after acetylation.

Mohanty *et al*. [56] explored the interfacial properties of sisal fibre reinforced HDPE composites. Sisal fibres were modified with different concentrations (0.3, 0.5, 1, and 2%) of maleic anhydride grafted PE (MAPE). The SEM micrographs of the untreated composites showed fibre pull out, which is an indication of poor interfacial adhesion. In contrast, in the MAPE treated composites, the fibres were uniformly coated by layers of matrix material. Furthermore, it was observed that the layers of matrix material were pulled out together with the fibres during tensile fracture. These observations were evidence of good interfacial adhesion. Besides SEM, FTIR spectroscopy was also used to characterize the interface for untreated composites and treated ones. In the case of treated composites, formation of ester linkage at the interface was proved by the presence of a peak around 1751 cm^{-1}. Additionally, the stretching absorptions of (—C—H) and (C—CH_3), which are characteristic of the PE spectrum, were confirmed by the presence of two absorption bands around 2931 cm^{-1} and 2844 cm^{-1}. Similar results were also reported by Mohanty *et al*. [57] for HDPE reinforced with MAPE treated jute fibres.

The effects of addition of maleic anhydride (MA)-grafted polypropylene (MAPP) and MA-grafted polyethylene on the morphology of bio-flour-filled polypropylene and low-density polyethylene composites were examined by Kim *et al*. [58]. The interfacial bonding and chemical reaction between the fibre and the polymers were characterized by attenuated total reflectance FTIR (FTIR-ATR). The results demonstrated the formation of ester bonding between the hydroxy groups of the fibre and the anhydride functional groups of MAPP and MAPE. This was confirmed by the presence of carbonyl absorption bands of the ester functional group at 1740 cm^{-1} for the MAPP treated samples and at 1730 cm^{-1} for the MAPE treated samples.

2.5.2.2 Mechanical properties of polyolefin/natural fibre composites

It is well known from literature [45,48-50,52,62] that the mechanical performance of natural fibre-reinforced polymers depends strongly on the interface between the fibres and the matrix. The adhesion is usually stronger in polar polymers, which are capable of forming hydrogen bonds with hydroxy groups available on the fibre surface [62]. Conversely, non-polar polymers, due to their hydrophobic nature, are incompatible with cellulosic fibres and hence modification of the fibre surfaces, the polymer, or both of them, is usually required [45,48-50,52]. The improvement in the mechanical properties after modification of the interface between the polymer and the fibre is usually attributed to the better stress transfer efficiency between the polymer matrix and the filler. Furthermore, it was also reported that the mechanical properties of natural fibre-polymer composites depend on several other factors such as the type of cellulosic fibres, fibre length, loading, and orientation, as well as the processing conditions during composite preparations [44,63].

The mechanical properties of cellulosic fibres reinforced plastic composites, which were frequently reported in the literature [44,52,55-61,64-68], include tensile, impact, and flexural properties. In most of these studies, the influence of the fibre surface treatments, fibre loading, fibre length and orientation as well as the polymer matrix modifications on the mechanical properties have been investigated. It can be concluded from these studies that untreated composites usually have worse mechanical properties than the neat polymers or treated composites due to poor interfacial bonding between the fibre and the polymer matrix.

The effects of chemical treatments of sisal fibres with alkali, isocyanate, permanganate, and peroxide on the tensile properties of short sisal-LDPE composites were studied as a function of fibre loading, fibre length, and orientation [44]. The results showed that the treatments enhanced the tensile properties, but to varying degrees. The tensile modulus and tensile strength of the unidirectionally oriented composites at 30% fibre loading displayed that dicumyl peroxide treated and CTDIC treated composites showed superior tensile properties compared to others.

Martin *et al.* [52] investigated the tensile as well as the impact Izod properties of the surface functionalized sisal fibres and HDPE in sisal/HDPE composites. Dichlorosilane (DS) was

used to modify both sisal fibres and HDPE on a radio-frequency plasma reactor. The composites were prepared from DS plasma-treated HDPE/untreated sisal (T/UN), and DS plasma-treated HDPE/DS plasma-treated sisal (T/T), as well as untreated HDPE/untreated sisal (UN/UN). They found that the tensile strength of the composites prepared from HDPE/sisal (T/UN) was the highest compared to the neat polymer, other treated composites, and untreated ones. On the other hand, the tensile strength of HDPE/sisal (T/T) was found to be comparable to that resulting from untreated composites. The authors attributed this to the decomposition processes of the surface layer structures of sisal fibres exposed to the plasma. The tensile modulus of all HDPE/sisal (70/30) composites were found to be higher than that of the neat polymer, and the highest values (> 400 %) were reported for the T/UN and T/T composites. The Izod impact properties of notched and unnotched HDPE/sisal composites were also determined. The results again showed that the highest impact toughness values were associated with the T/UN composites.

Fávaro *et al*. [55] studied the effect of chemical modification of sisal fibres and HDPE on the tensile, flexural, and impact Izod properties of sisal fibres reinforced recycled HDPE. Sisal was first mercerized with NaOH solution and then acetylated by using acetic anhydride in acidic medium, whereas PE was oxidized with potassium permanganate ($KMnO_4$) solution. Their results demonstrated a gradual decrease in the tensile strength of the treated and untreated composites with fibre loading 5 and 10%, compared to neat and oxidized HDPE. In addition, the composites with oxidized HDPE and unmodified or acetylated sisal showed lowest tensile strength values. This was explained by the absence of phase compatibility between the sisal fibres and the polymer surface after chemical treatment. On the other hand, the tensile modulus of the composites, which were prepared from modified or unmodified HDPE with 10% fibre loading of treated or untreated sisal fibres, increased significantly. An increase of up to 115% was reported. Their findings also revealed that the flexural strength and modulus for all the composite samples increased compared to the neat and oxidized HDPE. However, the flexural strength for oxidized HDPE composites showed values lower than the untreated composites and almost comparable with the neat matrices. Moreover, an increase up to 40% in the Izod impact strength of the unmodified HDPE composites with 10% fibre content of modified sisal fibres was reported, and again the oxidized HDPE composites displayed lower values relative to pure HDPE. This behaviour was attributed to

the increase in hydrophilic character of the polymer surface, in combination with the increase in hydrophobic character of the sisal fibre surface after acetylation.

Mohanty *et al*. [56,57] and Choudhury [64] reported the mechanical (tensile, flexural, and impact) properties of HDPE reinforced with sisal [56,64] and jute [57] fibres. They found that treatment of sisal and jute fibres with MAPE [56,57] increased the tensile, flexural, and impact strengths of the composites. It was also reported that above 30% fibre loading, the mechanical properties were significantly deteriorated. In agreement with the previous results [56,57], Choudhury [64] reported superior mechanical properties of ionomer treated sisal fibre/HDPE composites in comparison to the pure polymer. The author also found that the mechanical properties increased with increasing fibre content (5, 10, 15, and 20 %).

The mechanical properties of cellulosic fibres reinforced LDPE composites were reported by a number of researchers [61,65,66]. Bendahou *et al*. [61] studied the tensile modulus, upper yield stress, and absorbed energy per unit volume at the yield stress of maleic anhydride modified short date palm tree fibres reinforced LDPE and PP composites. The mechanical properties were studied as a function of fibre and compatibilizer content. Their results showed that the mechanical performance was different for the two thermoplastic matrices. The yield stress and the energy at yield stress decreased for the PP reinforced with unmodified fibres, whereas the tensile modulus remained roughly constant. On the other hand, the tensile modulus of LDPE reinforced with unmodified fibres was significantly enhanced, while both the yield stress and the energy at yield stress tended to decrease and stabilize for higher filler loadings. The authors ascribed the difference in mechanical behavior between PP and LDPE to the difference in degree of crystallinity between the two thermoplastic matrices. In contrast, the modification of the fibres improved all the mechanical properties of PP and LDPE. However, their results showed that there was a critical compatibilizer content, beyond which degradation of the mechanical performance occurred. This was attributed to a plasticizing effect resulting in a decrease of the degree of crystallinity of the matrix for both sets of composites. Similar improvement in mechanical properties after adding a compatibilizer or modifying the fibre or the polymer matrix was reported by Habibi *et al*. [65] and Sever [66]. Cotton stalk, rice straw, bagasse, and banana fibres extracted from Egyptian agricultural wastes were used to reinforce LDPE [65]. Maleic anhydride grafted LDPE (MLDPE) as well as neat LDPE were used as matrices. In the case of neat LDPE,

stearic acid was used as compatibilizer to prepare the composite samples. It was found that the tensile modulus increased with increasing fibre loading for all the composites prepared with LDPE or MLDPE. However, it was observed that the MLDPE composites had higher values compared to LDPE. Moreover, it was reported that the tensile strength for the MLDPE composites increased, whereas a decreasing trend was seen for the LDPE composites. These results were explained by the fact that maleated polyethylene improved the adhesion between the filler and the matrix, which resulted in better stress transfer from the matrix to the filler. In contrast, the elongation at break decreased upon fibre addition for both sets of composites regardless of the nature of the fibre. This was due to the effect of the addition of cellulosic fibres, which exhibited brittle behaviour with a subsequent loss of toughness of the composite material. Sever [66] reported that treatment of jute fibres with akali and oligomeric siloxane improved the tensile and flexural properties as well as interlaminar shear strength of their LDPE composites.

The effects of wood fibre content as well as the addition of compatibilizers and coupling agents on the mechanical properties of LLDPE reinforced wood fibre composites were studied by Bin and He [67] and Kuan *et al*. [68]. In agreement with literature, Bin and He [67] found that maleated polyethylene enhanced the tensile strength and Izod impact of LLDPE-wood fibre composites. The authors ascribed this to esterification reactions between hydroxyl groups on the wood fibre surface and anhydride groups on the polyethylene chain, which led to better interfacial adhesion. Similar results were reported by Kuan *et al*. [68]. Vinytrimethoxysilane was used to treat the composites during compounding and then moisture-crosslinked in hot water. The effects of different crosslinking time and wood flour content on the tensile, impact, and flexural properties of LLDPE/wood flour composites were studied. Their results demonstrated that water crosslinking significantly increased the tensile strength, flexural strength, and flexural modulus of the composites. Furthermore, the values of these properties were found to increase with increase in time of crosslinking as well as with an increase in wood content. However, elongation at break was found to decrease with an increase in wood content and water crosslinking time. On the other hand, the notched impact strength was found to decrease with increasing in fibre loading, whereas time of crosslinking did not have a significant effect on the values. The enhancement in composite mechanical properties was attributed to the crosslinking network formation between the fibres and the LLDPE polymer chains.

2.5.2.3 Dynamic mechanical properties of polyolefin/natural fibre composites

Dynamic mechanical analysis (DMA) had become a widely used technique for determining the dynamic mechanical properties (storage modulus E', loss modulus E" and damping capacity tan δ), and the interphase interaction of heterogeneous polymeric systems over a wide range of temperature. DMA analysis also helps to evaluate the viscoelastic behavior of the polymer matrix in fiber-reinforced composites in the glass transition (T_g) region [48,69]. The mechanical properties of polyethylene at a particular temperature are dependent on the T_g. At the T_g, the material changes from a glassy hard state to a soft tough state because certain molecular segments become more mobile. Phase transitions are major phenomena in many amorphous polymers where mechanical properties may change in the order of decades when the material goes through a glass-rubber transition known as the T_g. For semi-crystalline polymers in the temperature range between the crystalline melting point and liquid nitrogen temperature (-196 ^oC), at least three relaxation processes are often found. These are the α, β, and γ relaxations in order of decreasing temperature. In the case of PE, the α-relaxation is observed between 20 and 60 ^oC. The intensity of the α-relaxation increases with increasing density of PE but then levels off at higher densities. The β relaxation occurs between -35 and -5 ^oC depending on the type of PE, its intensity being high for LDPE and very low for HDPE. It is due to the cooperative segmental mobility of the disordered chains and is connected to the glass transition. However, the assignment of the β relaxation to the glass transition temperature is a controversial issue in the literature, but according to many authors [70-72] this temperature region has gained considerable credibility as a glass transition temperature for PE. The γ relaxation for HDPE occurs at -170 ^oC and at -111 and -114 ^oC for linear and branched LDPE, respectively. Its intensity decreases with increasing density. The γ relaxation is caused by small, local, short-range segmental motion of amorphous PE, involving three or four methylene groups, or it could be due to the defects in the crystalline phase [71]. Much work has been carried out on the dynamic mechanical properties of cellulosic fibres reinforced polyolefin composites as a function of the fibre surface (or polymer matrix) treatments, fibre content, as well as fibre length and orientation [48,52,68,56-58,73-76].

George *et al*. [48] examined the dynamic mechanical properties of treated pineapple leaf fibre (PALF)/LDPE composites. Fibre treatments were done using isocyanate, silane, and

peroxide. The storage modulus and tan δ of the neat polymer and the composites were determined as a function of temperature, frequency, fibre loading, and fibre treatments. Their results for modified and unmodified composite samples showed that at low temperatures the fibres do not contribute much to impart stiffness to the polymer. However, on increasing the temperature the storage modulus was found to increase with fibre loading. This indicates that LDPE is stiffened by the addition of fibres. Compared to composite samples, the storage modulus of a neat polymer drops steeply on increasing the temperature due to the increased segmental mobility. Significant improvement in E' of the treated composites was observed, which is attributed to the increase in interfacial stiffness achieved through more intense fibre-matrix interaction. Of all the treatments, the isocyanate treatment showed the maximum improvement in E'. This is because of the formation of covalent bonds between the ─OH group of cellulose and the ─N═C═O group of isocyanate. Furthermore, two transitions were observed in tan δ; one at a low temperature (-65 ^{o}C) and the other at a higher temperature (78 ^{o}C). The authors concluded that for pure LDPE, the transition at a temperature of -65 ^{o}C is due to the glass transition of LDPE, whereas the higher temperature transition at 78 ^{o}C is associated with the onset of melting of LDPE crystallites. In the case of the composite samples, the tan δ results displayed a significant shift in the glass transition from -65 to -55 ^{o}C and the onset of melting from 70 to 120 ^{o}C. This was attributed to the decreased mobility of the polymer chains by the addition of the fibres. They also observed that the damping peaks of the composites were lower and broader than that of LDPE. This was ascribed to the fact that, when strain was applied to the fibres, the greater stiffness of the fibres caused the strain to be controlled by the fibres in such a way that the interface, which was assumed to be the more dissipative component of the composite, was strained to a lesser degree.

The above results are consistent with the observations of many other researchers [52,53,56-58], where incorporation of biofibres and treatments increased the storage modulus and decreased the damping values in comparison with the untreated composites and the neat polymer matrices.

The effects of addition of two different compatibilizing agents (MAPP and MAPE), as well as their content (0 to 5%), on the viscoelastic properties of rice husk flour (RHF)-filled polypropylene and low-density polyethylene composites were studied by Kim *et al*. [58]. Their results showed that the E' values of PP and LDPE significantly decreased with

increasing the temperature due to the increased polymer chain mobility of the matrix at higher temperatures. However, with incorporation of RHF in PP and LDPE, the E' of PP and LDPE was significantly increased at higher temperatures. This was attributed to the increased stiffness of PP and LDPE with the reinforcing effect imparted by the RHF, which allows for greater stress transfer at the interface from the matrix to the RHF. Furthermore, they observed that the E' values of filled PP composites slightly increased with increasing MAPP and MAPE content, in comparison to the untreated composites. 5% MAPP and MAPE showed maximum enhancement in the E' values. The authors attributed this to the improved compatibility between the RHF and PP, resulting in an enhanced stiffness of the composites. On the other hand, the stiffness of the MAPE treated LDPE composites were not significantly changed by the addition of MAPE. In the case of tan δ, their results demonstrated that with increasing temperature, the tan δ values of PP and the composites increased due to the increased polymer chain mobility. They also found that the T_g of the composite was slightly shifted to a higher temperature with increasing MAPP content, which may indicate better interfacial interaction between RHF and the matrix at the interface. Moreover, they reported that the tan δ values of the MAPP treated composites were lower than their untreated counterparts, over the complete temperature range. This indicates that the energy dissipation of the MAPP treated composites was less than that of untreated composites. The authors did not report the temperature dependence of tan δ of the LDPE composites. Instead they reported the variation of E" of LDPE and RHF-filled LDPE composites at different MAPE content. They observed that the E" peak temperature of LDPE and MAPE treated composites was in the range of -23 ^{o}C to -19 ^{o}C. This was ascribed to the β relaxation, which was shifted to higher temperatures for the composites with increasing MAPE content. The authors attributed this to the additional bonding between the RHF and LDPE, which decreased the polymer chain mobility and thus increased the β relaxation temperature of the MAPE treated composites.

The effect of nano-silica on the dynamic mechanical properties of LDPE and their wood flour (WF) composites, which were prepared in the presence and absence of DCP, were reported by Mishra and Luyt [73]. Their results showed that the incorporation of the wood flour increased the storage modulus of the LDPE matrix in comparison to the neat polymer. However, the presence of nano-silica caused a decrease in the E', which was attributed to the better interfacial properties in the case of LDPE-WF compared to LDPE-nano-silica. Their

results also showed that the E' of the DCP-treated composites was higher than that of the DCP-treated LDPE and that the presence of the nano-silica further increased the E'. The authors ascribed this to the stronger interaction between the nano-silica and the rest of the composites after DCP treatment.

Similarly, Abdelmouleh *et al*. [74] reported that the presence of treated and untreated cellulosic fibres (avicel, technical, alfa pulps, and pine fibres) enhanced the E' of the LDPE matrix. The fibres were treated with γ–metacryloxypropyltrimethoxy, γ-mercaptopropyltrimethoxy, and hexadecyltrimethoxy-silanes. Again the fibre surface treatments increased the E' of the samples compared to the untreated ones. The results of tan δ showed that the peak intensities for treated composites were lower than those of the untreated composites and the neat matrix. The decrease in tan δ values after fibre treatments could be due to the movement restriction of the polymer chain near the fibre surfaces induced by the chemical bridging through the interface. Moreover, results of tan δ showed two relaxation processes located around -20 ^{o}C (labeled α) and 60-65 ^{o}C (labeled α_c). The authors concluded that the first relaxation process was associated with the chain segment mobility of the polymer branches, whereas the second one was associated with the molecular motion within the crystalline phase. The α-relaxation did not exhibit any change in its temperature position, whereas the α_c-relaxation was shifted from 60 to 67 ^{o}C after the fibre addition. This could be due to segmental immobilization of the polymer chain at the fibre surface.

Mohanty *et al*. [56,57], and Bengtsson *et al*. [75] reported an increase in the stiffness and a decrease in the damping [56,57,75] with the incorporation of surface treated sisal, jute and wood flour in the HDPE matrix. Similarly, the storage modulus of the untreated as well as the plasma functionalized sisal fibres and the HDPE composites were found to increase in comparison to the neat HDPE and the plasma functionalized HDPE [52].

Contrary to the above studies, Pasquini *et al.* [76] reported that the storage modulus of the chemically treated sugar cane bagasse (obtained from organosolv/supercritical carbon dioxide pulping process) reinforced LDPE composites was lower than that of the untreated ones. The fibres were treated with octadecanoyl and dodecanoyl chloride acids in order to make it more hydrophobic in nature. The authors ascribed this unexpected behaviour to the degradation of the cellulose molecules during the surface modification process as was observed from the

degree of polymerization measurements and from the zero tensile strength values. The cellulose degradation and the corresponding decrease in the aspect ratio of the fibres led to a reduction of the mechanical properties of the cellulose fibres and consequently to a reduction in the rubbery storage modulus. However, their results revealed that the incorporation of untreated or treated cellulose fibres in LDPE resulted in stiffer material compared to the virgin polymer. This was attributed to the reinforcing effect of the cellulose fibres.

2.5.2.4 The thermal properties of polyolefin/natural fibres

Thermal analysis is an important analytical method in understanding the structure-property relationship as well as in measuring different transitions such as melting, crystallization, and glass transition temperatures in polymers and composite materials. Moreover, it is a useful technique to determine the thermal stability of the materials [77]. Thermogravimetric analysis (TGA) and differential scanning calorimetry (DSC) are the most frequently used techniques to study the thermal properties of polymeric materials and composites.

A number of research reports [48,53,56-59,68,78,79] focused on studies of the thermal stability of natural fibres reinforced polyolefin composites. In general, the thermal stability of the neat polymer matrices along with their treated and untreated fibre-reinforced composites was investigated in these papers. Based on the findings of these studies, and as it was reported earlier, one of the drawbacks of using cellulosic fibres as reinforcement in plastic composites is their thermal instability, with their thermal degradation starting at temperatures around 200 °C [31]. Consequently, this restricts the choice of matrix material as well as the highest processing temperatures. It was demonstrated by some researchers [56-58,68] that the treatments of the composite materials resulted in thermally more stable composites compared to their individual components. Whereas in other cases, no significant influence of the treatments was detected [53,59], or even a decrease in thermal stability was observed [78,79].

George et al. [48] investigated the effects of fibre loading and surface modification on the thermal stability of LDPE reinforced pineapple leaf fibre (PALF). Their results showed that the degradation of the PALF alone occurred in the temperature range of 75 to 175 °C as well as at a temperature of 350 °C, whereas the pure polymer degrades at a temperature of 400 °C. On the other hand, the degradation of untreated PALF-LDPE composites containing 20%

fibre loading displayed a minor peak at 410 °C corresponding to the degradation of PE and a major peak at 510 °C corresponding to the degradation of dehydrocellulose. The treated composites with the same fibre content (20%) showed small increases in thermal stability compared to untreated ones. These results indicate an increase in thermal stability of the composites compared to the individual components. The authors attributed these results to the improved fibre-matrix interaction after incorporation of the fibre and the surface treatments. Similar results were reported by Mohanty et al. [56,57] and Kuan et al. [68]. HDPE reinforced unmodified sisal [56] and jute [57] fibres as well as MAPE modified fibres were studied. Their results showed better thermal stability for the fibre-reinforced composites compared to neat polymer matrices. It was also found that the first and the second decomposition temperatures were higher in the case of the treated composites and their corresponding mass loss percentages were lower than those of the untreated composites. The authors concluded that both the fibre reinforcement and the MAPE treatment increased the thermal stability of the HDPE matrix. Additionally, water crosslinked composites of wood flour reinforced LLDPE were reported to have higher thermal stability than the neat LLDPE matrix, and a further increase in stability was observed with increasing water-crosslinking time [68]. Freire et al. [53] and Lei et al. [59], on the other hand, found that the chemical treatments of the composites did not have a significant influence on the thermal stability of the polymer matrices reinforced with cellulosic fibres. The effect of the modification of cellulosic fibres (industrial Eucalyptus globulus bleached kraft pulp) with different fatty acids on the thermal stability of their LDPE composites was also studied [53]. The results showed a decrease in the thermal stability of the polymer matrix in the treated composites. However, the thermal stability of the cellulosic fibres increased, which was attributed to good adhesion between the esterified cellulose fibres and the PE matrix. Similarly, three different coupling agents [59] were used to treat recycled HDPE reinforced with pine wood flour and bagasse composites. The results showed little influence of the coupling agents' treatments on the thermal degradation of the composites. Moreover, Tajvidi and Takemura [79] displayed that the thermal stability of HDPE reinforced kenaf fibres, wood flour, newsprint, and rice hulls composites were lower compared to neat HDPE, and the presence of the compatibilizer did not alter the degradation temperatures of the components of the composite.

It is known in the literature [58,61,64,65,76,78,80-83] that the crystallization kinetics of semi-crystalline thermoplastic polymer matrices are strongly modified in the presence of

fibres. It was reported by some authors [64,65,78,80] that the incorporation of natural fibres in semi-crystalline matrices (e.g. PE) results in increasing of the crystallinity of the polymer matrix in the composites, with a further increase with increasing fibre content. It was concluded that the surfaces of the fibres act as nucleating sites for the crystallization of the matrix polymer, promoting the growth and formation of transcrystalline layers in the composites. It was observed in other cases [58,61,81] that the nucleating ability of the fibres increased in treated composites compared to untreated ones. However, there were some cases where the presence of cellulosic fibres did not significantly affect the crystallinity and melting behaviour of the polymer matrix [53,76]. On the other hand, it was reported by some authors [82,83] that the presence of fibres decreased the crystallinity of the polymer matrix.

Kim *et al.* [58] investigated the influence of the addition of two compatibilizing agents (MAPP and MAPE) on the thermal properties of bio-flour-filled PP and LDPE composites. They found that the melting temperature T_m of the composites was not significantly changed by the addition of MAPP and MAPE. Moreover, the crystallinity of the composites showed a slight increase with increasing MAPP and MAPE content, due to the coupling effect of the compatibilizers. In the case of the PP composites, the glass transition temperature T_g was slightly shifted to a higher temperature with increasing MAPP content, which was ascribed to the improved adhesion imparted by MAPP addition.

The effect of biofibres and coupling agents (MAPP and MAPE) contents on the thermal properties of LDPE and PP reinforced palm tree fibres was studied by Bendahou [61]. In the case of the LDPE composites, it was observed that the presence and content of the fibres did not have an effect on the melting temperature and the crystallinity of the polymer matrix, as their values remained constant. On the other hand, low contents of MAPE were found to increase both the melting temperature (T_m) and the crystallinity (X_c) of LDPE, whereas high contents decreased them. The first increase in T_m and X_c was explained by the enhanced adhesion of the composites, but as the MAPE content was increased, the crystallization was hindered by the irregularity of the polymeric chains. However, the addition of fibres was found to increase both the melting temperature and the crystallinity of PP composites. This was attributed to the nucleating effect of the fibres on the crystallization of PP. The fibre loading did not have an effect on T_m. It was also found that the crystallinity as well as the melting temperature both increased in the presence of MAPP. However, T_m showed a

continuous increase with addition of MAPP whereas X_c significantly increased for low amounts of MAPP, and decreased for high amounts. The last point was interpreted in a similar way to the LDPE composites. Similar results were reported by Choudhury [64]. The isothermal crystallization behaviour of ionomer-treated sisal fibres reinforced HDPE was investigated. The results demonstrated that the T_m of HDPE decreased after addition of the sisal fibres and further decreased with increasing fibres loading. The author attributed this to the nucleating effects of the fibre surfaces, which shortened the time required for crystallization of HDPE and hence limiting the isothermal thickening of HDPE crystals and consequently decreasing T_m. On the other hand, the author found that the percent crystallinity of HDPE was significantly increased by fibre addition, which indicates the nucleating ability of the fibres.

The thermal properties of LDPE and MLDPE reinforced with cellulosic fibres (cotton stalk, rice straw, bagasse, and banana plant waste) extracted from Egyptian agricultural wastes was studied by Habibi *et al.* [65]. They found that both the melting temperature and the crystallinity of MLDPE were higher than those of LDPE. Furthermore, it was observed that the melting temperatures of the neat polymer matrices as well as the crystallinity of the MLDPE matrix in the fibre reinforced composites remained roughly constant after addition of cellulosic fibres. However, the crystallinity of the LDPE matrix slightly increased when cellulosic fibres were added. Similar results were reported by Pasquini *et al.* [76].

In his effort to enhance the compatibility between an LDPE matrix and bleached kraft wood pulp, Sailaja [82] modified the wood with polymethylmethacrylate (PMMA) *via* graft copolymerization. The influence of poly(ethylene-co-glycidyl methacrylate) as a compatibilizer was also examined. The author found that the melting temperatures for the composite samples were slightly lower than that of the neat polymer matrix. The crystallinity also decreased with increasing filler content, which could be due to the inhibition of close packing of LDPE chains caused by the incorporation of grafted wood pulp.

Barone [83] studied keratin fibres reinforced polyethylenes of varying crystallinity. The author concluded that keratin fibres inhibited the crystallization in polyethylenes of low crystallinity, but enhanced crystallization in high crystallinity polyethylenes.

2.6 Poly(lactic acid)/sisal whiskers nanocomposites

2.6.1 Cellulose nanofibres

In recent years, nanocomposite materials have attracted significant scientific interest because of their exceptional electrical, thermal, barrier, and mechanical properties. They are defined as composite materials for which one of the phases has at least one dimension in the nanometer range (1-100 nm). Nano-reinforcements are also unique in that they will not affect the clarity of the polymer matrix. Only a few percentages of these nano-materials are normally incorporated (1- 5 %) into the polymer and the improvement is vast due to their large surface area [84-86].

The extraction and production of nano-scale cellulose fibres from different cellulosic sources (e.g. wood, bacterial cellulose, tunicate, etc.) has gained increasing attention due to their abundance, high strength and stiffness, low weight, and biodegradability. Cellulose (see 2.2.1.1) has a hierarchical structure, which forms *via* cellulose chains aggregation during the biosynthesis into the repeated crystalline structure to form microfibrils in the plant cell wall. The cross dimensions of the microfibrils range from 2 to 20 nm, depending on the source of celluloses. The aggregation phenomenon occurs primarily *via* van der Waals forces and intra- and inter-molecular hydrogen bonds. As they are devoid of chain folding and contain only a small number of defects, each microfibril can be considered as a string of cellulose crystals that are linked together by amorphous domains [85,86].

In general, cellulose nanofibres have been obtained in two forms or types depending on the method of extraction as well as the dimensions and the morphologies of the final product. Microfibrillated cellulose (MFC) is also known by other terms in the literature, such as microfibril, microfibril aggregates, microfibrillar cellulose, nanofibrils, and nanofibres. They are long flexible nanoparticles consisting of alternating crystalline and amorphous strings. The diameter of MFC is in range of 10 to 40 nm and their length is greater than thousand nanometer (>1,000). Several methods have been reported in the literature to isolate and produce MFC. So far, mechanical treatments, cryocrushing, and grinding are the major methods for production of MFC. Pre-treatments such as alkaline, oxidation, and enzymes of the cellulosic materials prior to the above-mentioned methods of extraction are often used.

The aim of these pre-treatments is to purify the cellulose by removing other constituents [85-88]. On the other hand, cellulose whiskers, that are also known as nanowhiskers, monocrystals, or nanocrystals, are elongated crystalline rod-like nanoparticles that can be extracted from plant material or animal sources (such as bacteria and tunicate) through controlled acid hydrolysis. Their precise morphological characteristics (e.g., length, width, and shape) are usually studied by microscopy (TEM, AFM, E-SEM) or light scattering techniques, including small angle neutron scattering (SANS). It has been reported in the literature that their diameters range between 2 to 20 nm, but there is a wide length distribution from 100 to 600 nm and even more than 1000 nm was reported in some cases. The dimensions of the cellulose whiskers depend on the origin of the cellulose, as well as on the conditions of the acid hydrolysis process such as time, temperature, acid concentration, and the nature of the acid. Typical procedures currently employed for production of cellulose whiskers consist of removing other constituents associated with cellulose by chemical treatments. Subsequently, pure cellulose is subjected to strong acid hydrolysis under strictly controlled conditions, which is followed by water dilution and successive washing using centrifugations. The resultant suspension is dialyzed against water to remove the free acid and then a sonication step is crucial to disrupt the solid aggregates. In addition, a filtration step is needed to exclude the microfibres and produce a stable colloidal suspension of the cellulose whiskers. Sulphuric and hydrochloric acids have been extensively used for whiskers preparation, but phosphoric and hydrobromic acids have also been reported for such purposes. During acid hydrolysis, the amorphous regions in the cellulose chains are more susceptible to acid attack, which promotes the hydrolytic cleavage of the glycosidic bonds and finally releasing individual crystallites. It was observed that the acid hydrolysis of cellulose by using sulphuric acid produced more stable colloidal suspensions of whiskers compared to hydrochloric acid. This can be explained by the fact that the sulphuric acid-treated cellulose whiskers have an important charge density on the surface compared to hydrochloric-treated cellulose whiskers, which are uncharged. This charge density results from grafting of the sulphate groups onto the surface of the whiskers, which induces a negative electrostatic layer covering the whiskers. The electrostatic repulsion between the negatively charged particles on the surface leads to whiskers suspensions that neither precipitate nor flocculate [85,86,89-96].

Due to the near perfect crystalline arrangement of the cellulose whiskers, they have a high modulus. The modulus of the perfect crystal of native cellulose was estimated to be 150 GPa, which is similar to that of aramid fibres (Kevlar). Using Raman spectroscopic techniques the modulus of cellulose whiskers extracted from the mantle of a tunicate sea animal was reported to be 143 GPa. Furthermore, the specific surface area for the cellulose whiskers extracted from tunicate was determined to be in the range of 150 to 170 $m^2 g^{-1}$ [85,86,89,97].

It was reported in the literature that concentrated colloidal suspensions of cellulose whiskers exhibited nematic liquid crystalline alignment. The microscopic studies demonstrated that in dilute suspensions, cellulose whiskers are randomly oriented (isotropic phase) and they appear as spheroids or ovaloids and the initial ordered domains are similar to tactoids. As the concentration of the whiskers increases (e.g. evaporation of water), the tactoids coalesce to form an anisotropic phase, which is characterized by a unidirectional self-orientation of the CNs rods. It was found that this chiral nematic structure could be preserved after complete water evaporation to provide iridescent films of cellulose whiskers [91,92].

Thanks to their good mechanical properties coupled with their high surface area as well as their availability, renewability, recyclability, and biodegradability, cellulose whiskers have more potential as reinforcing materials in polymer matrices. However, there are some drawbacks of cellulose whiskers, such as their time consuming preparation procedures with very low yield, highly hydrophilic surface, lack of commercial availability, low thermal stability, and poor dispersion due to a tendency to agglomerate [85,86,89].

2.6.2 Poly(lactic acid) (PLA)

Polylactic acid is one of the most promising biobased and biodegradable polymers, which has attracted the attention of polymer scientists during the last decade as a potential biopolymer to substitute the conventional petroleum based plastics. It belongs to the family of aliphatic polyesters commonly made from α-hydroxy acids. PLA is made up of lactic acid (2-hydroxy propionic acid) as a building block, which is produced by converting sugar or starch obtained from vegetable sources using either bacterial fermentation or a petrochemical route. Lactic acid is a highly water-soluble, three-carbon chiral acid that exists as two optically active configurations, namely the L- and D-isomers. The designation L- and D- are used to represent

the ability of the molecule to rotate the plane of the polarized light either clockwise (L-) or counterclockwise (D-).

Polymerization of lactic acid to PLA can be achieved by a direct condensation process that involves solvents under high vacuum. Alternatively, in a solvent-free process, a cyclic dimer intermediate called lactide (ester of the acid) is formed followed by catalytic ring opening polymerization of the cyclic lactide. In addition, PLA can be produced *via* azeotropic dehydrative condensation of lactic acid. Both azeotropic dehydrative condensation and ring opening polymerization produce high molecular weight PLA whereas the direct condensation process yields a low molecular weight, brittle, and unstable polymer. The properties of PLA depend on its molecular characteristics, as well as on the presence of ordered structures, such as crystalline thickness, crystallinity, spherulite size, morphology, and degree of chain orientation. The optical purity of PLA has many profound effects on the structural, thermal, barrier, and mechanical properties of the polymer. Depending on the composition of the optically active isomers (L- or D-), as well as on the thermal history, PLA in the solid state can be either semi-crystalline or totally amorphous. For amorphous PLAs, the glass transition (T_g) determines the upper use temperature for most commercial applications. For semi-crystalline PLAs, both the glass transition and melting (T_m) temperatures are important for determining the use temperatures across various applications. Both of these transitions, T_g and T_m, are strongly affected by the overall optical composition, primary structure, thermal history, and molecular weight.

Besides the fact that it complies with the current environmental concerns, as an eco-friendly polymer matrix (e.g. recyclable, biocompatible, compostable), PLA is a unique polymer that performs a lot like polypropylene. It has a broad range of applications because of its ability to be stress crystallized, thermally crystallized, impact modified, filled, copolymerized, and processed in most polymer processing equipment. However, there are some drawbacks of PLA, such as poor toughness, slow degradation, hydrophobicity, lack of reactive side-chain groups, and high production cost. Several modification methods have been used to improve the performance and the different end-use applications of PLA. Copolymerization, surface treatment, blending, and stereo-complexation were reported to have significant effects on the properties of PLA, as well as on its degradation pattern. Moreover, the incorporation of organic/inorganic fillers was also reported to have good effects on the mechanical, barrier,

and thermal properties of a PLA matrix. Due to its bioresorbability and biocompatibility in the human body, PLA has been used in medical applications, such as fracture fixation devices like screws, sutures, delivery systems, and micro-titration plates. Furthermore, PLA has also found an increasing use for different consumer packaging such as yogurt cups, cutlery, rigid thermoformed containers, high value films, and coated papers, because of its renewability, biodegradability, and transparency [98-106].

2.6.3 Properties of PLA/cellulose whiskers nanocomposites

As mentioned above, cellulose whiskers have great potential as reinforcing fillers in polymer matrices due to their good mechanical properties, high surface area, and high aspect ratio. The extent of the reinforcement of the cellulose nanofibres in polymer matrices is largely dependent, among other factors, on how well the nanofibres disperse in the polymer matrix, and the nature of interfacial interaction between the nanofibres and the polymer phase [85,86,89]. One drawback of using cellulose whiskers as reinforcement is the difficulty to disperse them uniformly in the non-polar medium because of their polar surface. So far, only aqueous or polar systems have been used successfully as matrices for the dispersion of cellulose whiskers because of the hydrophilic nature of both components [107,108]. The solid nanocomposites films are obtained by mixing, casting, and evaporating the aqueous polymer solutions and the aqueous suspensions. On the other hand, cellulose whiskers reinforced hydrophobic polymer matrices have not been studied extensively due to poor dispersion/compatibility, which results in agglomeration of the fibres and deterioration of the mechanical properties of the resulting composites. Various methods, which include modification of the cellulose whiskers surfaces [109-111], addition of surfactants [109,112], using compatibilizers [113], and modification of the polymer matrices [114], have been tried to overcome the poor dispersion and enhance the interfacial bonding in these systems. By using these approaches, many researchers have been able to obtain stable suspensions of the modified whiskers in non-aqueous solvents (organic solvents), either through solvent exchange methods [115] or *via* freeze-drying and re-dispersion in organic solvents through the aid of sonication treatment [94]. The approach of producing stable suspensions of modified whiskers in organic solvents have given the possibility of obtaining well dispersed and better adhered nanocomposites [94,112,115-118] through also dissolving PLA in the same organic solvents and subsequently mixing the two components, casting the mixture, and

evaporating the solvents. Although melt mixing techniques are the most suitable and practical methods for industrial applications, very limited works [119,120] have been published on melt mixing of cellulose whiskers and a PLA polymer matrix in the dry phase. Oksman and co-workers [113,114] have tried to develop an extrusion compounding method, which can be used industrially by pumping the suspensions of the cellulose whiskers into the molten polymer matrix.

2.6.3.1 Morphology of PLA/cellulose whiskers nanocomposites

The morphology of PLA reinforced cellulose whiskers nanocomposites have been studied by several authors [94,112-115,117,119-121]. The conclusion, which can be drawn from these studies, is that scanning electron microscopy (SEM) and transmission electron microscopy (TEM) are the most widely used techniques to inspect the structures and morphologies of these nanocomposite materials. It was, however, reported in the literature that atomic force microscopy (AFM) is a powerful alternative to TEM where contrast between the whiskers and the matrix is limited and the beam sensitivity is a major challenge [94]. The major issues during these examinations (SEM, TEM, and AFM) are the dispersion of the cellulose whiskers within the polymer matrix, the presence of voids and aggregates, as well as the interfacial adhesion between the nanofibres and the polymer matrix. FTIR spectroscopy was reported as an effective technique to investigate the possible interfacial interactions between the polymer and the cellulose nanofibres.

The dispersion of the nanofibres, as well as the presence of voids and aggregates, are strongly dependent on the processing techniques and the conditions. On the other hand, the interfacial adhesion between the components of the nanocomposites depends among other factors on their compatibility. It has been reported that solution casting (from organic solvents) of the nanofibres, which are modified through surfactant treatment [94,112], grafting of maleic anhydride [115,117], and grafting of poly(ε-caprolactone) [118,121], have resulted in homogeneous dispersion of the nanofibres within the polymer matrix, particularly at lower loadings. Thereafter, with an increase in nanofibre loadings, aggregation of the nanofibres to microparticles was observed. The results also demonstrated good interfacial adhesion. Conversely, solution casting (from organic solvents) for unmodified nanofibres was reported to have poor dispersion within the polymer matrix and the surface morphology of the samples

showed a rough and uneven distribution of the fillers, which increased with the amount of nanofibres. The fractured samples showed separation of two distinct zones from each other with circulated wrinkles on the surface and fibre pull-out. These observations are clear evidence of poor interfacial adhesion.

In the case of melt compounding of the cellulose whiskers and the PLA matrix in the dry phase, different chemical modifications of the cellulose whiskers such as addition of polyvinyl alcohol (PVOH) [113], silane treatment [119], and addition of surfactants [120] were used. Grafting of maleic anhydride to PLA (PLA-MA) [114] was also reported to have good effects on the dispersion of the whiskers and the interfacial adhesion of the resultant nanocomposites. The morphologies of the treated and untreated nanocomposites under SEM and TEM examinations have shown significant differences. Cryogenic fracturing of the untreated nanocomposites displayed uneven fracture surfaces and agglomeration of the nanofibres. Weak adhesion between the whiskers and PLA was evidenced by the presence of several fibres pull-outs and gaps between the nanofibres and the PLA matrix. In contrast, treated nanocomposites demonstrated better filler dispersion within the polymer matrix, and a thin layer of the polymer on the surface of the nanofibres was observed in some cases. This was attributed to improved interfacial adhesion. However, aggregations to microparticles were noticed with an increase of the amount of the nanofibres.

2.6.3.2 Thermal properties of PLA/cellulose whiskers nanocomposites

The physical properties of polymers depend on their molecular characteristics as well as ordered structures such as crystalline thickness, crystallinity, spherulite size, morphology, and degree of orientation. In the case of PLA, based on the composition of the optically active isomers (L- and D-) as well as the thermal history, PLA in the solid state can be either semi-crystalline or completely amorphous. PLA resins containing more than 93% of L-lactic acid are semi-crystalline, while PLA with 50-93% L-lactic acid is strictly amorphous [122]. Differential scanning calorimetry (DSC) can be used to determine the glass transition (T_g), crystallization (T_c), and melting (T_m) temperatures, as well as the crystallization and melting enthalpies of the polymeric materials. Furthermore, the thermal stability of these materials can be examined by using thermogravimetric analysis (TGA). The thermal properties of PLA reinforced cellulose whiskers nanocomposites were reported by a few authors

[112,115,117,121,123]. Only two papers could be found on the effects of the presence of cellulose whiskers on the glass transition as well as melting and crystallization behaviour of PLA [121,123]. In both these publications, a solution-casting method (from organic solvents) was used to prepare the nanocomposites. Lin *et al.* [121] have reported on PLA reinforced-cellulose whiskers-grafted-polycaprolactone, whereas Liu *et al.* [123] have studied PLA/cellulose whiskers nanocomposites without using any treatments. The results showed that the glass transition temperature of the PLA matrix in the presence of the grafted whiskers was shifted from 58 to 52 °C. This was ascribed to the presence of the rubbery poly(ε-caprolactone) (PCL), which improved the motion of the PLA segments in the amorphous region. In addition, the results showed two melting peaks for the nanocomposite samples which contained more than 4 wt % fibre. The first melting peak was located at a lower temperature of 140-143 °C, and the other melting peak was close to that of the unfilled polymer. This indicated a change in the original structure of PLA because of the interactions between PLA and the PCL grafted whiskers. Moreover, the melting enthalpies of the nanocomposite samples were all higher than that of the unfilled PLA. This was due to the nucleation effects of the PCL grafted cellulose whiskers that improved the crystallinity of the PLA matrix. The results of Liu *et al.* [123] demonstrated almost the same glass transition temperature between 55-56 °C for the nanocomposites and the unfilled PLA. The crystallization temperature of the nanocomposites showed a considerable decrease compared to unfilled PLA. Additionally, the crystallization and melting enthalpies increased with the addition of whiskers to the PLA matrix. These results proved that cellulose whiskers in this system acted as nucleating agents.

The effects of the incorporation of cellulose whiskers, as well as the different modifications, on the thermal stability of their PLA nanocomposites were investigated by a few authors [112,115,117]. As was reported earlier [31], one of the drawbacks of using cellulosic fibres as reinforcement in polymer composites is their thermal instability, with their thermal degradation starting at temperatures around 200 °C. Furthermore, it was observed that the modification of the hydroxy groups could alter the thermal stability of the fibres. The changes in degradation temperatures were found to depend on the type of modification agent applied [112,124]. Moreover, it was found that the introduction of sulphate groups during sulphuric acid hydrolysis of the cellulosic materials to produce the whiskers have caused a significant decrease in degradation temperatures of the resultant nanofibres. The content of the sulphate

groups was found to increase with acid concentration, acid to cellulose ratio, and hydrolysis time [115,117,125].

Pandey *et al.* [115,117] studied the influence of the incorporation of maleic anhydride-grafted cellulose whiskers on the thermal stabilities of their PLA nanocomposites. They found that the nanocomposite samples had lower thermal stability and faster degradation in comparison with neat PLA, and the thermal stability decreased with increasing filler content. A similar trend was observed for the nanocomposite samples with unmodified whiskers, which were degraded at slightly higher temperatures than the treated ones. The authors attributed this to the acid treatment during the nanofibres preparation, which probably generated some defects along the longitudinal cellulose chains, or to esterification reactions that caused the unfolding of ordered cellulose chains. In contrast to the previous observations, Oksman and co-workers [112] found that the surfactant treatment of cellulose whiskers resulted in higher thermal stability compared to the neat polymer and the untreated nanocomposites. They did, however, only study the thermal stability of the samples in the temperature range 20 to 220 °C (where all the samples are thermally stable). In this temperature range the untreated samples as well as the samples, that were prepared *via* exchanging water with tert-butyl alcohol, were less thermally stable than the unfilled PLA.

2.6.3.3 Mechanical properties of PLA/cellulose whiskers nanocomposites

The mechanical properties of PLA/cellulose whiskers nanocomposites are dependent on how well the whiskers are dispersed in the polymer matrix, as well as on the nature of the interfacial adhesion between the polymer and the cellulose whiskers. The effects of the method of preparation (solution casting or melt compounding), as well as the applied treatments, on the mechanical properties of PLA/whiskers nanocomposites have been reported in the literature [114,118,120,123]. The solution casting [123] of the unmodified PLA (T_g = 56 °C, T_m = 140 °C)/whiskers nanocomposites have shown that the Young's modulus and tensile strength for the untreated nanocomposites increased compared to unfilled PLA, whereas the elongation at break decreased. Conversely, the melt compounding of unmodified PLA (T_g = 68 °C, T_m = 160 °C)/cellulose whiskers [120] displayed that the Young's modulus was almost constant compared to unfilled PLA, while tensile strength and elongation at break both decreased.

Oksman and co-workers [114], have reported that the compatibilizer (PLA-MA), the processing aid (polyethylene glycol-PEG), and the pumping medium (N,N-dimethyl formamide/lithium chloride (DMAc/LiCl)) all had negative effects on the mechanical properties of the PLA reinforced cellulose whiskers nanocomposites. The nanocomposite samples were prepared by pumping a suspension of the cellulose whiskers into the molten polymer and additives during the extrusion process. Their results showed that the tensile properties of the untreated and unfilled PLA were better compared to all samples where one or more additive was used to process the samples. The authors tried to compare the effects of the presence of cellulose whiskers on the mechanical properties of the treated samples. When using the same pumping medium (DMAc/LiCl), the PLA/PLA-MA/whiskers sample showed a significant increase in Young's modulus and maximum strength compared to the PLA/PLA-MA/PEG/whiskers. However, the elongation at break for the PLA/PLA-MA/PEG/whiskers sample increased dramatically (800 %) compared to the PLA/PLA-MA/whiskers sample due to the plasticizing effect of PEG. Comparing unfilled PLA with PLA/PLA-MA/whiskers, that were both prepared by using DMAc/LiCl as pumping medium, the nanocomposite sample showed a significant improvement in Young's modulus, maximum strength, and elongation at break.

In another study, Oksman and co-workers [120] revealed that the surfactant treatment of the nanocomposites, that were prepared by melt compounding, showed different effects based on the percentage of the surfactant. The authors compared only surfactant treated PLA samples with or without cellulose whiskers to examine the reinforcing capability of the nanofibres. The sample (PLA/whiskers/surfactant) treated with 5% of the surfactant displayed a considerable improvement in Young's modulus, tensile strength, and elongation at break in comparison to PLA treated with 5 % surfactant (PLA/surfactant). As the percentage of the surfactant increased to 10 wt %, the tensile strength and the elongation at break both increased compared to PLA with only surfactant added sample, but the Young's modulus remained almost unchanged. Gel permeation chromatography measurements of the PLA and the PLA treated samples demonstrated significant degradation of the PLA in the surfactant treated samples.

In contrast to the previously reported studies, Yu *et al.* [118] reported a considerable enhancement in tensile properties of PLA reinforced with starch nanocrystals grafted-polycaprolactone (StN-g-PCL) compared to the unfilled PLA matrix. They found that for 5 wt % fibre loadings both the tensile strength as well as the elongation to break increased, whereas the Young's modulus decreased. However, as the nanofibres content increased, both the Young's modulus and the elongation to break gradually decreased, but the elongation to break remained higher than that of the unfilled PLA at all fibre loadings used in this study. In contrast, the results displayed that the tensile strength decreased abruptly and even became lower than that of neat PLA for higher nanofibres loadings. The authors observed an improvement in tensile properties for the nanocomposite sample only up to a level of 5 wt % nanofibres in the grafted PCL, which was due to the enhanced interfacial adhesion between the whiskers and PLA matrix. However, as the amount of PCL increased with an increase in nanofibre loadings, the plasticizing effect of PCL dominated its compatibilization role.

2.6.3.4 Dynamic mechanical properties of PLA/cellulose whiskers nanocomposites

Dynamic mechanical analysis (DMA) is presented as a powerful tool to investigate the linear mechanical behaviour of nanocomposites in different temperature/frequency ranges. Moreover, DMA can provide information on molecular relaxations as well as interactions taking place in the nanocomposite materials as the temperature is varied. DMA is more sensitive than DSC for observing weak thermal transitions (such as the glass transition), because it can reflect the motion of segments at molecular level, in contrast with the domain scale reflected by DSC. The glass transition temperature of cellulose whiskers filled polymer composites is an important parameter, which controls different properties of the resulting composite such as its mechanical behaviour and the matrix chain dynamics. The glass transition temperature of PLA is strongly dependent on the structural parameters such as the molecular weight, the optical purity, and crystallinity of the polymer. The thermal history of the polymer matrix and the way in which the glass transition is measured also affect the value of the reported glass transition. The typical PLA glass transition temperature (T_g) ranges from 50 to 80 °C [98,112,118,119].

The effects of the dispersion (by using solution casting or melt compounding) of the cellulose nanofibres, as well as the nature of the interfacial adhesion between the cellulose whiskers

and the polymer matrix, on the dynamic mechanical properties of PLA/cellulose whiskers nanocomposites have been investigated by a number of researchers [112,113,118-120]. Solution casting and/or melt compounding were used to prepare the PLA nanocomposite materials. Depending on the method of the preparation as well as the various chemical modifications, the effects of incorporation of cellulose whiskers on the storage modulus and tan δ (glass transition) were found to differ significantly. Oksman and co-workers have noticed a drastic shift in the glass transition temperature (up to 20 °C) for the surfactant treated PLA/whiskers nanocomposites [112], whereas in other cases it remained almost unchanged or even decreased [113,118]. The chemical modification of the cellulose whiskers or the polymer matrix was demonstrated to have a positive effect on the storage moduli of the nanocomposites [112]. However, in other cases the storage moduli of the nanocomposites were found to be lower than that of the neat PLA [118,120].

2.7 Poly(furfuryl alcohol) nanocomposites

2.7.1 Poly(furfuryl alcohol)

In recent years, due to both environmental and economical concerns, increasing attention has been given to materials that are derived from renewable resources as promising alternatives to their petroleum based counterparts [126,127]. Furan derivatives are ubiquitous in nature in a wide variety of structures, but all of them appear in very modest amounts within specific vegetables and animal species. The chemistry associated with the furan heterocycle has been the subject of extensive studies over the past century and is still a very active field of research because of its important consequences in areas such as synthons, pharmaceuticals and other fine chemicals, liquid crystals, as well as polymer science and technology. Furfural or 2-furancarboxaldehyde is produced industrially from agricultural residues such as sugarcane bagasse, corn cobs, cotton seeds, and wheat or forestry wastes *via* acid-catalyzed depolymerization and dehydration. Most of the furfural produced worldwide is converted into furfuryl alcohol (FA) by simple reduction processes. FA is the dominant furan commodity on the market, which has found a number of applications in different technological areas. It is a liquid at room temperature and has a high solubility in water and many organic solvents [127-129]. FA can easily be polymerized to produce a thermally crosslinked thermosetting polymer (poly(furfuryl alcohol) (PFA)). The polymerization process requires acid catalysis

and always leads to a black crosslinked product. The structure of the resin depends on the experimental conditions such as temperature, solvent and initial concentration of initiator. The acid catalyzed oligomerization and resinification of FA have been studied extensively in the past years and generally the features of the process are understood. However, many aspects of the process, including the initiation mechanism, are still unknown. Two main mechanisms for initiation of the process were suggested. The first pathway consists of a condensation reaction between the hydroxy (–OH) moiety of the methylol group of one furan ring and the 5-position of another furan ring (head-to-tail structure), leading to water elimination and the formation of a methylene linkage. This process can continue and lead to the formation of long oligomeric chains. The other pathway involves a condensation reaction between the –OH moiety of the methylol group of one furan ring and the methylol group of another furan ring (head-to-head structure) to form a dimethylene ether linkage. This mechanism can explain the formation of the dimeric species but not the polymeric ones. These pathways and the resulting structures predict only linear macromolecules without any chromophore, and therefore these materials are expected to be colourless. However, the experimental observations prove the formation of an intense coloured product, which suggests the presence of other reactions besides the condensation steps. Formation of conjugated sequences in the polymer chains was proposed as a mechanism to explain the development of the coloured species [128, 130,131].

PFA has found successful applications and usage in different fields include metal-casting cores and moulds, corrosion resistant coatings, polymer concrete, wood adhesives and binders, sand consolidation and well plugging, materials processing low flammability and low smoke release, and carbonaceous products comprising industrial graphitic electrodes [128,132,133]. Furthermore, in recent years, PFA has found an increasing attention in natural fibres reinforced polymer composites. Treatment of natural fibre surfaces with PFA to enhance their compatibility with polymer matrices [134], usage of FA (PFA) as a processing agent [135], and exploitation of PFA as a polymer matrix [136] have been reported in the literature.

2.7.2 Poly(furfuryl alcohol)/cellulose whiskers nanocomposites

Very few works have been published on PFA reinforced cellulose whiskers (CW) nanocomposites [126,137]. Pranger *et al.* [126] used a novel approach to prepare a completely biobased nanocomposite material by using *in situ* polymerization of furfuryl alcohol with cellulose whiskers. The monomer (FA) was used to serve first as a solvent for effective dispersion of the nanofibres (both hydrophilic), and later as a monomeric precursor for the *in situ* polymerization to form PFA. The cellulose whiskers, on the other hand, were used to catalyze the polymerization of FA by the sulfonic acid residues on its surfaces, which originate from the acid hydrolysis step during the preparation of the whiskers, and at the same time they serve as reinforcement for the PFA. The resinification of FA under experimental conditions was followed by FTIR spectroscopy. Formation of PFA is characterized by an increase in the intensities of the peaks at 1562 $cm^{-1}$and 1712 cm^{-1}, which are assigned to the skeletal vibration of the 2,5-disubstituted furan rings and the carbonyl stretching vibration of the γ-diketones, respectively. The formation of PFA is also accompanied by a decrease in the peak intensities around 3200-3600 cm^{-1} and at 3120 cm^{-1}, which are respectively assigned to the hydroxy stretching vibration and the in-plane stretching of the hydrogen at the C5 position of the furan ring. Thermal analysis (non-oxidative degradation) showed that the onset of degradation for the nanocomposite sample was significantly increased and the sample had a higher residual weight compared to the neat PFA. This was attributed to the ability of the whiskers to restrict the thermal motion of the matrix polymer.

Very recently, Pranger *et al.* [137] used the same approach to prepare a biobased nanocomposite of PFA and cellulose whiskers. The resinification of the FA was again followed using FTIR spectroscopy. The oxidative and the non-oxidative thermal analyses of the nanocomposite sample and the pure PFA showed similar results to those reported previously [126]. The tensile properties of the nanocomposite sample was determined and compared to those of other PFA based composites reported elsewhere. In general, the incorporation of a small amount of cellulose whiskers (0.75 phr) improved the toughness of the PFA matrix compared to those of previously studied PFA based materials. The modulus of the PFA/CW sample was found to be much lower than the previously reported results, whereas the tensile strength was comparable.

2.8 References

1. A. Bismarck, S. Mishra, T. Lampke. Plant fibres as reinforcement for green composites. In: A.K. Mohanty, M. Misra, L.T. Drzal (Eds.). Natural Fibres, Biopolymers, and Biocomposites. Taylor & Francis Group, Boca Raton, USA (2005) p.1-14.
2. M. Möller, C. Popescu. Natural fibres. In: R. Höfer (Ed.). Sustainable Solutions for Modern Economics. The Royal Society of Chemistry (2009); p.386-387.
3. A.K. Bledzki, J. Gassan. Composites reinforced with cellulose based fibres. Progress in Polymer Science 1999; 24:221-274.
   DOI: 10.1016/S0079-6700(98)00018-5
4. J.M. John, S. Thomas. Biofibres and biocomposites: Review. Carbohydrate Polymers 2008; 71:343-364.
   DOI: 10.1016/j.carbpol.2007.05.040
5. A.K. Mohanty, M. Mishra, G. Hinrichsen. Biofibres, biodegradable polymers, and biocomposites: An overview. Macromolecular Materials and Engineering 2000; 276/277:1-24.
   DOI: 10.1002/(SICI)1439-2054(20000301)276
6. K.G. Satyanarayana, J.L. Guimaraes, F. Wypych. Studies on lignocellulosic fibres of Brazil. Part 1. Source, production, morphology, properties, and applications. Composites: Part A 2007; 38:1694-1709.
   DOI: 10.1016/j.compositesa.2007.02.006
7. R.M. Rowell, J.S. Han, J.S. Rowell. Characterization and factors affecting fiber properties. In: E. Frollini, A.L. Leão, L.H.C. Mattoso (Eds.). Natural Polymers and Agrofibres Composites. USP/UNESP and Embrapa, São Carlos, Brazil (2000); ISBN 85-86463-06-X, p.115-134.
8. J.L. Guimarães, E. Frollini, C.G. da Silva, F. Wypych, K.G. Satyanarayana. Characterization of banana, sugarcane bagasse and sponge gourd fibers of Brazil. Industrial Crops and Products 2009; 30:407-415.
   DOI: 10.1016/j.indcrop.2009.07.013
9. W.G. Glasser. Cellulose and associated heteropolysaccharides. In: B. Fraser-Reid, K. Tatsuta, J. Thiem (Eds.). Glycoscience. Springer-Verlag Berlin Heidelberg (2008); p.1473-1512.

DOI: 10.1007/978-3-540-30429-6_36

10. D. Klemm, B. Heublein, H-P. Fink, A. Bohn. Cellulose: Fascinating biopolymers and sustainable raw material. Angewandte Chemie International Edition 2005; 44:3358-3393.
DOI: 10.1002/anie.200460587

11. N. Reddy, Y. Yang. Biofibers from agricultural byproducts for industrial applications. Trends in Biotechnology 2005; 23:22-27.
DOI: 10.1016/j.tibtech.2004.11.002

12. B. Xiao, X.F. Sun, R.C. Sun. Chemical, structural, and thermal characterizations of alkali-soluble lignins and hemicelluloses, and cellulose from maize stems, rye straw, and rice straw. Polymer Degradation and Stability 2001; 74:307-319.
DOI: 10.1016/S0141-3910(01)00163-x

13. P.S. Mukherjee, K.G. Satyanarayana. Structure and properties of some vegetable fibres: Part 1 Sisal fibre. Journal of Materials Science 1984; 19:3925-3934.
DOI: 10.1007/BF00980755

14. A.G. Kulkarni, K.G. Satyanarayana, P.K. Rohatgi. Mechanical properties of banana fibres (Musa sepientum). Journal of Materials Science 1983; 18:2290-2296.
DOI: 10.1007/BF00541832

15. P.S. Mukherjee, K.G. Satyanarayana. Structure and properties of some vegetable fibres: Part 2 Pineapple fibre (Anannus Comosus). Journal of Materials Science 1986; 21:51-56.
DOI: 10.1007/BF01144698

16. K.G. Satyanarayana, K.K. Ravikumar, K. Sukumaran, P.S. Mukherjee, S.G.K. Pillai, A.G. Kulkarni. Structure and properties of some vegetable fibres: Part 3 Talipot and palmyrah fibres. Journal of Materials Science 1986; 21:57-63.
DOI: 10.1007/BF01144699

17. S.S. Munawar, K. Umemura, S. Kawai. Characterization of the morphological, physical, and chemical properties of seven nonwood plant fibre bundles. Journal of Wood Science 2007; 53:108-113.
DOI: 10.1007/s10086-006-0836-x

18. Y. Li, Y-M. Mai, L. Ye. Sisal fibre and its composites: A review of recent developments. Composites Science and Technology 2000; 60:2037-2055.
DOI: 10.1016/S0266-3538(00)00101-9

19. K.G. Satyanarayana, J.L. Guimarães, F. Wypych. Studies on lignocellulosic fibres of Brazil. Part 1: Source, production, morphology, properties and applications. Composites: Part A 2007; 38:1694-1709.
DOI: 10.1016/j.compositesa.2007.02.006

20. Y. Li, Y-W. Mai, L. Ye. Sisal fibre and its composites: a review of recent developments. Composites Science and Technology 2000; 60:2037-2055.
DOI: 10.1016/S0266-3538(00)00101-9

21. T.H.D. Sydenstricker, S. Mochnaz, S.C. Amico. Pull-out and other evaluations in sisal-reinforced polyester biocomposites. Polymer Testing 2003; 22:375-380.
DOI: 10.1016/s0142-9418(02)00116-2

22. J.D. Megiatto, F.B. Oliveira, D.S. Rosa, C. Gardrat, A. Castellan, E. Frollini. Renewable resources as reinforcement of polymeric matrices: Composites based on phenolic thermosets and chemically modified sisal fibres. Macromolecular Bioscience 2007; 7:1121-1131.
DOI: 10.1002/mabi.200700083

23. J.M.F. Paiva, E. Frollini. Unmodified and modified surface sisal fibres as reinforcement of phenolic and lignophenolic matrices composites: Thermal analyses of fibres and composites. Macromolecular Materials and Engineering 2006; 291:405-417.
DOI: 10.1002/mame.200500334

24. V.R. Bataro, G. Siqueira, J.D. Megiatto, E. Frollini. Sisal fibres treated with NaOH and benzophenonetetracarboxylic dianhydride as reinforcement of phenolic matrix. Journal of Applied Polymer Science 2010; 115:269-276.
DOI: 10.1002/app.31113

25. M.A. Martins, P.K. Kiyohara, I. Joekes. Scanning electron microscopy study of raw and chemically modified sisal fibres. Journal of Applied Polymer Science 2004; 94:2333-2340.
DOI: 10.1002/app.21203

26. M.A. Martins, L.H.C. Mattoso. Short sisal fibre-reinforced tire rubber composites: Dynamic and mechanical properties. Journal of Applied Polymer Science 2004; 91:670-677.
DOI: 10.1002/app.13210

27. P. Gañan, S. Garbizu, R. liano-Ponte, I. Mondragon. Surface modification of sisal fibres: Effect on the mechanical and thermal properties of their epoxy composites. Polymer Composites 2005; 26:121-127.
DOI: 10.1002/pc.20083

28. S. Mishra, A.K. Mohanty, L.T. Drzal, M. Misra, G. Hinrichsen. A review on pineapple leaf fibres, sisal fibres and their biocomposites. Macromolecular Materials and Engineering 2004; 289:955-974.
DOI: 10.1002/mame.200400132

29. N. Chand, S. Sood, D.K. Singh, P.K. Rohatgi. Structural and thermal studies on sisal fibre. Journal of Thermal Analysis 1987; 32:595-599.
DOI: 10.1007/BF01912712

30. J.D. Megiatto, W. Hoareau, C. Gardrat, E. Frollini, A. Castellan. Sisal fibres: Surface chemical modification using reagent obtained from a renewable source; characterization of hemicellulose and lignin as model study. Agricultural and Food Chemistry 2007; 55:8576-8584.
DOI: 10.1021/jf071682d

31. D. Saikia. Investigation on structural characteristics, thermal stability, and hygroscopicity of sisal fibres at elevated temperatures. International Journal of Thermophysics 2008; 29:2215-2225.
DOI: 10.1007/s10765-008-0539-1

32. D. Nwabunma. Overview of Polyolefin Composites. In: D. Nwabunma, T. Kyu (Eds.). Polyolefin Composites. John Wiley & Sons Inc., USA (2008) p.3-8.

33. L.H. Sperling. Introduction to Physical Polymer Science. John Wiley & Sons Inc., (2006) p.757-760.

34. A.J. Peacock. Handbook of Polyethylene: Structures, Properties, and Applications. Marcel Dekker Inc., New York (2000) p.1-6, 43-66.

35. D. Malpass. Introduction to Industrial Polyethylene: Properties, Catalysts, and Processes. John Wiley & Sons Inc., USA (2010) p.1-22.

36. A. Prasad. Polyethylene, low-density. In: J.E. Mark (Ed.). Polymer Data Handbook. Oxford University Press Inc., New York (1999) p.518-519.

37. A. Prasad. Polyethylene, linear low-density. In: J.E. Mark (Ed.). Polymer Data Handbook. Oxford University Press Inc., New York (1999) p.508-516.

38. L. Mandelkern, R.G. Alamo. Polyethylene, linear high-density. In: J.E. Mark (Ed.). Polymer Data Handbook. Oxford University Press Inc., New York (1999) p.493-504.
39. S. Kalia, B.S. Kaith, I. Kaur. Pretreatment of natural fibres and their application as reinforcing material in polymer composites – A review. Polymer Engineering and Science 2009; 49:1253-1272.
DOI: 10.1002/pen.21328
40. M.J. John, R.D. Anandjiwala. Recent developments in chemical modification and characterization of natural fiber-reinforced composites. Polymer Composites 2008; 29:187-207.
DOI: 10.1002/pc.20461
41. X. Li, L.G. Tabil, S. Panigrahi. Chemical treatment of natural fiber for use in natural fiber-reinforced composites: A review. Journal of Polymers and the Environment 2007; 15:25-33.
DOI: 10.1007/s10924-006-0042-3
42. J. George, M.S. Sreekala, S. Thomas. A review on interface modification and characterization of natural fiber reinforced plastic composites. Polymer Engineering and Science 2001; 41:1471-1485.
DOI: 10.1002/pen.10846
43. L.A. Pothan, A.S. Luyt, S. Thomas. Polyolefin/natural fibre composites. In: D. Nwabunma, T. Kyu. Polyolefin Composites. John Wiley & Sons Inc., USA (2008) p.68-81.
44. K. Joseph, S. Thomas, C. Pavithran. Effect of chemical treatment on the tensile properties of short sisal fibre-reinforced polyethylene composites. Polymer 1996; 37:5139-5149.
DOI: 10.1016/0032-3861(96)00144-9
45. M.A. Mokoena, V. Djoković, A.S. Luyt. Composites of linear low density polyethylene and short sisal fibres: The effect of peroxide treatment. Journal of Materials Science 2004; 39:3403-3412.
DOI: 10.1023/B:JMSC.0000026943.47803.0b
46. M.E. Malunka, A.S. Luyt, H. Krump. Preparation of EVA-sisal fibre composites. Journal of Applied Polymer Science 2006; 100:1607-1617.
DOI: 10.1002/app.23650

47. A.S. Luyt, M.E. Malunka. Composites of low-density polyethylene and short sisal fibres: The effect of wax addition and peroxide treatment on thermal properties. Thermochimica Acta 2005; 426:101-107.
DOI: 10.1016/j.tca.2004.07.010

48. J. George, S.S. Bhagawan, S. Thomas. Thermogravimetric and dynamic mechanical thermal analysis of pineapple fibre reinforced polyethylene composites. Journal of Thermal Analysis 1996; 47:1121-1140.
DOI: 10.1007/BF01979452

49. I. Janigová, F. Lednický, Z. Nógellá, B.V. Kokta, I. Chodák. The effect of crosslinking on properties of low-density polyethylene filled with organic filler. Macromolecular Symposia 2001; 169:149-158.
DOI: 10.10026/1521-3900(200105)

50. G. Kalaprasad, B. Francis, S. Thomas, C.R. Kumar, C. Pavithran, G. Groeninckx, S. Thomas. Effect of fibre length and chemical modifications on the tensile properties of intimately mixed short sisal/glass hybrid fibre reinforced low-density polyethylene composites. Polymer International 2004; 53:1624-1638.
DOI: 10.1002/pi.1453

51. M. Mičušík, M. Omastová, Z. Nógellová, P. Fedorko, K. Olejníková, M. Trchová, I. Chodák. Effect of crosslinking on the properties of composites based on LDPE and conducting organic filler. European Polymer Journal 2006; 42:2379-2388.
DOI: 10.1016/j.europolymj.2006.05.024

52. A.R. Martin, F.S. Denes, R.M. Rowell, L.H.C. Mattoso. Mechanical behavior of cold plasma-treated sisal and high-density polyethylene composites. Polymer Composites 2003; 24:464-474.
DOI: 10.1002/pc.10045

53. C.S.R. Freire, A.J.D. Silvestre, C.P. Neto, A. Gandini, L. Martin, I. Mondragon. Composites based on acylated cellulose fibres and low density polyethylene: Effect of the fibre content, degree of substitution and fatty acid chain length on final properties. Composites Science and Technology 2008; 68:3358-3364.
DOI: 10.1016/j.compscitech.2008.09.008

54. A. Viksne, L. Rence, M. Kalnins, A.K. Bledzki. The effect of paraffin on fibre dispersion and mechanical properties of polyolefin-sawdust composites. Journal of Applied Polymer Science 2004; 93:2385-2393.

DOI: 10.1002/app.20664

55. S.L. Fávaro, T.A. Ganzerli, A.G.V. de Carvalho Neto, O.R.R.F. da Silva, E. Radovanovic. Chemical, morphological, and mechanical analysis of sisal fibre-reinforced high-density polyethylene composites. eXPRESS Polymer Letters 2010; 4:465-473.
DOI: 10.3144/expresspolymlett.2010.59

56. S. Mohanty, S.K. Nayak. Interfacial, dynamic mechanical, and thermal fibre reinforced behavior of MAPE treated sisal fibre reinforced HDPE composites. Journal of Applied Polymer Science 2006; 102:3306-3315.
DOI: 10.1002/app.24799

57. S. Mohanty, S.K. Verma, S.K. Nayak. Dynamic mechanical and thermal properties of MAPE treated jute/HDPE composites. Composites Science and Technology 2006; 66:538-547.
DOI: 10.1016/j.compscitech.2005.06.014

58. H-S. Kim, S. Kim, H-J, Kim, H-S, Yang. Thermal properties of bio-flour-filled polyolefin composites with different compatibilizing agent type and content. Thermochimica Acta 2006; 451:181-188.
DOI: 10.1016/j.tca.2006.09.013

59. Y. Lei, Q. Wu, F. Yao, Y. Xu. Preparation and properties of recycled HDPE/natural fiber composites. Composites: Part A 2007; 38:1664-1674.
DOI: 10.1016/j.compositesa.2007.02.001

60. X. Colom, F. Carrasco, P. Pagès, J. Cañavate. Effects of different treatments on the interface of HDPE/lignocellulosic fiber composites. Composites Science and Technology 2003; 63:161-169.
DOI: 10.1016/S0266-3538(02)00248-8

61. A. Bendahou, H. Kaddami, H. Sautereau, M. Raihane, F. Erchiqui, A. Dufresne. Short palm tree fibres polyolefin composites: Effect of filler content and coupling agent on physical properties. Macromolecular Materials and Engineering 2008; 293:140-148.
DOI: 10.1002/mame.200700315

62. K. Joseph, S. Varghese, G. Kalaprasad, S. Thomas, L. Prasannakumari, P. Koshy, C. Pavithran. Influence of interfacial adhesion on the mechanical properties and fracture behavior of short sisal fibre reinforced polymer composites. European Polymer Journal 1996; 32:1243-1250.

DOI: 10.1016/S0014-3057(96)00051-1

63. P.V. Joseph, K. Joseph, S. Thomas. Effects of processing variables on the mechanical properties of sisal-fibre-reinforced polypropylene composites. Composites Science and Technology 1999; 59:1625-1640.
DOI: 10.1016/S0266-3538(99)00024-X

64. A. Choudhury. Isothermal crystallization and mechanical behavior of ionomer treated sisal/HDPE composites. Materials Science and Engineering A 2008; 491:492-500.
DOI: 10.1016/j.msea.2008.03.011

65. Y. Habibi, W.K. El-Zawawy, M.M. Ibrahim, A. Dufresne. Processing and characterization of reinforced polyethylene composites made with lignocellulosic fibres from Egyptian agro-industrial residues. Composites Science and Technology 2008; 68:1877-1885.
DOI: 10.1016/j.compscitech.2008.01.008

66. K. Sever. The improvement of mechanical properties of jute fibre/LDPE composites by fibre surface treatment. Journal of Reinforced Plastics and Composites 2010; 29:1921-1929.
DOI: 10.1177/0731684409339078

67. B. Li, J. He. Investigation of mechanical property, flame retardancy, and thermal degradation of LLDPE-wood-fibre composites. Polymer Degradation and Stability 2004; 83:241-246.
DOI: 10.1016/S0141-3910(03)00268-4

68. C-F. Kuan, H-C. Kuan, C-C.M. Ma, C-M. Huang. Mechanical, thermal, and morphological properties of water-crosslinked wood flour reinforced linear low-density polyethylene composites. Composites: Part A 2006; 37:1696-1707.
DOI: 10.1016/j.compositesa.2005.09.020

69. S-M. Lai, F-C. Yeh, Y. Wang, H-C. Chan, H-F. Shen. Comparative study of maleated polyolefins as compatibilizers for polyethylene/wood flour composites. Journal of Applied Polymer Science 2003; 87(3):487-96.
DOI: 10.1002/app.11419

70. U. Gaur, B. Wunderlich. The glass transition temperature of polyethylene. Macromolecules 1980; 13:445-446.
DOI: 10.1021/ma60074a045

71. C. Vasile, M. Pascu. Practical Guide to Polyethylene. Rapra Technology Ltd, UK (2005) p.41-45.
72. M. Tajvidi, R.H. Falk, J.C. Hermanson, C. Felton. Influence of natural fibres on the phase transitions in high-density polyethylene composites using dynamic mechanical analysis. Seventh International Conference on Wood Fibre-Plastic Composites, Madison, Wisconsin, USA (2003) p.187-195.
73. A.K. Mishra, A.S. Luyt. Effect of sol-gel derived nano-silica and organic peroxide on the thermal and mechanical properties of low-density polyethylene/wood flour composites. Polymer Degradation and Stability 2008; 93:1-8.
DOI: 10.1016/j.polymdegradstab.2007.11.006
74. M. Abdelmouleh, S. Boufi, M.N. Belgacem, A. Dufresne. Short natural-fibre reinforced polyethylene and natural rubber composites: Effect of silane coupling agents and fibres loading. Composites Science and Technology 2007; 67:1627-1639.
DOI: 10.1016/j.compscitech.2006.07.003
75. M. Bengtsson, P. Gatenholm, K. Oksman. The effect of crosslinking on the properties of polyethylene/wood flour composites. Composites Science and Technology 2005; 65:1468-1479.
DOI: 10.1016/j.compscitech.2004.12.050
76. D. Pasquini, E.M. Teixeira, A.A.S. Curvelo, M.N. Belgacem, A. Dufresne. Surface esterification of cellulosic fibres: Processing and characterization of low-density polyethylene/cellulose fibres composites. Composites Science and Technology 2008; 68:193-201.
DOI: 10.1016/j.compscitech.2007.05.009
77. N.P. Cheremisinoff. Polymer Characterization: Laboratory Techniques and Analysis. Noyes Publication, Westwood, New Jeresy, USA (1996) p.17-23.
78. J.R. Araújo, W.R. Waldman, M.A. De Paoli. Thermal properties of high-density polyethylene composites with natural fibres: Coupling agent effect. Polymer Degradation and Stability 2008; 93:1770-1775.
DOI: 10.1016/j.polymdegradstab.2008.07.021
79. M. Tajvidi, A. Takemura. Effect of fibre content and type, compatibilizer, and heating rate on thermogravimetric properties of natural fibre high-density polyethylene composites. Polymer Composites 2009; 30:1226-1233.
DOI: 10.1002/pc.20682

80. H. Quan, Z-M. Li, M-B. Yang, R. Huang. On transcrystallinity in semi-crystalline polymer composites. Composites Science and Technology 2005; 65:999-1021.
DOI: 10.1016/j.compscitech.2004.11.015

81. P.V. Joseph, K. Joseph, S. Thomas, C.K.S. Pillai, V.S. Prasad, G. Groeninckx, M. Sarkissova. The thermal and crystallization studies of short sisal fibre reinforced polypropylene composites. Composites: Part A 2003; 34:253-266.
DOI: 10.1016/S1359-835X(02)00185-9

82. R.R.N. Sailaja. Mechanical and thermal properties of bleached kraft pulp-LDPE composites: Effect of epoxy functionalized compatibilizer. Composites Science and Technology 2006; 66:2039-2048.
DOI: 10.1016/j.compscitech.2006.01.029

83. J.R. Barone. Polyethylene/keratin fibre composites with varying polyethylene crystallinity. Composites: Part A 2005; 36:1518-1524.
DOI: 10.1016/j.compositesa.2005.03.006

84. M. Alexander, P. Dubois. Polymer-layered silicate nanocomposites: Preparation, properties, and uses of a new class of materials. Materials Science and Engineering 2000; 28:1-63.
DOI: 10.1016/S0927-796X(00)00012-7

85. S. Kamel. Nanotechnology and its application in lignocellulosic composites, a mini review. Express Polymer Letters 2007; 1:546-575.
DOI: 10.3144/expresspolymlett.2007.78

86. S.J. Eichhorn, A. Dufresne, M. Aranguren, N.E. Marcovich, J.R. Capadona, S.J. Rowan, C. Weder, W. Thielemans, M. Roman, S. Renneckar, W. Gindl, S. Veigel, J. Keckes, H. Yano, K. Abe, M. Nogi, A.N. Nakagaito, A. Mangalam, J. Simonsen, A.S. Benight, A. Bismarck, L.A. Berglund, T. Peijs. Review: current international research into cellulose nanofibres and nanocomposites. Journal of Materials of Science 2010; 45:1-33.
DOI: 10.1007/s10853-009-3874-0

87. G. Siqueira, J. Bras, A. Dufresne. Cellulose whiskers versus microfibrils: Influence of the nature of the nanoparticle and its surface functionalization on the thermal and mechanical properties of nanocomposites. Biomacromolecules 2009; 10:425-432. DOI: 10.1021/bm801193d

88. I. Siró, D. Plackett. Microfibrillated cellulose and new nanocomposite materials: A review. Cellulose 2010; 17:459-494.
DOI: 10.1007/s10570-010-9405-y

89. M.A.S. Aziz Samir, F. Alloin, A. Dufresne. Review of recent research into cellulosic whiskers, their properties, and their application in nanocomposites field. Biomacromolecules 2005; 6:612-626.
DOI: 10.1021/bm0493685

90. H. Håkansson, P. Ahlgren. Acid hydrolysis of some industrial pulps: Effect of hydrolysis conditions and raw material. Cellulose 2005; 12:177-183.
DOI: 10.1007/s10570-004-1038-6

91. Y. Habibi, L.A. Lucia, O.J. Rojas. Cellulose nanocrystals: Chemistry, self-assembly, and application. Chemical Reviews 2010; 110:3479-3500.
DOI: 10.1021/cr900339w

92. M.M. de Souza Lima, R. Borsali. Rodlike cellulose microcrystals: Structure, properties, and applications. Macromolecular Rapid Communications 2004; 25:771-787.
DOI: 10.1002/marc.200300268

93. S. Beck-Candanedo, M. Roman, D.G. Gray. Effect of reaction conditions on the properties and behavior of wood cellulose nanocrystals suspensions. Biomacromolecules 2005; 6:1048-1054.
DOI: 10.1021/bm049300p

94. I. Kvien, B.S. Tanem, K. Oksman. Characterization of cellulose whiskers and their nanocomposites by atomic force and electron microscopy. Biomacromolecules 2005; 6:3160-3165.
DOI: 10.1021/bm050479t

95. D. Bondeson, A. Mathew, K. Oksman. Optimization of the isolation of nanocrystals from microcrystalline cellulose by acid hydrolysis. Cellulose 2006; 13:171-180.
DOI: 10.1007/s10570-006-9061-4

96. P. Lu, Y-L. Hsieh. Preparation and properties of cellulose nanocrystals: Rods, spheres, and network. Carbohydrate Polymers 2010; 82:329-336.
DOI: 10.1016/j.carbpol.2010.04.073

97. A. Šturcová, G.R. Davies, S.J. Eichhorn. Elastic modulus and stress-transfer properties of tunicate cellulose whiskers. Biomacromolecules 2005; 6:1055-1061.

DOI: 10.1021/bm049291k

98. L. Avérous. Polylactic acid: Synthesis, properties, and applications. In: M.N. Belgacem, A. Gandini (Eds.). Monomers, Polymers and Composites from Renewable Resources. Elsevier Ltd. The Netherlands (2008).p.433-447.

99. A.K. Mohanty, M. Misra, L.T. Drzal, E. Selke, B.R. Harte, G. Hinrichsen. Natural fibres, biopolymers, and biocomposites: An introduction. In: A.K. Mohanty, M. Misra, L.T. Drzal (Eds.). Natural Fibres, Biopolymers, and Biocomposites. Taylor & Francis Group. Boca Raton, USA (2005).p.1-6.

100. D.E. Henton, P. Gruber, J. Lunt, J. Randall. Polylactic acid technology. In: A.K. Mohanty, M. Misra, L.T. Drzal (Eds.). Natural Fibres, Biopolymers, and Biocomposites. Taylor & Francis Group. Boca Raton, USA (2005).p.1-37.

101. S. Inkinen, M. Hakkarainen, A-C. Albertsson, A. Södergård. From lactic acid to poly (lactic acid) (PLA): Characterization and analysis of PLA and its precursors. Biomacromolecules 2011; 12:523-532.
DOI: 10.1021/bm101302t

102. Y. Cheng, S. Deng, P. Chen, R. Ruan. Polylactic acid (PLA) synthesis and modifications: A review. Frontiers of Chemistry in China 2009; 4:259-264.
DOI: 10.1007/s11458-009-0092-x

103. R.M. Rasal. A.V. Janorkar, D.E. Hirt. Poly(lactic acid) modifications. Progress in Polymer Science 2010; 35:338-356.
DOI: 10.1016/j.progpolymsci.2009.12.003

104. L-T. Lim, R. Auras, M. Rubino. Processing technologies for poly(lactic acid). Progress in Polymer Science 2008; 33:820-852.
DOI: 10.1016/j.progpolymsci.2008.05.004

105. W. Amass, A. Amass, B. Tighe. A review of biodegradable polymers: Uses, current developments in the synthesis and characterization of biodegradable polyesters, blends of biodegradable polymers and recent advances in biodegradation studies. Polymer International 1998; 47:89-144.
DOI: 10.1002/(SICI)1097-0126(1998100)

106. K.G. Satyanarayana, G.G.C. Arizaga, F. Wypych. Biodegradable composites based on lignocellulosic fibers – An overview. Progress in Polymer Science 2009; 34:982-1021.
DOI: 10.1016/j.progpolymsci.2008.12.002

107. N.L. Garcia de Rodriguez, W. Thielemans, A. Dufresne. Sisal cellulose whiskers reinforced polyvinyl acetate nanocomposites. Cellulose 2006; 13:261-270.
DOI: 10.1007/s10570-005-9039-7

108. A.J. Uddin, J. Araki, Y. Gotoh. Characterization of the poly(vinyl alcohol)/cellulose whisker gel spun fibers. Composites Part A: Applied Science and Manufacturing 2011; 42:741-747.
DOI: 10.1016/j.compositesa.2011.02.012

109. N. Ljungberg, C. Bonini, F. Bortolussi, C. Boisson, L. Heux, J.Y. Cavaillé. New nanocomposites materials reinforced with cellulose whiskers in atactic polypropylene: Effect of surface and dispersion characteristics. Biomacromolecules 2005; 6:2732-2739.
DOI: 10.1021/bm050222v

110. H. Yuan, Y. Nishiyama, M. Wada, S. Kuga. Surface acylation of cellulose whiskers by drying aqueous emulsion. Biomacromolecules 2006; 7:696-700.
DOI: 10.1021/bm050828j

111. G. Siqueira, J. Bras, A. Dufresne. New process of chemical grafting of cellulose nanoparticles with along chain isocyanate. Langmuir 2010; 26:402-411.
DOI: 10.1021/la9028595

112. L. Petersson, I. Kvien, K. Oksman. Structure and thermal properties of poly(lactic acid)/cellulose whiskers nanocomposite materials. Composites Science and Technology 2007; 67:2535-2544.
DOI: 10.1016/j.compscitech.2006.12.012

113. D. Bondeson, K. Oksman. Polylactic acid/cellulose whiskers nanocomposites modified by polyvinyl alcohol. Composites: Part A 2007; 38:2486-2492.
DOI: 10.1016/j.compositesa.2007.08.001

114. K. Oksman, A.P. Mathew, D. Bondeson, I. Kvien. Manufacturing process of cellulose whiskers/polylactic acid nanocomposites. Composites Science and Technology 2006; 66:2776-2784.
DOI: 10.1016/j.compscitech.2006.03.002

115. J.K. Pandey, C.S. Lee, S-H. Ahn. Preparation and properties of bio-nanoreinforced composites from biodegradable polymer matrix and cellulose whiskers. Journal of Applied Polymer Science 2010; 115:2493-2501.
DOI: 10.1002/app.31205

116. N. Lin, G. Chen, J. Huang, A. Dufresne, P.R. Chang. Effects of polymer-grafted natural nanocrystals on the structure and mechanical properties of poly(lactic acid): A case of cellulose whisker-grafted-polycaprolactone. Journal of Applied Polymer Science 2009; 113:3417-3425.
DOI: 10.1002/app.30308

117. J.K. Pandey, W.S. Chu, C.S. Kim, C.S. Lee, S.H. Ahn. Bio-nano reinforcement of environmentally degradable polymer matrix by cellulose whiskers from grass. Composites: Part B 2009; 40:676-680.
DOI: 10.1016/j.compositesb.2009.04.013

118. J. Yu, F. Ai, A. Dufresne, S. Gao, J. Huang, P.R. Chang. Structure and mechanical properties of poly(lactic acid) filled with (starch nanocrystals)-grafted-poly(ε-caprolactone). Macromolecular Materials and Engineering 2008; 293:763-770.
DOI: 10.1002/mame.200800134

119. A.N. Frone, S. Berlioz, J-F. Chailan, D.M. Panaitescu, D. Donescu. Cellulose fiber-reinforced polylactic acid. Polymer Composites 2011; 32:976-985.
DOI: 10.1002/pc.21116

120. D. Bondeson, K. Oksman. Dispersion and characteristics of surfactant modified cellulose whiskers nanocomposites. Composite Interfaces 2007; 14:617-630.
DOI: 10.1163/156855407782106519

121. N. Lin, G. Chen, J. Huang, A. Dufresne, P.R. Chang. Effects of polymer-grafted natural nanocrystals on the structure and mechanical properties of poly(lactic acid): A case of cellulose whisker-grafted-polycaprolactone. Journal of Applied Polymer Science 2009; 113:3417-3425.
DOI: 10.1002/app.30308

122. R. Auras, B. Harte, S. Selke. An overview of polylactides as packaging materials. Macromolecular Bioscience 2004; 4:835-864.
DOI: 10.1002/mabi.200400043

123. D.Y. Liu, X.W. Yuan, D. Bhattacharyya, A.J. Easteal. Characterization of solution cast cellulose nanofibre-reinforced poly(lactic acid). eXPRESS Polymer Letter 2010; 4(1):26-31.
DOI: 10.3144/expresspolymlett.2010.5

124. A. Alemdar, M. Sain. Isolation and characterization of nanofibres from agricultural residues-wheat straw and soy hull. Bioresource Technology 2008; 99: 1664-1671.

DOI: 10.1016/j.biortech.2007.04.029

125. M. Roman, W.T. Winker. Effect of sulfate groups from sulfuric acid hydrolysis on the thermal degradation behavior of bacterial cellulose. Biomacromolecules 2004; 5:1671-1677.
DOI: 10.1021/bm034519

126. L. Pranger, R. Tannenbaum. Biobased nanocomposites prepared by in situ polymerization of furfuryl alcohol with cellulose whiskers or montmorillonite clay. Macromolecules 2008; 41:8682-8687.
DOI: 10.1021/ma8020213

127. A. Gandini. Polymers from renewable resources: A challenge for the future of macromolecular materials. Macromolecules 2008; 41:9491-9504.
DOI: 10.1021/ma801735u

128. A. Gandini, M.N. Belgacem. Furans in polymer chemistry. Progress in Polymer Science 1997; 22:1203-1379.
DOI: 10.1016/S0079-6700(97)00004-X

129. A. Gandini, M.N. Belgacem. Furan derivatives and furan chemistry at the service of macromolecular materials. In: M.N. Belgacem, A. Gandini (Eds.). Monomers, Polymers and Composites from Renewable Resources. Elsevier Ltd. Amsterdam (2008) p.433-447.

130. S. Bertarione, F. Bonino, F. Cesano, A. Damin, D. Scarano, A. Zecchina. Furfuryl alcohol polymerization in H-Y confined spaces: Reaction mechanism and structure of carbocationic intermediates. Journal of Physical Chemistry B 2008; 112:2580-2589.
DOI: 10.1021/jp0739589q

131. M. Choura, N.M. Belgacem, A. Gandini. Acid-catalyzed polycondensation of furfuryl alcohol: Mechanism of chromophore formation and crosslinking. Macromolecules 1996; 29:3839-3850.
DOI: 10.1021/ma951522f

132. H. Wang, J. Yao. Use of poly(furfuryl alcohol) in fabrication of nanostructured carbons and nanocomposites. Industrial and Engineering Chemistry Research 2006; 45:6393-6404.
DOI: 10.1021/ie0602660

133. A.J.G. Zarbin, R. Bertholdo, M.A.F.C. Oliveira. Preparation, characterization and pyrolysis of poly(furfuryl alcohol)/porous silica glass nanocomposites: Novel route to carbon template. Carbon 2002; 40:2413-2422.
DOI: 10.1016/S0008-6223(02)00130-6

134. J.D. Megiatto, W. Hoareau, C. Gardrat, E. Frollini, A. Castellan. Sisal fibres: Surfaces chemical modification using reagent obtained from a renewable source; characterization of hemicellulose and lignin as model study. Journal of Agricultural and Food Chemistry 2007; 55:8576-3584.
DOI: 10.1021/jf071682

135. G. Toriz, R. Arvidsson, M. Westin, P. Gatenholm. Novel cellulose ester-poly(furfuryl alcohol)-flax fibre biocomposites. Journal of Applied Polymer Science 2003; 88:337-345. DOI: 10.1002/app.1170

136. N. Guigo, A. Mija, L. Vincent, N. Sbirrazzuoli. Eco-friendly composite resins based on renewable biomass resources: Polyfurfuryl alcohol/lignin thermosets. European Polymer Journal 2010; 46:1016-1023.
DOI: 10.1016/j.eurpolymj.2010.02.010

137. L. Pranger, G.A. Nunnery, R. Tannenbaum. Mechanism of the nanoparticle-catalyzed polymerization of furfuryl alcohol and the thermal and mechanical properties of the resulting nanocomposites. Composites: Part B (In press).
DOI: 10.1016/j.compositesb.2011.08.010

Chapter 3

Effects of organic peroxide and polymer chain structure on morphology and thermal properties of sisal fibre reinforced polyethylene composites

Abstract

The effect of polymer chain structure, addition of dicumyl peroxide (DCP) to initiate grafting onto the fibre, and different fibre loadings on the morphology and thermal properties of polyethylene/sisal fibre composites was investigated. The gel content results suggest both crosslinking between the polyethylene chains and grafting onto the sisal fibres. There were significant differences in gel contents between the composites because of the differences in the polyethylene molecular structures. The SEM micrographs of the samples show clear evidence of grafting, particularly in the case of the LDPE and LLDPE composites. The presence of the sisal fibres gave rise to thermally less stable composites compared to the neat matrices, whereas marginal differences in stability were observed between the untreated and peroxide treated composites. The DSC results show interesting trends in terms of the influence of fibre content and dicumyl peroxide treatment on the crystallization behaviour of the composites.

Keywords: Polyethylenes; sisal fibre; composites; crosslinking; grafting; morphology; thermal properties

3.1 Introduction

In recent years, increasing worldwide environmental awareness together with a decline of petroleum resources have incited material scientists and engineers to look for alternative materials that are more sustainable, renewable, low cost, and environmentally friendly. Therefore, over the past decade, natural fibres as reinforcing materials in polymer matrix composites have received increasing attention as potential candidates to substitute the synthetic reinforcing materials (e.g. glass fibres) because of their unique properties [1-8]. Compared to synthetic reinforcing materials, natural fibres have many advantages such as

low density and cost, wide availability, low energy consumption, biodegradability, recyclability and renewability [1-3,9]. Among the various natural fibres, sisal fibre is of particular interest. It is a hard fibre extracted from the leaves of the sisal plant (*Agava sisalana*), and it has a short renewal time, wide availability, ease of cultivation and low cost, associated with excellent physical and mechanical characteristics [2,6].

Polyethylenes (PEs) offer many characteristics, which make them one of the most widely used synthetic polymers as matrix materials for fibre composites. They have excellent value (cost and performance), chemical inertness, good electrical resistance, relatively modest physical properties, ease of processing, recyclability, and adequate mechanical properties. In addition, their properties can be improved *via* blending and composite technologies. There are three major classes of PEs, high-density PE (HDPE), low-density PE (LDPE), and linear low-density PE (LLDPE). The basic difference between these three types of PEs lies in the degree and regularity of branching. While HDPE has very few branches, LDPE is characterized by significant branching with long, irregular branches at irregular intervals. LLDPE, on the other hand, is characterized by short branches of regular length at regular intervals. The presence of chain branches decreases the size of the linear, crystallizable-sequence in the backbone (i.e. lamellar thickness) thus modifying the morphology and the degree of crystallinity. The physical and the mechanical properties of polyethylenes and other polymers depend on their molecular characteristics as well as on ordered structures such as crystalline thickness, crystallinity, spherulite size, morphology, and degree of orientation [10-14].

Despite the promise of natural fibres as alternative reinforcing materials, there are still some drawbacks. Besides their high moisture absorption, low microbial resistance, relatively high variability in diameter and length, and low thermal stability, natural fibres are incompatible with hydrophobic polymers due to their polar and hydrophilic nature. This incompatibility leads to weak interfacial adhesion as well as to non-uniform dispersion within the matrix during compounding. Because of this weak interface, a decrease in the mechanical properties with the incorporation of natural fibres is one of the inherent problems [2,3,5]. To overcome this, several strategies have been tested to enhance the adhesion between the lignocellulosic fillers and the polymer matrices. These strategies generally involve modifications of the fibre and/or the matrix by physical or chemical methods. Chemical modifications such as

acetylation, mercerization, cyanoethylation, peroxide treatments, graft copolymerization (methylmethacrylate, acrylamide, and acrylonitrile) as well as various coupling agents (silane, isocyanate and titanate based compounds), have been studied and reviewed by many researchers [4,7,15,16]. Among all these treatments, organic peroxides have shown a better compatibilization effect in polyethylene based natural fibre and wood composites associated with easy processability [17-23]. Organic peroxides are most commonly used to initiate crosslinking of polymer chains *via* thermal decomposition into radicals that abstract hydrogen atoms from the surrounding polymer chains, thus forming macroradicals. Crosslinks are then formed through a radical combination of these macroradicals. In addition, organic peroxides are frequently used to initiate grafting reactions such as grafting of short chain molecules to polymer backbones [24,25]. Luyt and co-workers [18,19], have reported that the presence of DCP have led to grafting of EVA and LLDPE chains onto sisal fibres. Other studies have also suggested grafting between the polymer matrices and cellulosic fibres, which resulted in enhanced properties of the composites after addition of DCP [17,22]. Joseph *et al* [17] suggested an expected mechanism of the peroxide initiated radical reaction between the polymer (LDPE) matrix and cellulosic sisal fibres. It was generally concluded that organic peroxides are very effective as compatibilizers by generating better interfacial adhesion.

We could not find, in the available literature, a detailed study that proved the grafting between PE chains and cellulosic fibres, and that reported on the influence of PE structure and crystallinity on the efficiency of such grafting processes. Here we report and discuss results where dicumyl peroxide was used to improve the interfacial adhesion between sisal fibres and polyethylenes with different structures and morphologies (LDPE, LLDPE, and HDPE). The influence of the presence of different amounts of sisal fibre, as well as dicumyl peroxide initiated crosslinking/grafting, on the morphology and thermal properties were investigated and the results are reported and explained.

3.2 Experimental

3.2.1 Materials

Sisal fibre was obtained from the National Sisal Marketing Committee in Pietermaritzburg, South Africa. LDPE and LLDPE were supplied in pellet form by Sasol Polymers,

Johannesburg, South Africa, and HDPE was supplied by Safripol Ltd, Sasolburg, South Africa. They have the following specifications:
LDPE: MFI = 2 g/10 min at 190 ºC / 2.16 kg, density = 0.922 g cm^{-3}, M_n = 30302 g mol^{-1}, M_w = 206797 g mol^{-1};
LLDPE: MFI = 1 g / 10 min at 190 ºC / 2.16 kg, density = 0.924 g cm^{-3}, M_n = 68409 g mol^{-1}, M_w = 290056 g mol^{-1};
HDPE: MFI = 2 g / 10 min at 190 ºC / 5 kg, density = 0.956 g cm^{-3}, M_n = 27575 g mol^{-1}, M_w = 539389 g mol^{-1};

Dicumyl peroxide (bis(α,α-dimethylbenzyl)peroxide) was supplied by Merck, South Africa. It has a minimum assay of 98%. Petroleum ether was also supplied by Merck. Xylene (boiling point of 139.3 ºC) was supplied by Minema.

3.2.2 Treatments of sisal fibres

The sisal fibres were cut into an average length of between 5 and 10 mm, soaked in distilled water for 24 h to remove any surface impurities, filtered and washed thoroughly with distilled water before being allowed to dry in an oven at 80 ºC for 48 h. The dried fibres were washed with petroleum ether for 5 h at 50 ºC to remove waxy materials and natural oils, followed by oven drying at 80 ºC.

3.2.3 Preparation of polyethylene composites

The polyethylene-sisal fibre composites were prepared *via* melt mixing in a 55 mL mixing chamber of a Plastograph-W50EHT (Brabender®OHG, Germany) at 150 ºC, 30 rpm and 10 min. DCP treated samples were prepared by addition of 1 phr DCP to the mixture one minute before the end of the mixing. The melt pressing of the prepared samples was performed at 175 ºC and 50 bar for 10 min. Table 3.1 shows the compositions of the PE composite samples used in this study.

Table 3.1 Compositions of the PEs composite samples used in this study

LDPE/sisal/DCP (w/w)	LLDPE/sisal/DCP (w/w)	HDPE/sisal/DCP (w/w)
100/0/0	100/0/0	100/0/0
100/0/1	100/0/1	100/0/1
90/10/0	90/10/0	90/10/0
80/20/0	80/20/0	80/20/0
70/30/0	70/30/0	70/30/0
90/10/1	90/10/1	90/10/1
80/20/1	80/20/1	80/20/1
70/30/1	70/30/1	70/30/1

3.2.4 Characterization methods

FTIR transmittance spectra of the neat and the DCP treated polyethylenes were obtained using a Perkin Elmer Multiscope FT-IR microscope attached to a Perkin Elmer Spectrum 100 FTIR spectrometer. Thin films from the samples were obtained by using a microtome and then analyzed over a range of 600-4000 cm^{-1} with a resolution of 4 cm^{-1}. All spectra were averaged over 32 scans.

The gel contents of the DCP treated samples were determined *via* p-xylene extraction. The samples to be analyzed were cut into small pieces (the shapes and sizes of the pieces were the same for all the samples) and wrapped in 120-mesh stainless steel cloth cages, which were previously weighed. The cages with the samples were weighed again before immersion in a round-bottom flask containing p-xylene. The extraction was done in boiling p-xylene (140 ºC) under reflux for 24 h and the solvent was changed every 6 h. Extracted samples were then dried at 100 ºC until a constant weight was attained. The gel content of the different samples was determined as the average of three separate analyses and calculated according to Equation 1.

$$\% \text{ Extract} = (\text{mass loss during extraction}) / (\text{original sample mass} - \text{fibre mass})$$
$$\% \text{ Gel content} = 100 - \% \text{ Extract} \quad (1)$$

SEM was used to investigate both the morphology of the composite samples as well as the interface between the fibre and the polymer matrix through a Shimadzu SSX-550 Super-Scan scanning electron microscope. The samples were frozen under liquid nitrogen, fractured, mounted, sputter-coated with gold, and allowed to dry. The dried samples were viewed using an accelerating voltage of 10 kV. SEM micrographs were also taken for the samples that were extracted by xylene in the determination of the gel contents to examine their morphologies after the extraction process.

A polarized optical microscope (CETI-Topic B, Belgium) was used to examine the dispersion of the fibres within the polymer matrices as well as the morphologies of the composite samples. The micrographs of the untreated and the DCP treated polyethylene composites were taken at 4x (SP 4x/0.10/160/-) magnification.

Thermogravimetric analysis was used to study the thermal stabilities of the composite samples in a Perkin Elmer TGA7 thermogravimetric analyzer. Samples with weights in the range of 5 to 10 mg were heated under a flowing nitrogen atmosphere (20 mL min^{-1}) from 30 to 700 ºC at a heating rate of 10 ºC min^{-1}, and the corresponding mass loss was recorded.

DSC analyses were performed in a Perkin Elmer DSC7 differential scanning calorimeter. Each sample of 5 to 10 mg weight was sealed in an aluminum pan and heated under nitrogen flow (20 mL min^{-1}) from 30 to 170 ºC at a heating rate of 10 ºC min^{-1}, kept at this temperature for 1 min to erase the thermal history, and cooled and re-heated under the same conditions. At least three individual measurements were made to ensure reproducibility. The melting and the crystallization temperatures as well as the melting and crystallization enthalpies of the samples were determined from the cooling and re-heating runs as the average of three separate measurements. The degree of crystallinity (χ_c) of the samples was calculated according to the following Equation 2.

$$\% \text{ Crystallinity} = \Delta H_m / (\Delta H^o_m \times w) \qquad (2)$$

where $\Delta H^o_m = 288.8$ J g^{-1} is the heat of fusion for 100% crystalline polyethylene [16], ΔH_m (J g^{-1}) is the enthalpy of fusion, and (w) is the weight fraction of the polymer matrix material in the composites. The calculated melting enthalpies (ΔH_m^{calc} (J g^{-1})) were determined from the

observed melting enthalpies of the neat polymers, and the weight fractions of the polymers in the composites, according to Equation 3.

$$\Delta H_m^{calc} = w_{PE} \times \Delta H_m^{obs}(\text{neat PE}) \quad (3)$$

3.3 Results and discussion

FTIR microspectroscopy measurements were performed to examine the differences in the absorption peak for the vinyl groups before and after treatment with DCP. Although other unsaturated functional groups such as vinylidene and trans-vinylene are also present in the polyethylenes, only the vinyl groups (909 cm^{-1} and 990 cm^{-1}) were reported to be more reactive towards grafting and crosslinking reactions [26,27]. Figures 3.1 and 3.2 show the FTIR spectra of the neat and the crosslinked polyethylenes in the range of 1000 cm^{-1} to 880 cm^{-1}.

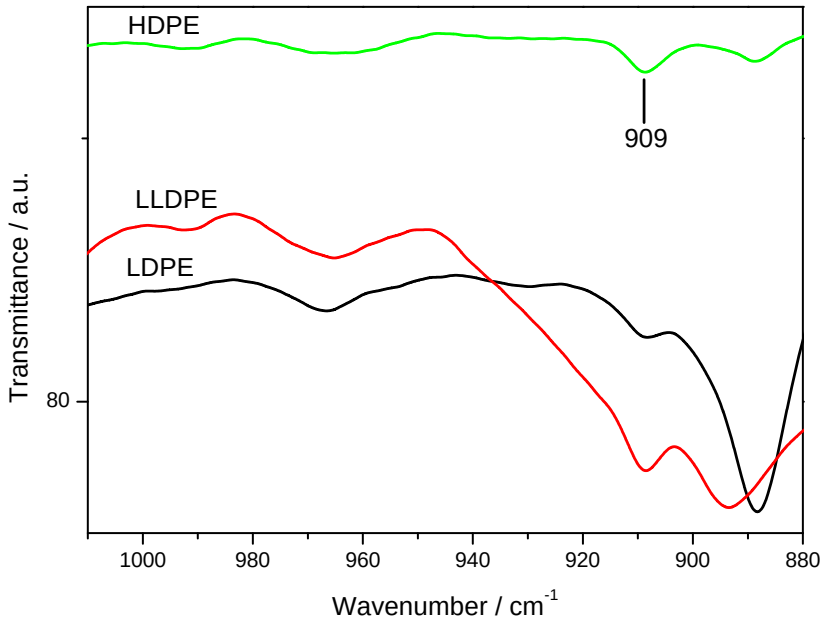

Figure 3.1 FTIR transmittance spectra of the neat polyethylenes

The absorption intensity of the vinyl groups in the case of LLDPE is higher than those of LDPE and HDPE, which indicates a higher content of vinyl groups in LLDPE. After addition of 1 phr DCP, the FTIR spectra in Figure 3.2 show that the absorption peak of the vinyl groups almost completely disappeared in the case of LLDPE, whereas it was reduced in the

case of LDPE and almost unchanged in the case of HDPE. These differences between the reduction in the number of vinyl groups for LLDPE and LDPE/HDPE could be due to the initial higher concentration of the vinyl groups in LLDPE, as well as to the presence of more tertiary carbon atoms (effect of branching), both of which are more prone to crosslinking/grafting. However, other structural parameters such as the number average molecular weight, the molecular weight distribution, and the number of chain branches as well as their length are also important in the ability of polyethylenes to effectively crosslink/graft.

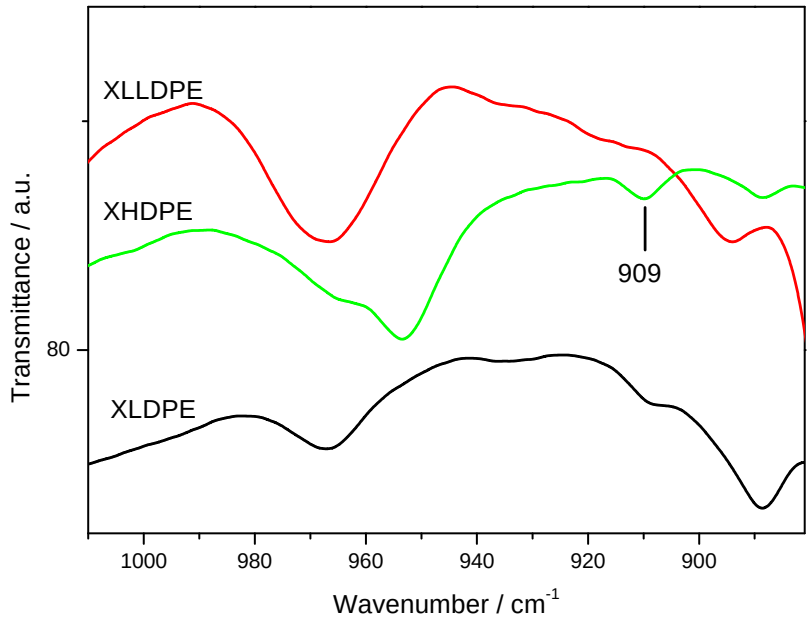

Figure 3.2 FTIR transmittance spectra of the DCP treated polyethylenes (XPEs)

Figure 3.3 shows the variation of gel contents with sisal fibre contents in the DCP treated composites. It is clear that the gel contents of the different polyethylene samples differ considerably. For the LDPE samples, there was a significant increase in gel content with increasing sisal fibre content compared to the neat polymer, whereas for the LLDPE samples the gel content remained very high, but almost unchanged with increasing fibre content. The gel content for the HDPE samples increased first for 10 wt % fibre loading and thereafter decreased with increasing fibre content, so that for the 30 wt % sisal fibre content the value approximately equaled that of the neat polymer. Differences in a number of different

molecular characteristics of these polymers could have contributed to the observed differences in crosslinking/grafting.

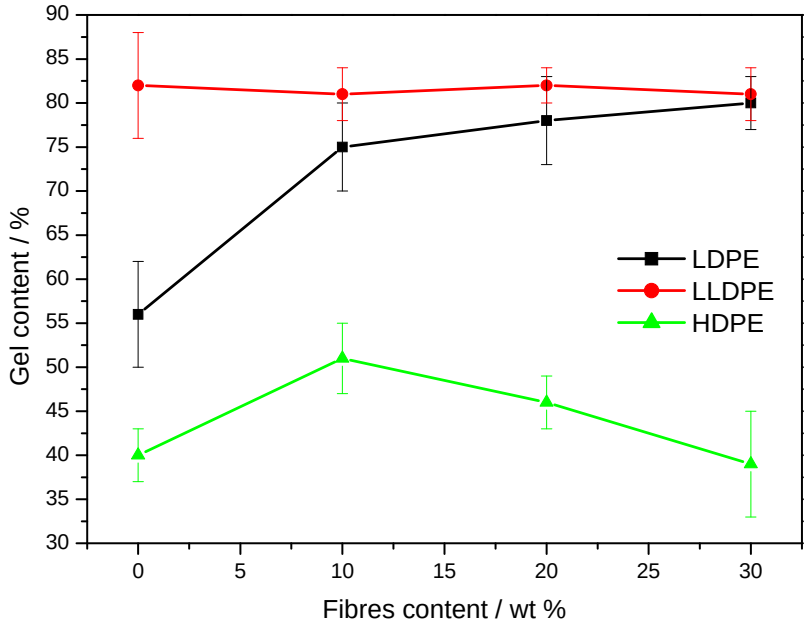

Figure 3.3 Gel content of the DCP treated polyethylenes and their composites samples

A number of authors [26-30] found that the molecular weight, the presence and content of vinyl groups, as well as the branching content and branching length have an influence on the effectiveness of polyethylene crosslinking/grafting. According to them crosslinking/ grafting should be most effective in PEs with higher molecular weights, higher contents of vinyl groups and more short to medium branches. This explains the very high gel content of LLDPE compared to those of the other two PEs. It is interesting that the gel content for LLDPE does not change with increasing fibre content, and we assume that at low fibre contents there is more crosslinking between the polymer chains, but as the fibre content increases, there is more grafting of the polymer chains onto the fibre. This is confirmed by the SEM results discussed below.

Pure LDPE shows a relatively low gel content compared to LLDPE. The reason is probably its much lower number-average molecular weight and the smaller number and much longer branches. In this case one would expect a fair amount of intramolecular crosslinking [28,30].

However, in the presence of sisal fibre and with increasing fibre content, grafting of the LDPE chains onto the fibre will preferably occur which would decrease the extent of intramolecular crosslinking. The grafting of LDPE onto the fibre has been confirmed by SEM as discussed further on. Therefore a significant increase in the gel content with increasing fibre content is observed for LDPE.

The generally low gel content in HDPE, in the absence and presence of sisal fibre, is probably due to its relatively low number-average molecular weight, its high polydispersity, and the absence of branching. We currently do not have an explanation for the trend observed for HDPE in Figure 3.3, but the SEM results (discussed further on) clearly show the absence of grafting between HDPE and the sisal fibres.

SEM was used to investigate the morphology and the possible interfacial adhesion between the polymers and the fibres in the composites. The SEM micrographs of the untreated and DCP treated composite samples, which contain 30 wt % sisal fibre, are shown in Figure 3.4. Generally, in the case of the composites treated with DCP (Figures 3.4b, 3.4d and 3.4f), strong adhesion between the sisal fibres and the polymer matrices is clearly observed. No fibre pullout can be seen, and the fibres are completely imbedded in the matrix, which indicates good wetting by the polymer. In addition, defibrillation and breakage of the sisal fibres are visible on the fractured surfaces of the composites. This is probably the result of grafting between the polymer chains and the fibre, and is in line with the gel content results. However, the effect of the DCP treatment seems to be less effective in the case of the HDPE composite (Figure 3.4f), which can be seen from the presence of holes, gaps between the fibres and the matrix, and poor wetting of the fibres by the polymer matrix. These results are also in agreement with the gel content results. Similar observations were also reported by other authors where peroxide treatments have resulted in better and improved interfacial adhesion between the polymer matrix and the cellulosic fibres [17-19,22].

In contrast, all the untreated composite samples (Figures 3.4a, 3.4c and 3.4e) show that the fibres appear to be free of any matrix interactions, and cracks, voids, and fibre pullouts are very obvious. In the case of HDPE (Figure 3.4e) the absence of any physical contact between the fibres and the polymer matrix is so obvious that the fibres were completely separated from the polymer with clean surfaces [18,31,32]. Although all the composites were prepared

under the same conditions, the ability of the polymer to wet the fibres seems to depend strongly on the polymer morphology. The LDPE and LLDPE, that are more branched and amorphous than HDPE, seem to penetrate the pores in the fibre structure and, as a result, adhere better to the surfaces of the fibres than HDPE, probably because of the chain folding and crystal growth that gives rise to HDPE's higher crystallinity.

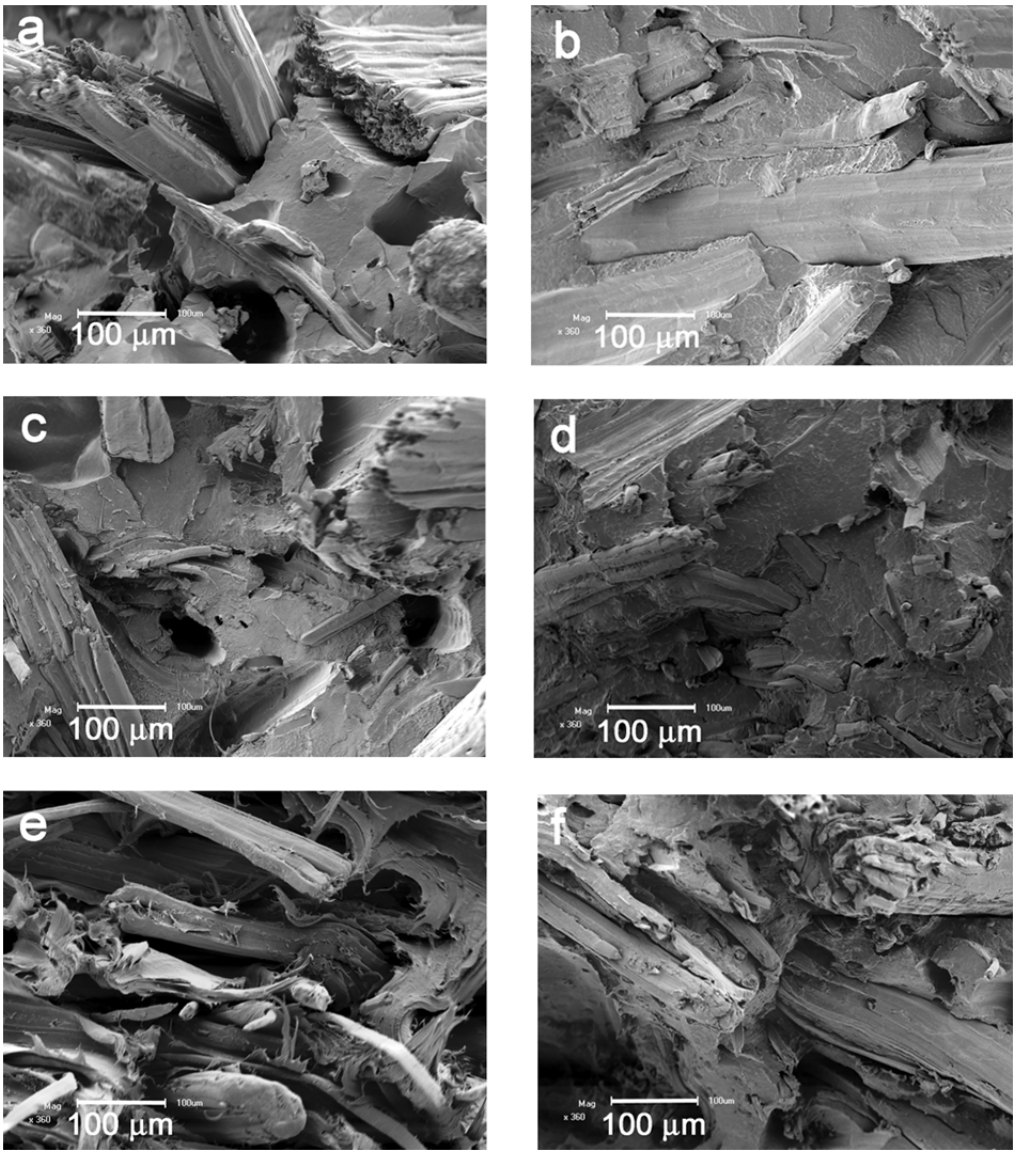

Figure 3.4 SEM micrographs of the cryofractured surfaces of polyethylene composites reinforced with 30 wt % sisal fibre (LDPE/sisal, (a) untreated and (b) treated; LLDPE/sisal, (c) untreated and (d) treated; HDPE/sisal, (e) untreated and (f) treated)

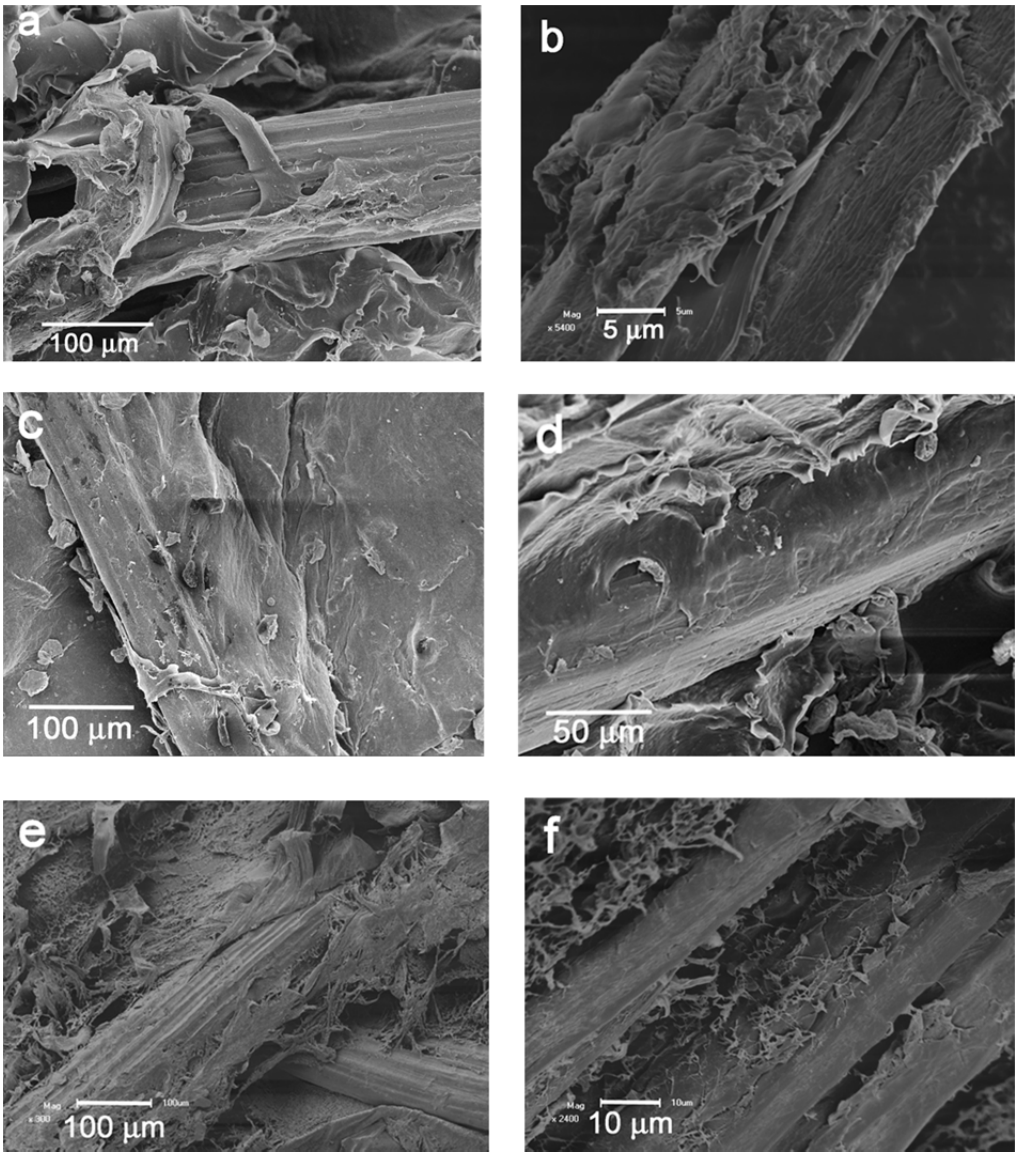

Figure 3.5 SEM micrographs of xylene-extracted polyethylene composites reinforced with 20 wt % sisal fibre (treated LDPE/sisal at magnifications of (a) 300x and (b) 5400x; treated LLDPE/sisal at magnifications of (c) 300x and (d) 540x; treated HDPE/sisal at magnifications of (e) 300x and (f) 2400x)

SEM micrographs were also taken of the samples that were exposed to xylene extraction in the determination of the gel content, in order to further examine the adhesion between the fibres and the polymer matrices. As can be seen from the SEM micrographs in Figure 3.5, thin layers of the polymers covering the surfaces of the fibres are visible for the LLDPE and LDPE samples (Figures 3.5a to 3.5d). These polymers could not be extracted because of chemical bonding between the fibres and the polymer matrices, which is due to the grafting of the polymer chains onto the fibre surfaces after DCP initiation. However, the SEM

micrographs of the HDPE sample (Figures 3.5e and 3.5f) do not show any evidence of polymer attached to the fibre surfaces. This confirms that the HDPE chains probably did not graft onto the fibre surfaces as was observed for LDPE and LLDPE.

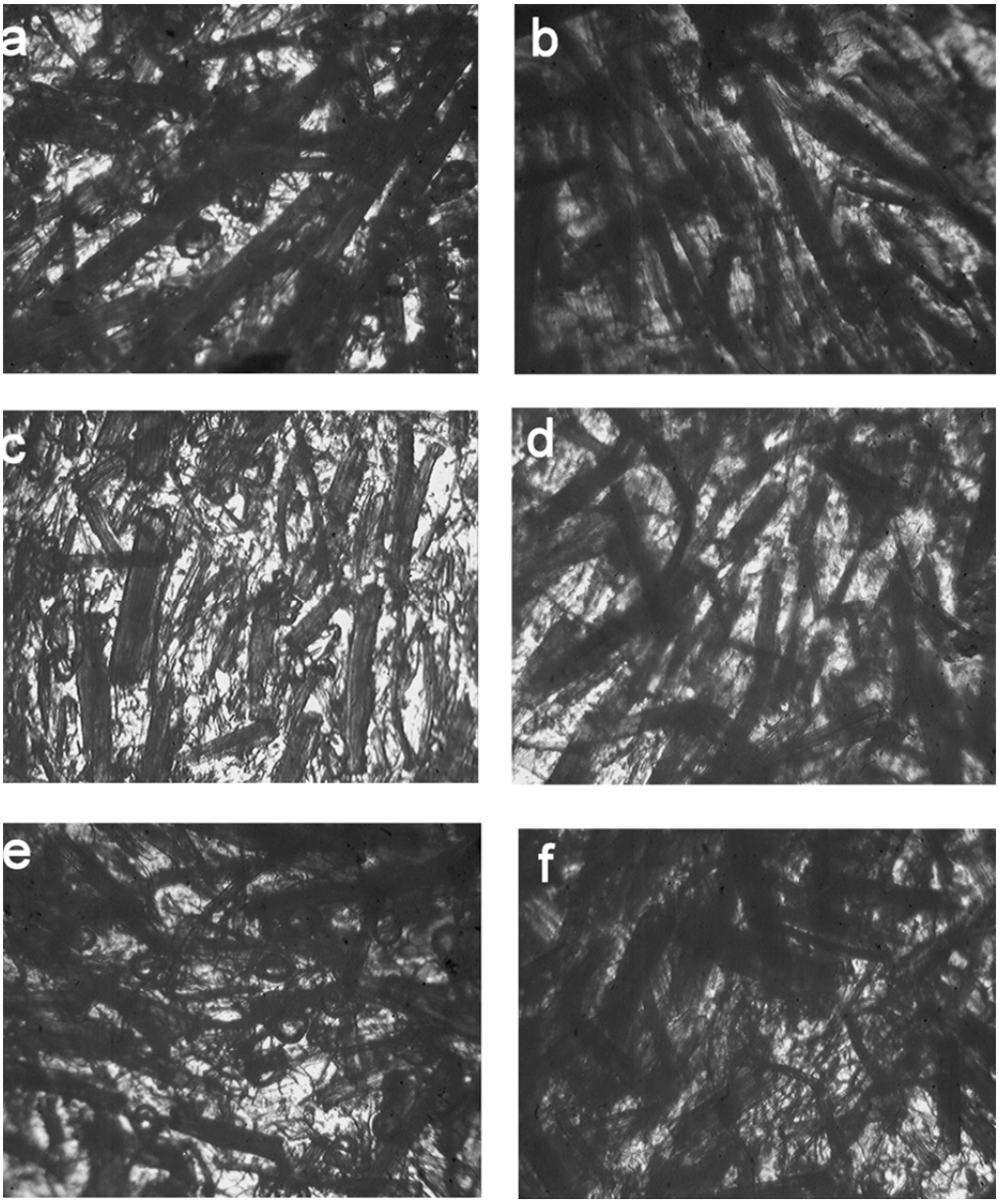

Figure 3.6 POM pictures (4x magnification) of microtomed thin films of polyethylene composites reinforced with 30 wt % sisal fibre (LDPE/sisal, (a) untreated and (b) treated; LLDPE/sisal, (c) untreated and (d) treated; HDPE/sisal, (e) untreated and (f) treated)

Polarized optical microscopy (POM) was used to inspect both the morphologies as well as the dispersion of the fibres within the polymer matrices. Figure 3.6 shows the POM micrographs of the treated and untreated samples. In general, the images show a good dispersion of sisal fibres within the polymer matrices for all the composite samples, with few agglomerations. This shows that the conditions of the composite preparation were good.

Figures 3.7 to 3.9 show the TGA curves of sisal fibre, the neat polyethylenes, the DCP treated polyethylenes and the DCP modified and unmodified composites as a function of temperature.

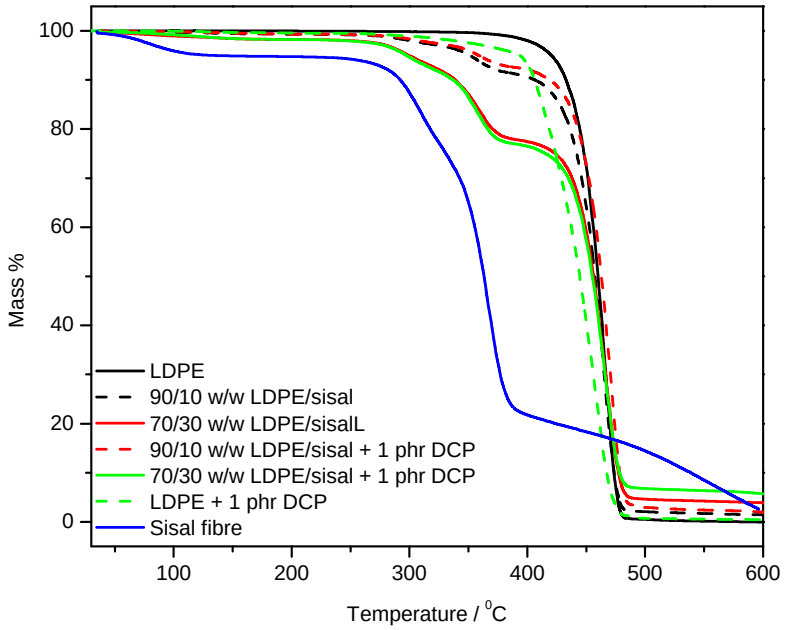

Figure 3.7 TGA curves of sisal fibre, LDPE, DCP treated LDPE, as well as untreated and DCP treated composites

All the reported temperature values are the decomposition peak temperatures obtained from the derivative TGA curves. In the case of sisal fibre, the TGA curve shows several decomposition steps. The first step around 80 °C is due to the evaporation of sorbed water from the fibre, while the step around 300 °C corresponds to the thermal decomposition of hemicellulose and the glycosidic links of cellulose. The step around 360 °C is the result of the thermal decomposition of α-cellulose [33-35]. The neat LDPE shows only one decomposition step around 466 °C, whereas DCP treated LDPE has a lower thermal stability with the

decomposition temperature shifting to 460 °C. This could be due to some thermal degradation of the LDPE chains induced by the DCP during processing, since crosslinking introduces tertiary carbon atoms in the polymer, which are more susceptible to thermal degradation [36]. For the unmodified and DCP modified composites no significant differences in thermal stability could be seen, and the mass loss after the first decomposition step corresponds well with the amount of fibre initially mixed into the samples. Contrary to the case of neat LDPE where the degradation moved to lower temperatures, the degradation temperature range of LDPE in the treated and untreated composites remained the same. This indicates that the DCP more probably initiated grafting between the polymer and the fibre, which reduced the number of tertiary carbon atoms in the polymer and its subsequent degradation.

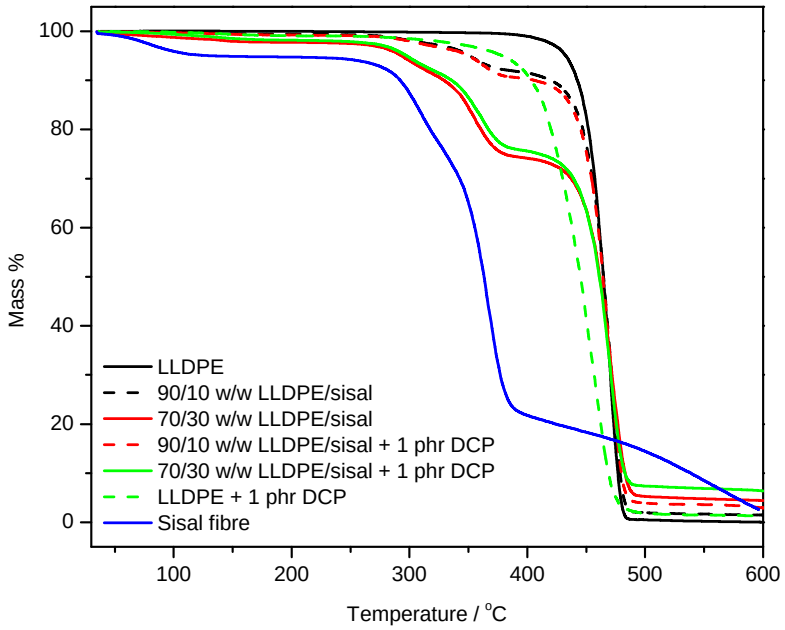

Figure 3.8 TGA curves of sisal fibre, LLDPE, DCP treated LLDPE, as well as untreated and DCP treated composites

In the case of pure LLDPE and DCP treated LLDPE (Figure 3.8), the thermal degradation also occurs in a single step, and the DCP treated LLDPE also shows a lower thermal stability. The reason for this is probably the same as in the case of LDPE. As in the case of LDPE, the DCP treatment did not influence the degradation behaviour of the composites at all the investigated fibre contents, and there is a good correlation between the mass loss after the

first degradation step and the amount of fibre initially mixed into the composite. This is also an indication of a fairly good fibre dispersion in the composites. As in the case of LDPE, the degradation temperature range of LLDPE was the same in the DCP treated and untreated composites, and the explanation is probably the same.

As was observed for LDPE and LLDPE, the DCP treated HDPE was also thermally less stable than the neat HDPE (Figure 3.9). In this case, however, the thermal stability of HDPE in the modified composites is lower than in their unmodified counterparts. The most probable explanation for this is that the DCP in this case did not initiate grafting between the polymer and the fibre, but rather degradation of the polymer chains, also because of the much lower extent of crosslinking in HDPE.

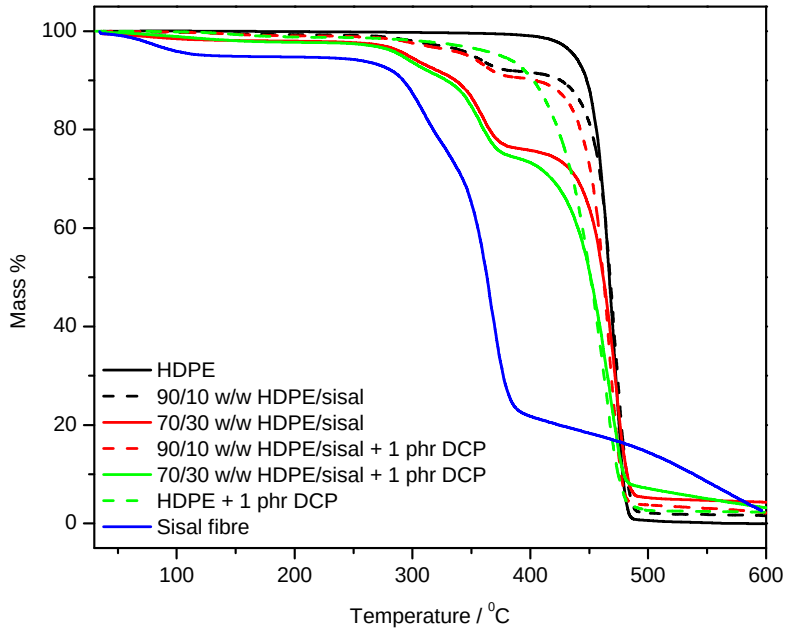

Figure 3.9 TGA curves of sisal fibre, HDPE, DCP treated HDPE, as well as untreated and DCP treated composites

DSC measurements were performed to characterize the thermal behaviour of neat and DCP treated polyethylenes, and their DCP modified and unmodified sisal composites. Tables 3.2 to 3.4 show the melting peak temperatures (T_m) and the melting enthalpies (ΔH_m), that were determined from the DSC curves, as well as the calculated melting enthalpies and degree of crystallinity (χ). Table 3.2 summarizes the thermal behaviour of LDPE and its sisal composites. The T_m values of LDPE in all the unmodified samples are the same (about 110

°C) regardless of the fibre content. This indicates that the size of the crystalline domains, which is directly related to T_m, is retained in the matrix. The melting enthalpy (ΔH_m), however, decreased with increasing fibre loading, as expected, due to the decrease in polymer matrix quantity. The degree of crystallinity, calculated from the respective melting enthalpies, remained fairly constant with increasing fibre content in the absence of DCP. This can also be seen in the fairly good correlation between the experimentally observed and calculated melting enthalpies. This indicates that the fibres had little influence on the crystallization behaviour of LDPE. In the case of the DCP treated LDPE the DSC melting peak is less intense and broader than that of pure LDPE, although the melting temperature and melting enthalpy, as well as the degree of crystallinity, are very similar to those of pure LDPE. It seems as if the DCP initiated crosslinking did not change the extent of crystallization, but certainly had an influence on crystal size and perfection. This may have been the result of intramolecular crosslinking, as mentioned previously. On the other hand, the DCP treated composites showed lower melting temperatures compared to the neat LDPE, the DCP treated LDPE, and the untreated samples, while the degree of crystallinity did not change significantly (Table 3.2). This indicates smaller sizes of the crystallites and thinner lamella, which could be due to the DCP initiated grafting of the polymer chains onto the sisal fibres. This grafting interaction obviously restricted the lamellar growth process.

The melting temperature of LLDPE slightly increased with increasing fibre content for the unmodified composites, but the temperature increase is not significant enough to relate it to specific morphological changes in the samples (Table 3.3) [18]. The degree of crystallinity also did not change appreciably with increasing fibre content, which is in line with the good correlation between the experimentally observed and calculated enthalpy values. It is therefore clear that the presence of fibre alone did not significantly influence the LLDPE crystallization process. For the DCP treated samples, both the melting temperature and the degree of crystallinity decreased with an increase in fibre loading, which means that both the sizes and amounts of the crystallites decreased [18]. As already mentioned in the above discussion, LLDPE (because of the larger number of short chain branches) showed a much larger extent of grafting to the sisal fibre, which would strongly impede the chain mobility and reduce the crystallization ability of the chains.

Table 3.2 Melting characteristics of LDPE composites: melting temperature (T_m), observed melting enthalpy (ΔH_m^{obs}), calculated melting enthalpy (ΔH_m^{calc}), and degree of crystallinity (χ_c)

LDPE/sisal (w/w)	T_m (°C)	ΔH_m^{obs} (J g^{-1})	ΔH_m^{calc} (J g^{-1})	χ_c (%)
Untreated LDPE composites				
100/0	110.6 ± 0.2	55.6 ± 1.2	55.6	19.3
90/10	110.6 ± 0.8	46.1 ± 2.2	50.0	17.7
80/20	110.9 ± 0.2	42.9 ± 2.1	44.5	18.6
70/30	110.7 ± 0.2	36.3 ± 2.9	38.9	18.0
DCP treated LDPE composites				
100/0	108.6 ± 2.0	56.0 ± 2.0	56.0	19.4
90/10	107.0 ± 0.2	44.7 ± 2.7	50.0	17.4
80/20	106.9 ± 0.7	43.3 ± 0.6	44.8	18.7
70/30	106.3 ± 0.4	35.4 ± 2.3	39.0	17.5

Table 3.3 Melting characteristics of LLDPE composites: melting temperature (T_m), observed melting enthalpy (ΔH_m^{obs}), calculated melting enthalpy (ΔH_m^{calc}), and degree of crystallinity (χ_c)

LLDPE/sisal (w/w)	T_m (°C)	ΔH_m^{obs} (J g^{-1})	ΔH_m^{calc} (J g^{-1})	χ_c (%)
Untreated LLDPE composites				
100/0	124.7 ± 0.2	58.5 ± 0.6	58.5	20.3
90/10	125.6 ± 0.2	52.1 ± 2.6	52.7	20.0
80/20	125.0 ± 0.8	46.6 ± 1.2	46.8	20.2
70/30	126.6 ± 0.4	43.2 ± 1.3	41.0	21.4
DCP treated LLDPE composites				
100/0	119.0 ± 1.7	60.9 ± 1.0	60.9	21.0
90/10	121.0 ± 0.4	46.2 ± 2.3	54.8	17.8
80/20	116.8 ± 0.6	39.2 ± 0.9	48.7	17.0
70/30	114.4 ± 0.7	32.2 ± 1.3	42.6	15.9

In the case of the DCP treated HDPE, it can be seen that the intensity of the melting peak decreased significantly and it broadened compared to that of neat HDPE (Table 3.4). However, the melting temperature remained almost unchanged, whereas the crystallinity decreased significantly, which could be attributed to a decrease in the amount of crystallites by the effect of crosslinking [37,38]. Because HDPE has such a high crystallinity, any degree of crosslinking will have a much stronger influence on the crystallizability of the uncrosslinked parts of the chains. For the untreated composite samples, the melting temperatures and the degree of crystallinity did not change significantly with increasing fibre content, which implies that the presence of the fibre did not influence the crystallization behaviour of HDPE. Similarly the presence of fibres in the DCP treated composites did not significantly change the melting peak temperature and crystallinity compared to those of the DCP treated neat HDPE. As observed and discussed earlier, the most probable reason for this is the lack of grafting between the HDPE chains and the sisal fibres.

Table 3.4 Melting characteristics of HDPE composites: melting temperature (T_m), observed melting enthalpy (ΔH_m^{obs}), calculated melting enthalpy (ΔH_m^{calc}), and degree of crystallinity (χ_c)

HDPE/sisal (w/w)	T_m (°C)	ΔH_m^{obs} (J g^{-1})	ΔH_m^{calc} (J g^{-1})	χ_c (%)
Untreated HDPE composites				
100/0	132.7 ± 0.4	176.7 ± 4.6	176.7	61.2
90/10	133.5 ± 1.1	160.5 ± 2.7	159.0	61.7
80/20	132.9 ± 0.2	146.0 ± 1.6	141.4	63.2
70/30	132.7 ± 0.4	124.8 ± 1.2	123.7	61.7
DCP treated HDPE composites				
100/0	132.0 ± 1.0	148.9 ± 1.0	148.9	51.6
90/10	132.2 ± 0.6	136.7 ± 1.5	134.0	52.6
80/20	130.9 ± 0.9	118.6 ± 0.4	119.0	51.0
70/30	130.7 ± 0.6	112.8 ± 0.7	104.0	55.8

3.4 Conclusions

The effects of polyethylene chain structure, the presence of DCP, and the fibre loadings on the morphologies and thermal properties of different sisal fibre reinforced polyethylene (LDPE, LLDPE, and HDPE) composites were investigated. The gel content results showed that the polyethylene chain structure plays a major role in the crosslinkability of the specific type of PE, and higher gel contents were observed for the LLDPE samples, followed by LDPE and then HDPE. SEM was used to investigate the morphology and the interfacial adhesion between the fibres and the polymer matrices in the composite samples. All the untreated samples showed poor adhesion between the polymer matrices and the fibres. On the other hand, the treated LDPE and LLDPE composites showed intimate contact between the polymers and fibres, which was not observed for the HDPE samples. This was confirmed by the SEM micrographs of the xylene-extracted samples, which clearly showed the presence of grafting between the fibres and both LDPE and LLDPE. The TGA results showed that all the composite samples were thermally less stable than the neat matrices, and that the thermal stabilities of the DCP treated composites were almost the same as those of the untreated composites in case of LDPE and LLDPE. The treated HDPE composite samples, however, were thermally less stable than the untreated samples. In general, the DSC results revealed that the presence of the fibre had little influence on the crystallization and melting behaviour of all three the investigated polymers. In the case of the DCP treated composites, the degree of crystallinity of LDPE and LLDPE slightly decreased, while that of HDPE decreased considerably. The melting temperatures of the HDPE composites remained almost unchanged with DCP treatment and increasing fibre content, whereas they decreased with DCP treatment but did not change significantly with increasing fibre content for the LDPE samples. The melting temperatures of the LLDPE samples decreased after addition of DCP and decreased even further with increasing fibre loadings for the DCP treated samples.

As a final conclusion it may be said that all the results described in this paper indicate the presence of grafting between the polymers and the fibre for the LDPE and LLDPE composites prepared in the presence of DCP, with the highest grafting efficiency in the case of LLDPE. In the case of HDPE there was very little or no grafting.

3.5 References

1. P. Wambua, J. Ivens, I. Verpoest. Natural fibres: Can they replace glass in fibre reinforced plastics? Composites Science and Technology 2003; 63:1259-1264.
   DOI: 10.1016/S0266-3538(03)00096-4
2. A.K. Bledzki, J. Gassan. Composites reinforced with cellulose based fibres. Progress in Polymer Science 1999; 24:221-274.
   DOI: 10.1016/S0079-6700(98)00018-5
3. A.K. Mohanty, M. Mishra, G. Hinrichsen. Biofibres, biodegradable polymers and biocomposites: An overview. Macromolecular Materials and Engineering 2000; 276/277:1-24.
   DOI: 10.1002/(SICI)1439-2054(20000301)276
4. S. Kalia, B.S. Kaith, I. Kaur. Pretreatment of natural fibres and their application as reinforcing material in polymer composites – A review. Polymer Engineering & Science 2009; 49:1253-1272.
   DOI: 10.1002/pen.21328
5. J.M. John, S. Thomas. Biofibres and biocomposites. Carbohydrate Polymers 2008; 71:343-364.
   DOI: 10.1016/j.carbpol.2007.05.040
6. Y. Li, Y-M. Mai, L. Ye. Sisal fibre and its composites: A review of recent developments. Composites Science and Technology 2000; 60:2037-2055.
   DOI: 10.1016/S0266-3538(00)00101-9
7. G. Jayamol, M.S. Sreekala, S. Thomas. A review on interface modification and characterization of natural fibre reinforced plastic composites. Polymer Engineering and Science 2001; 41:1471-1485.
   DOI: 10.1002/pen.10846
8. P.A. Fowler, J.M. Hughes, R.M. Elias. Biocomposites: Technology, environmental credentials, and market forces. Journal of the Science of Food and Agriculture 2006; 86:1781-1789.
   DOI: 10.1002/jsfa.2558
9. S.M. Huda, T.L. Drzal, M. Misra, K.A. Mohanty, K. Williams, F.D. Mielewski. Study on biocomposites from recycled newspaper fibre and poly(lactic acid). Industrial & Engineering Chemistry Research 2005; 44:5593-5601.

DOI: 10.1021/ie0488849

10. A.J. Peacock. Handbook of Polyethylene: Structures, Properties, and Applications. Marcel Dekker Inc., New York (2000) p.123-238.
11. D. Nwabunma. Overview of polyolefin composites. In: D. Nwabunma, T .Kyu (Eds.). Polyolefin Composites. John Wiley& Sons Inc., USA (2008) p.3-8.
12. D. Malpass. Introduction to Industrial Polyethylene: Properties, Catalysts, and Processes. John Wiley & Sons Inc., USA (2010) p.1-22.
13. C.A. Sperati, W.A. Franta, H.W. Starkweather. The molecular structure of polyethylene. V. The effect of chain branching and molecular weight on physical properties. Journal of the American Chemical Society 1953; 75:6127-6133.
    DOI: 10.1021/ja01120a009
14. L.C. Simon, R.F. de Souza, J.B.P. Soares, R.S. Mauler. Effect of molecular structure on dynamic mechanical properties of polyethylene obtained with nickel-diimine catalysts. Polymer 2001; 42:4885-4892.
    DOI: 10.1016/S0032-3861(00)00917-4
15. M.J. John, R.D. Anandjiwala. Recent developments in chemical modification and characterization of natural fiber-reinforced composites. Polymer Composites 2008; 29:187-207.
    DOI: 10.1002/pc.20461
16. X. Li, L.G. Tabil, S. Panigrahi. Chemical treatment of natural fiber for use in natural fiber-reinforced composites: A review. Journal of Polymers and the Environment 2007; 15:25-33.
    DOI: 10.1007/s10924-006-0042-3
17. K. Joseph, S. Thomas, C. Pavithran. Effect of chemical treatment on the tensile properties of short sisal fibre-reinforced polyethylene composites. Polymer 1996; 37:5139-5149.
    DOI: 10.1016/0032-3861(96)00144-9
18. M.A. Mokoena, V. Djoković, A.S. Luyt. Composites of linear low-density polyethylene and short sisal fibres: The effects of peroxide treatment. Journal of Materials Science 2004; 39:3403-3412.
    DOI: 10.1023/B:JMSC.0000026943.47803.0b
19. M.E. Malunka, A.S. Luyt, H. Krump. Preparation and characterization of EVA-sisal fibre composites. Journal of Applied Polymer Science 2006; 100:1607-1617.

DOI: 10.1002/app.23650

20. A.S. Luyt, M.E. Malunka. Composites of low-density polyethylene and short sisal fibres: The effect of wax addition and peroxide treatment on thermal properties. Thermochimica Acta 2005; 426:101-107.
DOI: 10.1016/j.tca.2004.07.010

21. J. George, S.S. Bhagawan, S. Thomas. Thermogravimetric and dynamic mechanical thermal analysis of pineapple fibre reinforced polyethylene composites. Journal of Thermal Analysis 1996; 47:1121-1140.
DOI: 10.1007/BF01979452

22. I. Janigová, F. Lednický, Z. Nógellová, B.V. Kokta, I. Chodák. The effect of crosslinking on properties of low-density polyethylene filled with organic filler. Macromolecular Symposia 2001; 169:149-158.
DOI: 10.1002/1521-3900(200105)

23. M. Mičušík, M. Omastová, Z. Nógellová, P. Fedorko, K. Olejníková, M. Trchová, I. Chodák. Effect of crosslinking on the properties of composites based on LDPE and conducting organic filler. European Polymer Journal 2006; 42:2379-2388.
DOI: 10.1016/j.europolymj.2006.05.024

24. J. Morshedian, P.M. Hoseinpour, H. Azizi, R. Parvizzad. Effect of polymer structure and additives on silane grafting of polyethylene. eXPRESS Polymer Letters 2009; 3(2):105-115.
DOI: 10.3144/expresspolymlett.2009.14

25. C. Li, Y. Zhang, Y. Zhang. Melt grafting of maleic anhydride onto low-density polyethylene/polypropylene blends. Polymer Testing 2003; 22(2):191-195.
DOI: 10.1016/S0142-9418(02)00079-X

26. A. Smedberg, T. Hjertberg, B. Gustafsson. Crosslinking reactions in an unsaturated low-density polyethylene. Polymer 1997; 38:4127-4138.
DOI: 10.1016/S0032-3861(96)00994-9

27. S. Nilsson, T. Hjertberg, A. Smedberg, Structural effects on thermal properties and morphology in XPLE. European Polymer Journal 2010; 46:1759-1769.
DOI: 10.1016/j.eurpolymj.2010.05.003

28. L.H.U. Andersson, T. Hjertberg. The effect of different structure parameters on the crosslinking behaviour and network performance of LDPE. Polymer 2006; 47:200-210.
DOI: 10.1016/j.polymer.2005.11.023

29. H. Azizi, J. Morshedian, M. Barikani. Silane grafting and moisture crosslinking of polyethylene: the effect of molecular structure. Journal of Vinyl and Additive Technology 2009; 15:184-190.
DOI: 10.1002/vnl.20194

30. L.H.U. Andersson, B. Gustafsson, T. Hjertberg. Crosslinking of bimodal polyethylene. Polymer 2004; 45:2577-2585.
DOI:10.1016/j.polymer.2004.01.073

31. S.L. Fávaro, T.A. Ganzerli, A.G.V. de Carvalho Neto, O.R.R.F. da Silva, E. Radovanovic. Chemical, morphological, and mechanical analysis of sisal fiber-reinforced recycled high-density polyethylene composites. eXPRESS Polymer Letters 2010; 4:465-473.
DOI: 10.3144/expresspolymlett.2010.59

32. A.R. Martin, F.S. Denes, R.M. Rowell, L.H.C. Mattoso. Mechanical behavior of cold plasma-treated sisal and high-density polyethylene composites. Polymer Composites 2003; 24:464-474.
DOI: 10.1002/pc.10045

33. N.Chand, S. Sood, D.K. Singh, P.K. Rohatgi. Structural and thermal studies on sisal fibre. Journal of Thermal Analysis 1987; 32:595-599.
DOI: 10.1007/BF01912712

34. J.D. Megiatto, W. Hoareau, C. Gardrat, E. Frollini, A. Castellan. Sisal fibres: Surface chemical modification using reagent obtained from a renewable source; characterization of hemicellulose and lignin as model study. Agricultural and Food Chemistry 2007; 55:8576-8584.
DOI: 10.1021/jf071682d

35. H. Yang, R. Yan, H. Chen, D.H. Lee, C. Zheng. Characteristics of hemicellulose, cellulose and lignin pyrolysis. Fuel 2007; 86:1781-1788.
DOI: 10.1016/j.fuel.2006.12.013

36. N.E. Marcovich, M.A. Villar. Thermal and mechanical characterization of linear low-density polyethylene/wood flour composites. Journal of Applied Polymer Science 2003; 90:2775-2784.
DOI: 10.1002/app.12934

37. H.A. Khonakdar, J. Morshedian, U. Wagenknecht, S.H. Jafari. An investigation of chemical crosslinking effect on properties of high-density polyethylene. Polymer 2003; 44:4301-4309.
DOI: 10.1016/S0032-3861(03)00363-X
38. H.A. Khonakdar, S.H. Jafari, M. Taheri, U. Wagenknecht, D. Jehnichen, L. Häussler. Thermal and wide angle x-ray analysis of chemically and radiation-crosslinked low and high density polyethylenes. Journal of Applied Polymer Science 2006; 100:3264-3271.
DOI: 10.1002/app.23073

Chapter 4

Effects of organic peroxide and polymer chain structure on mechanical and dynamic mechanical properties of sisal fibre reinforced polyethylene composites

Abstract

Three types of polyethylene, low-density (LDPE), linear low-density (LLDPE) and high-density (HDPE) polyethylenes were used as polymer matrices to prepare untreated as well as DCP treated sisal fibre composites. The effect of polymer chain structure, addition of dicumyl peroxide (DCP), and sisal fibre loadings on the mechanical and dynamic mechanical properties of the composite was investigated in this study. It was found that the extent of improvement in tensile properties of the composite samples varied with respect to the polymer molecular characteristics. The elongation at break for all the composites decreased significantly. Young's modulus and the tensile strength of the treated LDPE and LLDPE composites increased significantly compared to the untreated composites, while Young's modulus of the treated HDPE samples decreased observably compared to the untreated samples. DCP treatment, however, did not change the tensile strength of HDPE and its composites. The storage modulus results for all the polyethylene composites correlate well with the tensile testing results. In the case of the LDPE and LLDPE samples, the curves of the mechanical loss factor (tan δ) show a clear relaxation around -18 °C, which shifted to higher temperature in the treated composites, whereas for HDPE this transition was not seen.

Keywords: Polyethylenes; sisal fibre; composites; crosslinking; grafting; mechanical properties; dynamic mechanical properties

4.1 Introduction

During the last decade, the use of natural fibres as reinforcement in plastics has received considerable attention. Natural fibres have many advantages over their synthetic counterparts. They are cheap, widely available, renewable, recyclable, biodegradable, and have high

specific strength. These properties are in agreement with the recent tendency and legislation towards using materials that are renewable and environmentally friendly. Therefore, many studies have been carried out on natural fibres reinforced polymer composites as alternative to synthetic reinforcing materials [1-5]. Among natural fibres, sisal fibre has been widely used in polymer/natural fibre composites due to its wide availability, short renewable time, ease of cultivation, low cost and excellent physical and mechanical characteristics [1,6].

However, there are some shortcomings of natural fibres, which affect their reinforcing capabilities. Natural fibres have a tendency to absorb moisture due to their hydrophilic nature, as well as to form aggregates during processing. In addition, their thermal stability (start degrading above 200 °C) limits their utilization in certain polymer matrices. On top of that, owing to their hydrophilic nature, natural fibres are incompatible with hydrophobic polymers, which leads to weak interfacial bonding between the two components. Consequently, this will deteriorate the mechanical properties and performance of the resulting composites [1,7,8]. Hence, modification of the fibre and/or the polymer is required to improve the compatibility and consequently the performance of the composites.

Pretreatments of natural fibres can clean the fibre surface, chemically modify the surface, increase the surface roughness, and reduce the moisture absorption process. Modifications of the polymer matrix and the fibre during processing, and of the polymer matrix alone, have been reported to improve the interfacial bonding. These various strategies were reviewed by a number of researchers [9-13]. Among the various treatments, peroxide treatment of cellulose fibre, as well as the addition of peroxide to the molten polymer-fibre mixture during processing, has attracted the attention of various researchers due to easy processability and the improvement in the mechanical properties. Addition of dicumyl peroxide (DCP) to the composite mixture during melt mixing can give rise to crosslinking of the polymer chains and grafting between the polymer chains and the natural fibres. However, due to the presence of three reactive hydroxy groups on each cellulose unit, the grafting of the cellulose fibres to the polymer chains should dominate because of the higher free radical reactivity of the hydroxyl groups [14-16].

Polyethylenes have been widely used as matrix materials in natural fibre reinforced composites due to their excellent value (cost and performance), relatively modest physical

properties, ease of processing, recyclability, and adequate mechanical properties. There are three major classes of PEs, HDPE, LDPE, and LLDPE. The basic difference between these three types of PEs lies in the degree and regularity of branching. While HDPE has very few branches, LDPE is characterized by significant branching with long, irregular branches at irregular intervals. LLDPE, on the other hand, is characterized by short branches of regular length at regular intervals [17-19].The molecular structure of a polyethylene is an important characteristic influencing the physical and chemical properties. It has been reported that the structural parameters such as number average molecular weight, the molecular weight distribution, the presence of unsaturated functional groups (vinyl groups), and the content of branches as well as their length had important effects in the crosslinking/grafting behaviour of polyethylenes [20-23].

The objective of the present study is to investigate the effects of polyethylene molecular characteristics, the addition of DCP, and the sisal fibre loadings on the mechanical and the dynamic mechanical properties of sisal fibre reinforced LDPE, LLDPE, and HDPE composites. Dicumyl peroxide was used to improve the interfacial adhesion between the polyethylene matrices and sisal fibre through initiation of both crosslinking of polyethylenes chains and grafting of the chains onto the sisal fibre surfaces.

4.2 Experimental

4.2.1 Materials

Sisal fibre was obtained from the National Sisal Marketing Committee in Pietermaritzburg, South Africa. LDPE and LLDPE were supplied in pellet form by Sasol Polymers, Johannesburg, South Africa, whereas HDPE was supplied by Safripol Ltd, South Africa. They have the following specifications:

LDPE: MFI = 2 g/10 min at 190 ºC / 2.16 kg, density = 0.922 g cm^{-3}, M_n = 30302 g mol^{-1}, M_w = 206797 g mol^{-1};

LLDPE: MFI = 1 g / 10 min at 190 ºC / 2.16 kg, density = 0.924 g cm^{-3}, M_n = 68409 g mol^{-1}, M_w = 290056 g mol^{-1};

HDPE: MFI = 2 g / 10 min at 190 ºC / 5 kg, density = 0.956 g cm^{-3}, M_n = 27575 g mol^{-1}, M_w = 539389 g mol^{-1};

Dicumyl peroxide (bis(α,α-dimethylbenzyl)peroxide) was supplied by Merck, South Africa. It has a minimum assay of 98%. Petroleum ether was also supplied by Merck.

Sisal fibres were cut into an average length of between 5 and 10 mm, soaked in distilled water for 24 h to remove any surface impurities, filtered and washed thoroughly with distilled water before being allowed to dry in an oven at 80 ºC for 48 h. The dried fibres were washed with petroleum ether for 5 h at 50 ºC to remove waxy materials and natural oils, followed by oven drying at 80 ºC.

4.2.2 Preparation of polyethylene composites

The polyethylene-sisal fibre composites were prepared *via* melt mixing in a 55 mL mixing chamber of a Plastograph-W50EHT (Brabender®OHG, Germany) at 150 ºC, 30 rpm and 10 min. DCP treated samples were prepared by addition of 1 phr DCP to the mixture one minute before the end of the mixing. The melt pressing of the prepared samples was performed at 175 ºC and 50 bar for 10 min. Table 4.1 shows the compositions of the PE composite samples used in this study.

Table 4.1 Compositions of the composite samples used in this study

LDPE/sisal/DCP (w/w)	LLDPE/sisal/DCP (w/w)	HDPE/sisal/DCP (w/w)
100/0/0	100/0/0	100/0/0
100/0/1	100/0/1	100/0/1
90/10/0	90/10/0	90/10/0
80/20/0	80/20/0	80/20/0
70/30/0	70/30/0	70/30/0
90/10/1	90/10/1	90/10/1
80/20/1	80/20/1	80/20/1
70/30/1	70/30/1	70/30/1

4.2.3 Characterization methods

The tensile properties of the neat polymers and the composites were determined using a Hounsfield H5KS tensile tester at a crosshead speed of 50 mm min^{-1} at ambient temperature. Dumbbell-shaped test specimens of 75 mm total length, 13 mm width at the two ends, 5 mm neck width, 20 mm gauge length and 1.5 mm thickness were used. The stress and the elongation at yield, Young's modulus, as well as the tensile strength and elongation at break were determined from the stress-strain curves. At least eight samples were tested for each composition, and the mean values are reported.

The dynamic mechanical properties (storage and loss modulus as well as tan δ) of the samples were determined in a Perkin Elmer Diamond DMA dynamic mechanical analyzer. Rectangular bar specimens with dimensions of 50 x 10 x 1.5 mm were used for this study, there was no pretreatment after composite preparation, and the samples were stored in the dark under ambient conditions. The measurements were carried out in the dual cantilever bending mode and the corresponding viscoelastic properties were determined as a function of temperature. The samples were heated under nitrogen flow (30 mm min^{-1}) from -100 ºC to 100 ºC at a heating rate of 5 ºC min^{-1}, and at a frequency of 1 Hz.

4.3 Results and discussion

The tensile properties of the polyethylene/sisal fibre composites as a function of sisal fibre content are shown in Figures 4.1 to 4.3. As can be seen from Figure 4.1, the elongation at break of the treated and the untreated LDPE composites decreased significantly with incorporation of the sisal fibre, and it further decreased with increasing filler content. No significant differences in the elongation at break between the treated and the untreated samples could be seen. This can be explained by the sisal fibres imparting rigidity and brittleness to the LDPE matrix [24,25]. The tensile modulus of the composites (Figure 4.2) was found to increase significantly with the presence of sisal fibre as well as with the addition of DCP. The treated composites showed higher values compared to the untreated ones for all fibre loadings. The increase in the modulus upon fibre addition is ascribed to the higher modulus of the lignocellulosic fibres compared to LDPE, whereas the treatment of the composites with DCP resulted in better interfacial adhesion between the fibre and the

polymer matrix [24,25], as well as in crosslinking of the polymer that will contribute to the increase in stiffness. The improved interfacial adhesion leads to good stress transfer from the matrix to the fibre and the mechanical properties of the fibre are fully utilized. This result is in agreement with the morphological observations and gel contents that were described in another paper [26]. Figure 4.3 shows the tensile strength as a function of fibre loading of the treated and the untreated LDPE composites. The tensile strength of the untreated composites is lower than that of the unfilled polymer matrix and the treated composites. The treated composites show a gradual increase in tensile strength with increasing fibre content. An almost 20 % increase in tensile strength of the composite with 30 wt % fibre is observed compared to the neat LDPE [25,27]. This increase is a clear indication of the improved interfacial adhesion between the polymer matrix and the sisal fibre, which was described in our previous paper [26].

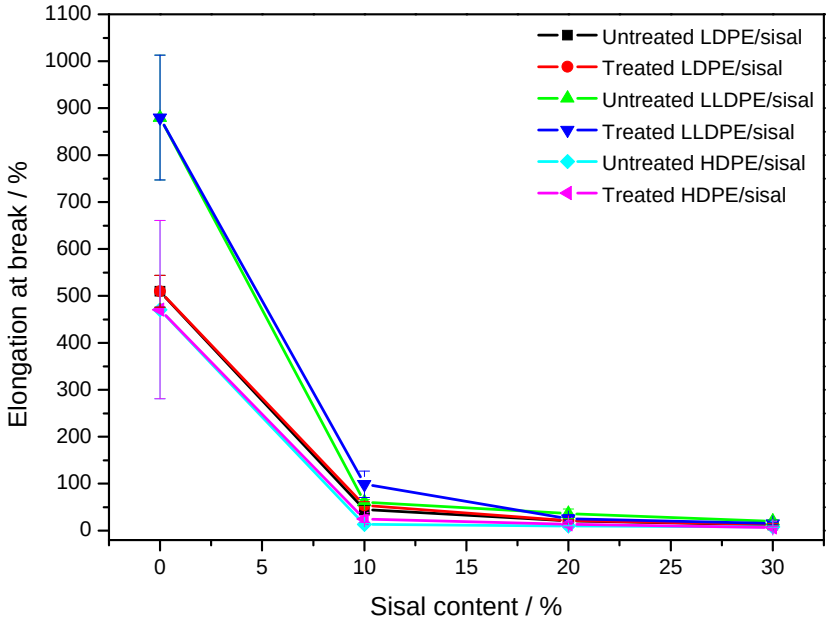

Figure 4.1 Elongation at break as function of sisal fibre content for untreated and DCP treated polyethylenes composites

The tensile results of LLDPE and its composites are summarized in Figures 4.1 to 4.3. As expected, the elongation at break of the LLDPE composites (Figure 4.1) decreased significantly with the presence of the sisal fibre, and even further decreased with increasing fibre content. A considerable increase in the tensile modulus (Figure 4.2) was observed with

increasing fibre content. The tensile modulus of the treated composites was higher than those of the untreated ones, especially at higher fibre loadings. The decrease in the elongation at break as well as the increase in the tensile modulus could be explained in the same way as for LDPE. Figure 4.3 shows the dependence of the tensile strength of the untreated and the treated LLDPE composites on the fibre content. The tensile strength of the untreated and treated composites decreased noticeably with the incorporation of 10 wt % sisal fibre, and thereafter the tensile strength of the untreated samples remained almost unchanged with increasing fibre loadings.

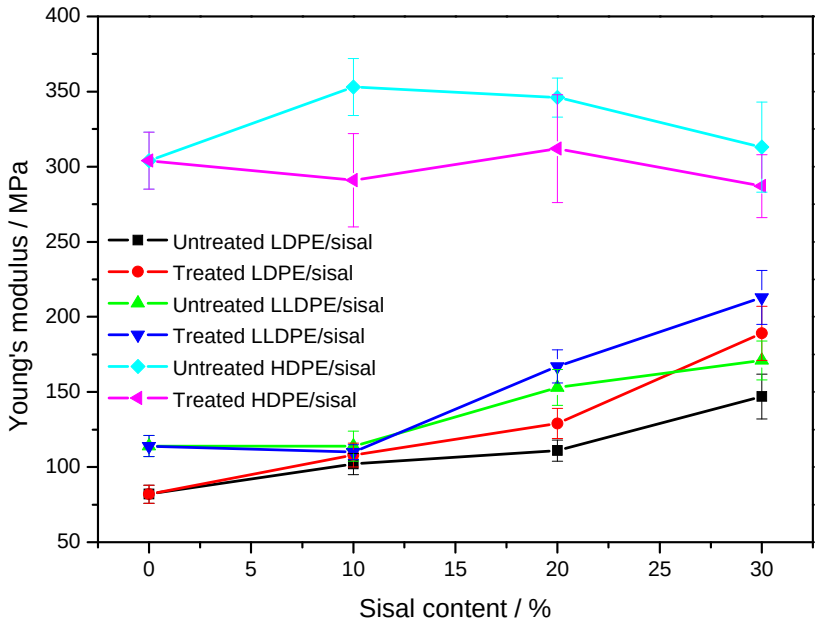

Figure 4.2 Tensile modulus as function of sisal fibre content for untreated and DCP treated polyethylenes composites

The tensile strength of the treated composites was, however, found to increase slightly with an increase in fibre content. The tensile strength of the treated 70/30 w/w LLDPE/sisal composite was about 80% higher than that of the untreated composite. This is the result of a lack of interfacial adhesion between the fibre and the polymer in the case of the untreated samples, which resulted in poor stress transfer from the polymer to the reinforcing filler. The grafting in the treated composites resulted in good stress transfer from the LLDPE matrix to the fibre.

In the case of the HDPE composites (Figures 4.1 to 4.3) the elongation at break of the treated and the untreated composites was found to decrease in a similar way as for the LDPE and LLDPE composites. The tensile modulus of the untreated HDPE composites increased by about 20% in the presence of 10 wt.% fibre, but decreased slightly at higher fibre contents (Figure 4.2). However, the tensile modulus for all the untreated HDPE composites was higher than that of neat HDPE because of the higher stiffness of the fibres. The tensile modulus of the treated composites did not change in the presence of fibre, and with increasing fibre content. This could have been due to the reduction in the crystallinity of the HDPE matrix after addition of DCP, as was observed from DSC results [26]. The increase in modulus as a result of the presence of the stiffer fibres was obviously balanced by the decrease in modulus as a result of the decreased crystallinity brought about by crosslinking in the presence of DCP. It was reported that the tensile modulus of polyethylene polymers depends strongly on its crystallinity.

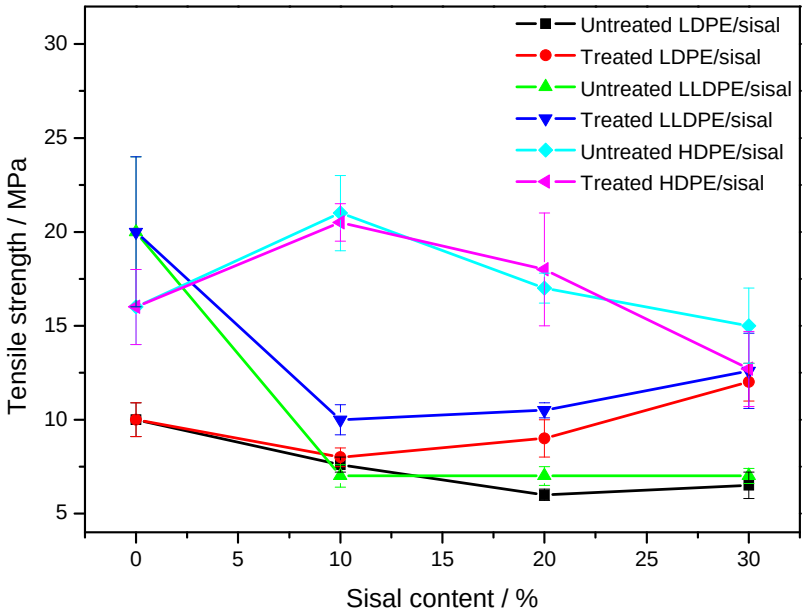

Figure 4.3 Tensile strength as function of sisal fibre content for untreated and DCP treated polyethylenes composites

In general, the tensile modulus changes approximately linearly with the degree of crystallinity [28]. The tensile strength of the untreated and the treated HDPE/sisal composites increased at lower fibre loadings, and then decreased with an increase in fibre loading (Figure

4.3). In general, no significant differences in tensile strength between the untreated and the treated composites were observed. The reason for this is that, because there was no grafting between the polymer chains and the fibres in the case of the DCP treated HDPE composites, the interaction (or lack thereof) between HDPE and the fibres was the same, whether the samples were prepared in the presence or absence of DCP.

Dynamic mechanical measurements were performed on the neat and DCP treated polyethylenes, as well as on the untreated and DCP treated sisal fibre composites to display the effect of the fibre loading, molecular characteristics of the polymer, and the DCP treatments on the viscoelastic properties of the composites. The storage modulus and tan δ of the composite samples as function of temperature are shown in Figures 4.4 to 4.9.

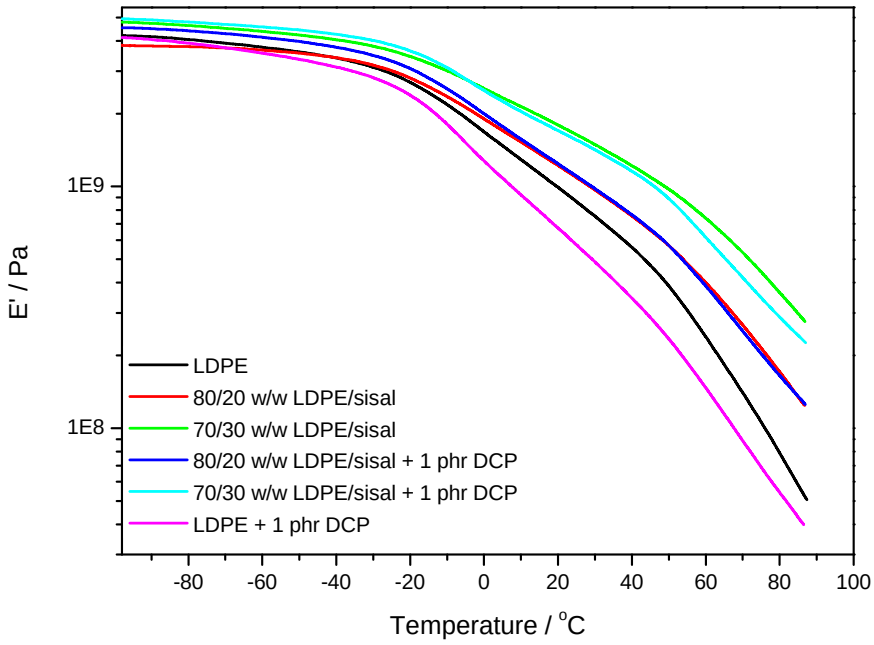

Figure 4.4 Storage modulus versus temperature for the neat and DCP treated LDPE, as well as the untreated and DCP treated LDPE/sisal composites

As can be seen in Figure 4.4, the storage modulus increases with increasing amount of sisal fibre, and all the composites show higher values than the neat and DCP treated LDPE, especially at temperatures above the glass transition. The curve of the storage modulus of the DCP treated LDPE shows the lowest values at temperatures around and above the glass transition temperature. It was expected that the introduction of the crosslinks in the LDPE

matrix would increase the rigidity of the polymer matrix, decrease the chain mobility, and consequently increase the modulus of the LDPE matrix. However, the results in Figure 4.4 show exactly the opposite trend. As the degree of crystallinity of the neat and the DCP treated LDPE is almost identical, this behaviour is probably associated with the decrease in the size of the crystalline domains [26], which enhances the free volume and the molecular motions of the amorphous phase. The DSC measurements [26] showed a slight decrease in the melting temperature (from 110.6 to 108.6) of the LDPE matrix after treatment with DCP. The treated composites also show slightly higher storage modulus values than their untreated counterparts at temperatures below the glass transition. However, at higher temperatures the curves of the treated and the untreated composites were almost overlapped. The increase in the storage modulus upon fibre addition is ascribed to the higher modulus of the lignocellulosic fibres compared to that of LDPE, while the DCP treatment of the composites resulted in better interfacial adhesion between the fibre and the polymer [24,25].

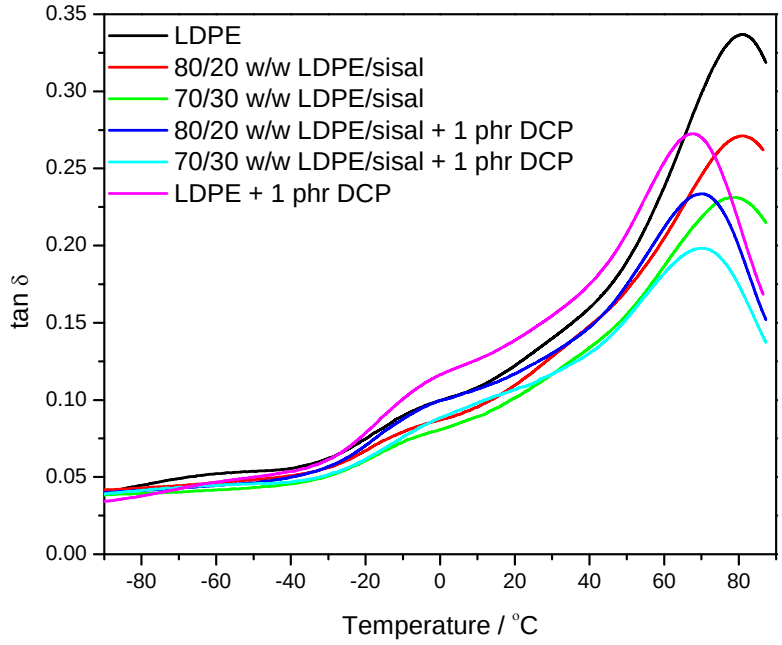

Figure 4.5 tan δ versus temperature for the neat and DCP treated LDPE, as well as the untreated and DCP treated LDPE/sisal composites

It has been reported that DMA measurements can give information on the interface between natural fibres and polymer matrices [29,30]. In the case of good adhesion between the natural fibres and the polymer matrix, a shift in the glass transition towards higher temperatures is

expected. Moreover, it was observed that good interfacial bonding has resulted in composite materials with lower energy dissipation than the poorly bonded or untreated composites.

Tan δ as function of temperature for the LDPE composites is shown in Figure 4.5. The tan δ curve of the DCP treated LDPE shows the highest energy dissipation at temperatures above the glass transition. This demonstrates that the polymer chain motions were enhanced by the reduction in the sizes of the crystallites due to the presence of the crosslinks. The tan δ curves of all the composites show lower values than the neat polymer matrix. The treated composites show slightly lower values than the untreated ones, especially at higher temperatures. Furthermore, the tan δ curves show two relaxation processes located around -18 °C (glass transition) and 69-80 °C (α-transition). The first relaxation process is called the β-relaxation, which is generally accepted as being the glass transition in polyethylenes [31,32]. For the treated composites, there is a slight shift to higher temperatures (-13 °C) of this transition, which is the result of the immobilization of the amorphous polymer chains through crosslinking/grafting. This is in agreement with the findings of the gel contents as well as the SEM observations, which confirmed an enhanced interfacial adhesion as a result of grafting in the treated composites [26]. The relaxation process in the temperature range 69-80 °C is associated with the molecular motion within the crystalline phase. For the neat LDPE and the untreated composites, this relaxation occurred around 80 °C, whereas for the treated composites it shifted to 69 °C. This could be explained by the fact that crosslinking/grafting reduced the lamellar thickness of the polymer matrix and hence eased the polymer chain motions. For the DCP treated LDPE sample, a slight decrease in the α-relaxation peak to lower temperatures was observed compared to the treated composites. This can be explained by the presence of grafting between the LDPE matrix and sisal fibre in the case of the treated composites, which restricts the polymer chain motions and stiffens the material. Sirotkin *et al*. [33] studied three polyethylene copolymers, which differed in short chain branch content, to establish the effect of the morphology on the α-, β-, and γ-relaxations. They found that the α-relaxation temperature increased with lamellar thickness, irrespective of the grade or crystallinity, and is associated with c-shear within the crystalline lamellae.

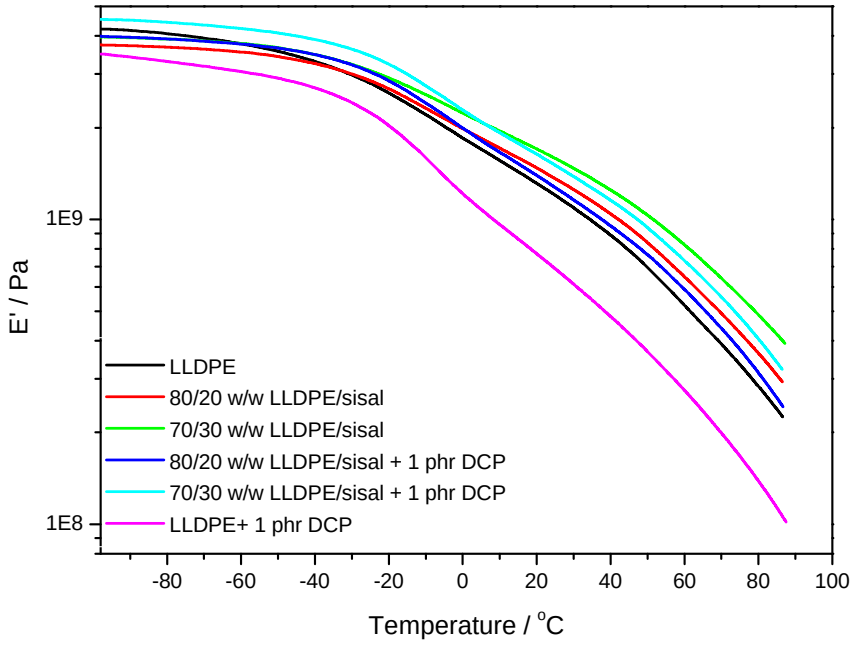

Figure 4.6 Storage modulus versus temperature for the neat and DCP treated LLDPE, as well as the untreated and DCP treated LLDPE/sisal composites

Figures 4.6 and 4.7 show the storage modulus and tan δ of the LLDPE composites as function of temperature. It is evident from Figure 4.6 that the storage modulus of all the composites is higher than that of the neat and DCP treated LLDPE at the glass transition and higher temperatures. Similar to the DCP treated LDPE, the DCP treated LLDPE shows the lowest storage modulus values over the temperature range used in this study. This can be explained in a similar way to DCP treated LDPE. However, in the case of LLDPE, even the crystallinity was slightly reduced [26], which would further enhance the molecular motions of the polymer chains. Figure 4.6 demonstrates that the molecular motions of DCP treated LLDPE were significantly enhanced after introduction of crosslinks. At temperatures above the glass transition the storage modulus of the untreated samples was somewhat higher than that of the treated ones. This is probably due to the slight decrease in the crystallinity of the polymer matrix after treatment with DCP, which was apparent from the DSC results [26].

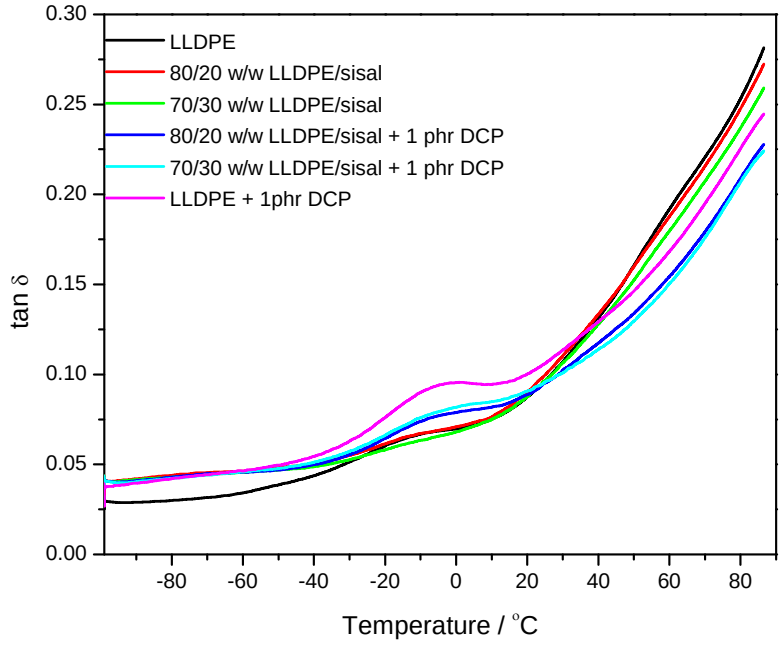

Figure 4.7 tan δ versus temperature for the neat and DCP treated LLDPE, as well as the untreated and DCP treated LLDPE/sisal composites

The tan δ curves of the LLDPE composites as a function of temperature are shown in Figure 4.7. It is obvious that the intensity of the glass transition at -16 °C of the treated samples increased, and that the transition shifted to higher temperatures, compared to both the untreated samples and the neat LLDPE matrix (-23 °C). The increase in the intensity of the glass transition peak is due to the increase in the volume fraction of the amorphous phase as a result of the crosslinking/grafting processes, which restricted the polymer chains packing and hence reduced the crystallinity of the matrix [26]. The shift in the glass transition is probably due to the improved interfacial interactions between the polymer matrix and the sisal fibre, which restricts the segmental mobility of the LLDPE chains in the amorphous phase and hence shifts the β-transition to higher temperatures. Furthermore, the observable reduction in the intensity of the β-relaxation for the DCP treated composites compared to the DCP treated LLDPE matrix suggests that the grafting between the polymer chains and the sisal fibre is more dominant than the crosslinking between the polymer chains. The SEM and gel content results for the treated LLDPE composite samples showed good interfacial bonding between the polymer and sisal fibre [26]. The tan δ values of the treated composites were also lower

than those of the untreated composites and the neat LLDPE above the glass transition temperature, which indicates better interfacial interactions and less dissipation of energy.

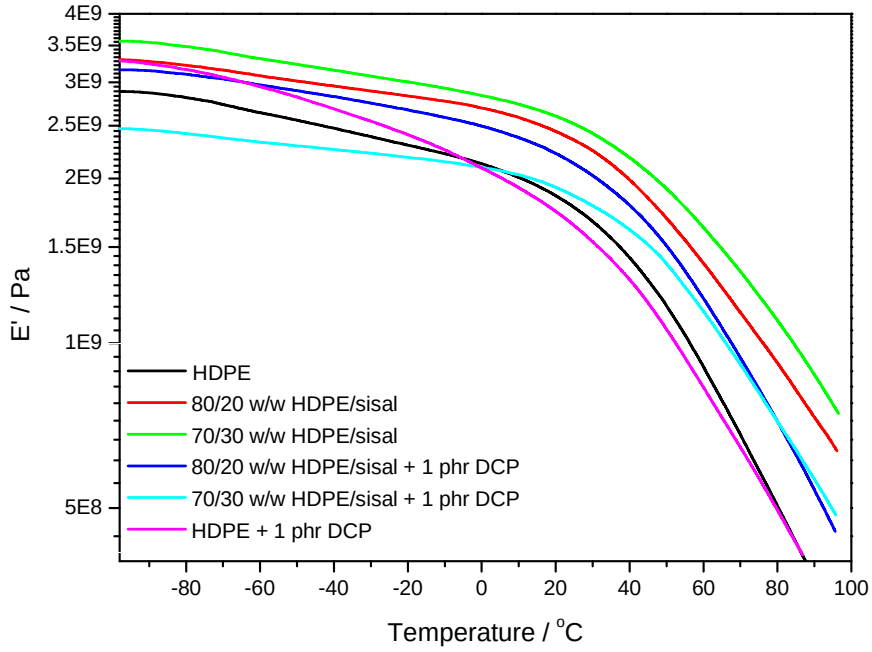

Figure 4.8 Storage modulus versus temperature for the neat and DCP treated HDPE, as well as the untreated and DCP treated HDPE/sisal composites

The variation of the storage modulus of HDPE and its composites as a function of temperature is shown in Figure 4.8. The storage modulus of the DCP treated HDPE shows a notably abrupt decrease with an increase in the temperature compared to the other samples, and at higher temperatures it showed the lowest values. This could also be interpreted in a similar way to the DCP treated LDPE and LLDPE. The storage modulus values of the untreated samples increased with increasing fibre content over the whole temperature range, and they were higher than those of the treated samples, which decreased with increasing fibre content. These results show the same trend as the tensile modulus results, and can be explained in the same way.

The dependence of tan δ of HDPE and its treated and untreated composites on temperature is shown in Figure 4.9. The β-relaxation, which was seen in the tan δ curves of the LDPE and LLDPE samples (Figures 4.5 and 4.7), is not clearly seen in the case of the neat and DCP treated HDPE, as well as the untreated and the DCP treated composites. This could be

ascribed to the higher crystallinity of the HDPE matrix. At higher temperatures the tan δ values of the untreated composites were lower than those of the neat HDPE, DCP treated HDPE, and the treated composites. This is probably due to the reduction in the crystallinity of the polymer matrix after treatment with DCP, which enhances the molecular motions of the amorphous phase and hence leads to higher dissipation of energy. It was expected that the reduction of the polymer's crystallinity due to DCP treatment would be counterbalanced by the enhanced interfacial bonding between the polymer matrix and the sisal fibres. However, the SEM and gel content results [26] both demonstrated poor interfacial bonding as well as less grafting in the case of the HDPE composites [26]. This can explain why the DCP treated composites had higher dissipation of energy compared to their untreated counterparts.

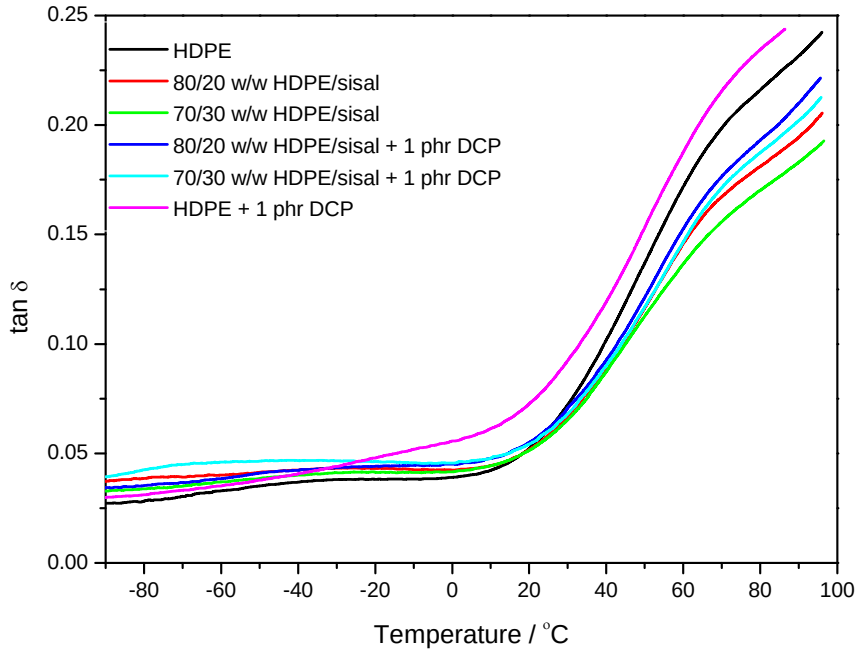

Figure 4.9 tan δ versus temperature for the neat and DCP treated HDPE, as well as the untreated and DCP treated HDPE/sisal composites

4.4 Conclusions

In this study the influence of the polyethylene molecular characteristics, the sisal fibre loadings, and DCP treatment on the mechanical and the dynamic mechanical properties of polyethylene based sisal fibre composites were investigated. It was found [26] that the

polyethylene molecular characteristics play a crucial role in its crosslinking/grafting behaviour. The degree of crosslinking/grafting was higher for the polyethylenes with higher number average molecular weights, higher contents of vinyl groups, relatively lower molecular weight distributions, and higher branching contents. In our study [26] it was found that the LLDPE had the highest crosslinking/grafting efficiency, followed by the LDPE and then the HDPE, for which no grafting was observed.

This crosslinking/grafting efficiency was clearly reflected in the mechanical and dynamic mechanical properties of the polyethylene composites. The elongation at break was found to decrease significantly for all the polyethylenes composites, and DCP treatment did not seem to make any difference. This is common for all particulate filled polyethylenes, and crosslinking/grafting was not expected to make any difference. The grafting did, however, positively influence the tensile strength and modulus of the LDPE and LLDPE composites, because of the improved interfacial bonding between the fibre and the matrix. In the case of the HDPE composites, the DCP treatment had a marginal influence on the tensile strength, whereas the tensile modulus of the treated composites was smaller than that of the neat HDPE and the untreated composites. This is probably due to a combination of the reduction in the crystallinity of the polymer matrix as a result of DCP treatment, and the absence of grafting between the fibre and the matrix.

The DMA results were also in line with the effect of DCP treatment on the composite structures. For all three polyethylenes the storage moduli above T_g of the DCP treated samples were lower than those of the untreated samples. It seems as if the decrease in crystallinity as a result of crosslinking/grafting more strongly influenced the storage modulus values than the grafting between the matrices and the fibres. For both LDPE and LLDPE the glass transition temperatures increased as a result of crosslinking/grafting due to the immobilization of the polymer chains, although the effect is more visible in the case of LLDPE. In the case of LDPE, the α-transition temperature observably decreased for the DCP treated samples, which is in line with the reduced lamellar thickness.

4.5 References

1. A.K. Bledzki, J. Gassan. Composites reinforced with cellulose based fibres. Progress in Polymer Science 1999; 24:221-274.
   DOI: 10.1016/S0079-6700(98)00018-5
2. M.S. Huda, L.T. Drzal, A.K. Mohanty, M. Misra. Chopped glass and recycled newspaper as reinforcement fibres in injection molded poly(lactic acid) (PLA) composites: A comparative study. Composites Science and Technology 2006; 66:1813-1824.
   DOI: 10.1016/j.compscitech.2005.10.015
3. D. Puglia, A. Tomassucci, J.M. Kenny. Processing, properties and stability of biodegradable composites based on Mater-Bi® and cellulose fibres. Polymers for Advanced Technologies 2003; 14:749-756.
   DOI: 10.1002/pat.390
4. P. Wambua, J. Ivens, I. Verpoest. Natural fibres: can they replace glass in fibre reinforced plastics ? Composites Science and Technology 2003; 63:1259-1264.
   DOI: 10.1016/S0266-3538(03)00096-4
5. X.P. Zhou, R.K.Y. Li, X.L. Xie, S.C. Tjong. Reinforcement of polypropylene using sisal fibres grafted with poly(methyl methacrylate). Journal of Applied Polymer Science 2003; 88:1055-1064.
   DOI: 10.1002/app.11818
6. Y. Li, Y-M. Mai, L. Ye. Sisal fibre and its composites: A review of recent developments. Composites Science and Technology 2000; 60:2037-2055.
   DOI: 10.1016/S0266-3538(00)00101-9
7. J.M. John, S. Thomas. Biofibres and biocomposites: Review. Carbohydrate Polymers 2008; 71:343-364.
   DOI: 10.1016/j.carbpol.2007.05.040
8. A.K. Mohanty, M. Mishra, G. Hinrichsen. Biofibres, biodegradable polymers, and biocomposites: An overview. Macromolecular Materials and Engineering 2000; 276/277:1-24.
   DOI: 10.1002/(SICI)1439-2054(20000301)276

9. S. Kalia, B.S. Kaith, I. Kaur. Pretreatment of natural fibres and their application as reinforcing material in polymer composites – A review. Polymer Engineering and Science 2009; 49:1253-1272.
DOI: 10.1002/pen.21328
10. M.J. John, R.D. Anandjiwala. Recent developments in chemical modification and characterization of natural fiber-reinforced composites. Polymer Composites 2008; 29:187-207.
DOI: 10.1002/pc.20461
11. X. Li, L.G. Tabil, S. Panigrahi. Chemical treatment of natural fiber for use in natural fiber-reinforced composites: A review. Journal of Polymers and the Environment 2007; 15:25-33.
DOI: 10.1007/s10924-006-0042-3
12. J. George, M.S. Sreekala, S. Thomas. A review on interface modification and characterization of natural fiber reinforced plastic composites. Polymer Engineering and Science 2001; 41:1471-1485.
DOI: 10.1002/pen.10846
13. L.A. Pothan, A.S. Luyt, S. Thomas. Polyolefin/natural fibre composites. In: D. Nwabunma, T. Kyu. Polyolefin Composites. John Wiley & Sons Inc., New Jersey (2008) p.68-81.
14. M.A. Mokoena, V. Djoković, A.S. Luyt. Composites of linear low density polyethylene and short sisal fibres: The effect of peroxide treatment. Journal of Materials Science 2004; 39:3403-3412.
DOI: 10.1023/B:JMSC.0000026943.47803.0b
15. M.E. Malunka, A.S. Luyt, H. Krump. Preparation of EVA-sisal fibre composites. Journal of Applied Polymer Science 2006; 100:1607-1617.
DOI: 10.1002/app.23650
16. K. Joseph, S. Thomas, C. Pavithran. Effect of chemical treatment on the tensile properties of short sisal fibre-reinforced polyethylene composites. Polymer 1996; 37:5139-5149.
DOI: 10.1016/0032-3861(96)00144-9
17. A.J. Peacock. Handbook of Polyethylene: Structures, Properties, and Applications. Marcel Dekker Inc., New York (2000) p.123-238.

18. D. Nwabunma. Overview of polyolefin composites. In: D. Nwabunma, T .Kyu (Eds.). Polyolefin Composites. John Wiley& Sons Inc., New Jersey (2008) p.3-8.
19. D. Malpass. Introduction to Industrial Polyethylene: Properties, Catalysts, and Processes. John Wiley & Sons Inc., New Jersey (2010) p.1-22.
20. L.H.U. Andersson, B. Gustafsson, T. Hjertberg. Crosslinking of bimodal polyethylene. Polymer 2004; 45:2577-2585.
DOI: 10.1016/j.polymer.2004.01.073
21. L.H.U. Andersson, T. Hjertberg. The effect of different structure parameters on the crosslinking behaviour and network performance of LDPE. Polymer 2006; 47:200-210.
DOI: 10.1016/j.polymer.2005.11.023
22. H. Azizi, J. Morshedian, M. Barikani. Silane grafting and moisture crosslinking of polyethylene: The effect of molecular structure. Journal of Vinyl and Additive Technology 2009; 15:184-190.
DOI: 10.1002/vnl.20194
23. A. Smedberg, T. Hjertberg, B. Gustafsson. Effect of molecular structure and topology on network formation in peroxide crosslinked polyethylene. Polymer 2003; 44:3395-3405.
DOI: 10.1016/S0032-3861(03)00179-4
24. M. Mičušík, M. Omastová, Z. Nógellová, P. Fedorko, K. Olejníková, M. Trchová, I. Chodák. Effect of crosslinking on the properties of composites based on LDPE and conducting organic filler. European Polymer Journal 2006; 42:2379-2388.
DOI: 10.1016/j.eurpolymj.2006.05.024
25. G. Kalaprasad, B. Francis, S. Thomas, C.R. Kumar, C. Pavithran, G. Groeninckx, S. Thomas. Effect of fibre length and chemical modifications on the tensile properties of intimately mixed short sisal/glass hybrid fibre reinforced low-density polyethylene composites. Polymer International 2004; 53:1624-1638.
DOI: 10.1002/pi.1453
26. E.E.M. Ahmad, A.S. Luyt. Effects of organic peroxide and polymer chain structure on morphology and thermal properties of sisal fibre reinforced polyethylene composites. Composites: Part A 2012; 43:703-710.
DOI: 10.1016/j.compositesa.2011.12.011

27. A.K. Mishra, A.S. Luyt. Effects of sol-gel derived nano-silica and organic peroxide on the thermal and mechanical properties of low-density polyethylene/wood flour composites. Polymer Degradation and Stability 2008; 93:1-8.
DOI: DOI: 10.1016/j.polymdegradstab.2007.11.006
28. A.J. Peacock. Handbook of Polyethylene: Structures, Properties, and Applications. Marcel Dekker Inc., New York (2000) p.128-145.
29. J. George, S.S. Bhagawan, S. Thomas. Thermogravimetric and dynamic mechanical thermal analysis of pineapple fibre reinforced polyethylene composites. Journal of Thermal Analysis 1996; 47:1121-1140.
DOI: 10.1007/BF01979452
30. H-S. Kim, S. Kim, H-J, Kim, H-S, Yang. Thermal properties of bio-flour-filled polyolefin composites with different compatibilizing agent type and content. Thermochimica Acta 2006; 451:181-188.
DOI: 10.1016/j.tca.2006.09.013
31. U. Gaur, B. Wunderlich. The glass transition temperature of polyethylene. Macromolecules 1980; 13:445-446.
DOI: 10.1021/ma60074a045
32. C. Vasile, M. Pascu. Practical Guide to Polyethylene. Rapra Technology Ltd, Shropshire (2005) p.41-45.
33. R.O. Sirotkin, N.W. Brooks. The dynamic mechanical relaxation behaviour of polyethylene copolymers cast from solution. Polymer 2001; 42:9801-9808.
DOI: 10.1016/S0032-3861(01)00535-3

Chapter 5

Morphology, thermal and dynamic mechanical properties of poly(lactic acid)/sisal whiskers nanocomposites

Abstract

In this study, sisal whiskers were used as biobased nanofillers to prepare polylactic acid based nanocomposites. Sisal whiskers (nanofibres) were obtained from sisal fibres *via* a sulphuric acid hydrolysis method. Freeze-drying of the aqueous whiskers suspension was carried out to reduce the strong hydrogen bonding between the nanofibres in the dry state and to obtain loosely packed dry sisal whiskers. The nanocomposite samples were prepared by a melt mixing method, followed by hot melt pressing. The effect of the freeze-drying of the nanofibres, the treatments of the samples with maleic anhydride (MA)/dicumyl peroxide (DCP) and with DCP, and the premixing of the powdered components, on the dispersion of the sisal whiskers within the PLA matrix and on the morphology, as well as the thermal, and dynamic mechanical properties, of the resultant nanocomposites were investigated. TEM micrographs show that the acid hydrolysis method has led to separation of the whiskers, which had an approximate length and diameter of 195 nm and 15 nm respectively. The TEM images of the nanocomposites show similar dispersion of the whiskers in the PLA matrix, whether untreated or MA/DCP or DCP treated. It was found that the crystallization behaviour of the PLA matrix changed somewhat depending on whether the samples were treated or not. The TGA results show a slight decrease in the thermal stabilities of the untreated and the MA/DCP treated nanocomposite samples compared to that of the neat PLA, whereas the DCP treatment slightly improved the thermal stability of the nanocomposites. The storage modulus of the nanocomposites increased over the investigated temperature region, and the incorporation of sisal whiskers reduced the intensity of the glass transition at 67 ºC.

Keywords: Biodegradable polymer, PLA; sisal whiskers; nanocomposites; freeze-drying; morphology; thermal properties; dynamic mechanical properties

5.1 Introduction

Due to the rising concern towards environmental issues, the present tendency in fibre-reinforced polymer composites is to use materials that are biodegradable, environmentally friendly, sustainable, and renewable. Therefore, over the last decades, bio-composites, which are a combination of cellulose fibres with polymer matrices from both nonrenewable resources (petroleum-based) and renewable resources, have found increasing attention as alternatives to glass fibre reinforced composites [1-7].

Compared to synthetic fibres, natural fibres have many advantages, such as low density and cost, high specific strength and modulus, wide availability, low energy consumption, biodegradability, recyclability, and renewability [1-4]. In recent years, the extraction and production of nano-scale cellulose fibres from different cellulosic sources (e.g. wood, bacterial cellulose, tunicate, etc.) has gained increasing attention due to their abundance, high strength and stiffness, low weight, and biodegradability. Cellulose whiskers that are also known as nanowhiskers, monocrystals, or nanocrystals, are elongated crystalline rod-like nanoparticles that can be extracted from plant material or animal sources (such as bacteria and tunicate) through controlled acid hydrolysis. Their precise morphological characteristics (e.g., length, width, and shape) are usually studied by microscopy (TEM, AFM, E-SEM) or light scattering techniques, including small angle neutron scattering (SANS). It has been reported that their diameters range from 2 to 20 nm, but there is a wide length distribution from 100 to 600 nm and even more than 1000 nm was reported in some cases. The dimensions of the cellulose whiskers depend on the origin of the cellulose, as well as on the conditions of the acid hydrolysis process such as time, temperature, acid concentration, and the nature of the acid. Sulphuric and hydrochloric acids have been extensively used for whiskers preparation, but phosphoric and hydrobromic acids have also been reported for such purposes. The amorphous regions in the cellulose chains are more susceptible to acid attack, which promotes the hydrolytic cleavage of the glycosidic bonds and finally releasing individual crystallites. It was observed that the acid hydrolysis of cellulose by using sulphuric acid produced more stable colloidal suspensions of whiskers compared to hydrochloric acid. This can be explained by the fact that the sulphuric acid-treated cellulose whiskers have an important charge density on the surface compared to hydrochloric acid-treated cellulose whiskers, which are uncharged. The electrostatic repulsion between the negatively charged

particles on the surface leads to whiskers suspensions that neither precipitate nor flocculate [8-16]. Thanks to their good mechanical properties coupled with their large surface areas as well as their availability, renewability, recyclability, and biodegradability, cellulose whiskers have a lot of potential as reinforcing materials in polymer matrices [8-11].

Biodegradable/biobased polymers such as poly(lactic acid) (PLA), polyhydroxybutyrate (PHB), soy-based plastic, aliphatic esters, poly(vinyl alcohol), cellulose esters, and starch plastic are a new generation of biobased polymeric products that can be obtained from renewable resources or synthesized from petroleum-based chemicals. They have offered scientists a possible solution to waste disposal problems associated with traditional petroleum-derived plastics. Biodegradable polymers may be defined as those that undergo microbially induced chain scission leading to photodegradation, oxidation, and hydrolysis, which can alter the polymer during the degradation process [17,18]. One of the most promising biobased and biodegradable polymers is poly(lactic acid) (PLA), which has attracted the attention of polymer scientists during the last decade as a potential biopolymer to substitute the conventional petroleum based plastics. It belongs to the family of aliphatic polyesters commonly made from α-hydroxy acids. PLA is made up of lactic acid (2-hydroxy propionic acid) as a building block, which is produced by converting sugar or starch obtained from vegetable sources using either bacterial fermentation or a petrochemical route. Lactic acid is a highly water-soluble, three-carbon chiral acid that exists as two optically active configurations, namely L- and D-isomers. The designation L- and D- are used to represent the ability of the molecule to rotate the plane of the polarized light either clockwise (L-) or counterclockwise (D-). The properties of PLA depend on its molecular characteristics, as well as on the presence of ordered structures, such as crystalline thickness, crystallinity, spherulite size, morphology, and degree of chain orientation. The optical purity (which indicates whether the PLA consists of only one optical isomer or a mixture of the two) of PLA has many profound effects on the structural, thermal, barrier, and mechanical properties of the polymer. Depending on the composition of the optically active isomers (L- or D-), as well as on the thermal history, PLA in the solid state can be either semi-crystalline or totally amorphous [19-24].

One drawback of using cellulose whiskers as reinforcement in composites is the difficulty to disperse them uniformly in the non-polar medium because of their polar surfaces. So far, only

aqueous or polar systems have been used successfully as matrices for the dispersion of cellulose whiskers because of the hydrophilic nature of both components [25,26]. Cellulose whiskers reinforced hydrophobic polymer matrices have not been studied extensively due to poor dispersion/compatibility, which results in agglomeration of the fibres and deterioration of the mechanical properties of the resulting composites. Various methods, which include modification of the cellulose whiskers' surfaces [27-29], addition of surfactants [30,31], using compatibilizers [32], and modification of the polymer matrices [33], have been tried to overcome the poor dispersion and enhance the interfacial bonding in these systems.

Although polymer melt processing techniques are the most suitable and practical methods for industrial applications, only a few papers have been published on melt processing of cellulose whiskers and biodegradable polyester matrices (PLA) in the dry phase [34,35]. Therefore, in this study, sisal whiskers reinforced poly(lactic acid) nanocomposites were prepared by a melt mixing method, followed by hot melt pressing. The influence of the freeze-drying of the nanofibres, the treatments of the samples with MA/DCP and with DCP, and the premixing of the powdered components, on the dispersion of the cellulosic whiskers within the PLA matrix and the morphology, as well as the thermal, and the dynamic mechanical properties of the nanocomposites were investigated.

5.2 Experimental

5.2.1 Materials

Polylactic acid (PLA), NatureWorks® PLA polymer 4032D (Cargill Dow LLC, Minnetonka, MN, USA), was used as a polymer matrix. Sisal fibres were obtained from the National Sisal Marketing Committee in Pietermaritzburg, South Africa. Maleic anhydride (assay ≥ 99%) and sulphuric acid (assay 95-99%) were all supplied by Merck Chemicals (Pty) Ltd. Dicumyl peroxide (assay 40%) was purchased from Shalom Chemicals, South Africa. Sodium hydroxide pellets (assay 97%) was supplied by Associated Chemical Enterprises (Pty) Ltd. Sodium hypochlorite was obtained from the local markets (JIK-household bleach, which contains sodium hypochlorite as an active ingredient with a concentration of 3.5% (w/v), Reckitte Benckiser (Pty) Ltd., South Africa).

5.2.2 Preparation of sisal nanofibres (nano-whiskers)

Sisal fibres were cut with a Tecator sample grinder (Cyclotec-1093 sample mill, made in Sweden) until fine particulate fibres were obtained. The fibres were then treated with a 4 wt% sodium hydroxide solution at 80 ºC in a water bath for 2 h under mechanical stirring. This treatment was done three times to remove constituents other than cellulose from the fibres. After each treatment, the fibres were filtered and washed with distilled water until the akali was removed. A subsequent bleaching treatment was carried out to bleach the fibres. The solution used in this treatment consisted of equal parts of an acetate buffer (27 g of NaOH and 75 mL glacial acetic acid, diluted to 1 L using distilled water) and aqueous chlorite (1.7 wt % $NaClO_2$ in water). The bleaching treatment was performed at 80 ºC for 4 h under mechanical stirring and was repeated four times. After each treatment, the fibres were filtered and washed with distilled water. The fibres were subsequently dried in an oven at 60 ºC for 24 h. The dried fibres were ground to a fine powder using a Philips grinder (HR2021-400 W). Acid hydrolysis of the fine fibre powder was performed at 50 ºC in a water bath, for about 50 min by using a 65 wt% sulphuric acid, under mechanical stirring. The fibre content during all these chemical treatments was in the range 5-6 wt%. The suspension was diluted with ice cubes to stop the reaction. Successive washings in a centrifuge (HARRIER 18/80 Refrigerated Centrifuge, Model MSB080.CR1.K, made in the UK) at 10 ºC and 5000 rpm for 30 min were then performed. Dialysis (SnakeSkin® Pleated Dialysis Tubing-3,500 MWCO) against distilled water was done to remove the free acid in the dispersion. This was verified by determining the neutrality of the dialysis effluent. Complete dispersion of nano-whiskers was obtained by a sonication step using a Cole-Parmer Ultrasonic Processor (Model CP 505, 500 Watts). The dispersion was then filtered through a No. 1 fritted glass filter to remove residual aggregates, and then freeze-dried using a Freeze Dryer (Flex-Dry™ µP-Microprocessor Control, FTS Systems, Inc., USA).

5.2.3 Preparation of polylactic acid (PLA) nanocomposites

The powdered PLA was dried first in an oven at 80 °C for 4 hours prior to sample preparation and then the untreated PLA nanocomposites were prepared by mechanical mixing of the powdered polymer with different amounts (2 and 6 wt %) of the freeze-dried whiskers. Each of the mechanically mixed samples was transferred into a 55 mL mixing chamber of a

Plastograph-W50EHT (Brabender®OHG, Germany) and then the mixing was conducted for 10 min at 180 ºC and a rotor speed of 80 rpm. The melt pressing of the prepared samples was carried out at 180 ºC and 50 bar for 5 min to form sheets with dimensions of 130 x 130 x 1.5 mm. Pure PLA and the treated samples were prepared under the same conditions. In the case of the MA/DCP treated samples, both MA and DCP were added first to PLA/sisal whiskers and thoroughly mixed before they were transferred to the mixer. The percentages of MA and DCP in all the samples were kept at 1 wt % (based on the weight of PLA) and 20 wt % (based on the weight of MA), respectively. The DCP treated samples were prepared by the addition of 0.15 phr DCP to the mixture (PLA/sisal whiskers) one minute before the end of the mixing time.

5.2.4 Characterization methods

The sisal whiskers suspension was examined using a transmission electron microscope, Philips (FEI) CM100 (The Netherlands), to confirm the separation of the nanofibres and to determine their dimensions. A drop of the diluted suspension was allowed to dry on a carbon coated grid at ambient conditions and then the sample was stained using a uranyl acetate solution (2 wt%). The stained sample was observed using an accelerating voltage of 60 kV.
The nanocomposites were examined by cutting very thin sections from the samples using ultramicrotomy. A 2 % uranyl acetate solution was used to stain these sections before they were viewed under TEM.

ATR-FTIR spectra of the pure PLA, sisal whiskers, untreated samples, as well as MA/DCP and DCP treated samples were obtained using a Perkin Elmer Spectrum 100 FTIR spectrometer. The samples were analyzed over a range of 600-4000 cm^{-1} with a resolution of 4 cm^{-1}. All the spectra were averaged over 16 scans.

DSC analyses were performed with a Perkin Elmer DSC7 differential scanning calorimeter. Each sample of 5 to 10 mg weight was sealed in an aluminum pan and heated under nitrogen flow (20 mL min^{-1}) from 25 to 190 ºC at a heating rate of 10 ºC min^{-1}, and kept at this temperature for 1 min to erase the thermal history. Subsequently, the sample was cooled and re-heated under the same conditions. At least three separate measurements were made to ensure reproducibility. The glass transition, cold crystallization, and melting temperatures as

well as the melting and cold crystallization enthalpies of the samples were determined from the second heating runs as the average of three measurements. The percent crystallinity of the melting and cold crystallization steps, as well as the overall crystallinity of the PLA and its nanocomposites were calculated according to Equations 1, 2, and 3.

$$\text{Crystallinity of the melting step } (X_m)\ \% = (\Delta H_m / (w_{PLA} \times \Delta H^o_m)) \times 100 \quad (1)$$

$$\text{Crystallinity of the cold crystallization step } (X_{cc})\ \% = (\Delta H_{cc} / (w_{PLA} \times \Delta H^o_m)) \times 100 \quad (2)$$

$$\text{Overall crystallinity } (X_m\text{-}X_{cc})\ \% = ((\Delta H_m - \Delta H_{cc}) / (w_{PLA} \times \Delta H^o_m)) \times 100 \quad (3)$$

where ΔH_m (J g^{-1}) and ΔH_{cc} (J g^{-1}) are the enthalpies of fusion and cold crystallization, respectively, ΔH_m^0 = 93.1 J g^{-1} is the heat of fusion for 100% crystalline polylactic acid (PLLA or PDLA homopolymers) [36], and w_{PLA} is the weight fraction of PLA in the nanocomposite. The calculated melting and cold crystallization enthalpies for the composites were determined from the observed melting and cold crystallization enthalpies of the neat PLA, and the weight fraction of the PLA in the nanocomposites, according to Equations 4 and 5.

$$\Delta H_m^{calc} = w_{PLA} \times \Delta H_m^{obs} \quad (4)$$

$$\Delta H_{cc}^{calc} = w_{PLA} \times \Delta H_{cc}^{obs} \quad (5)$$

Thermogravimetric analysis was used to study the thermal stabilities of the neat PLA, the sisal whiskers, and the nanocomposite samples in a Perkin Elmer TGA7 thermogravimetric analyzer. Samples with weights in the range of 5 to 10 mg were heated under a flowing nitrogen atmosphere (20 mL min^{-1}) from 30 ºC to 550 ºC at a heating rate of 10 ºC min^{-1}, and the corresponding mass loss was recorded.

The dynamic mechanical properties (storage and loss modulus, as well as dissipation factor) of the samples were determined in a Perkin Elmer Diamond DMA dynamic mechanical analyzer. The measurements were carried out in the dual cantilever-bending mode and the corresponding viscoelastic properties were determined as a function of temperature. Rectangular bar specimens with dimensions of 50 x 10 x 1.4 mm were used for this study. The samples were heated under nitrogen flow (30 mL min^{-1}) from -10 ºC to 150 ºC at a heating rate of 3 ºC min^{-1}, and at a frequency of 1 Hz.

5.3 Results and discussion

Figure 5.1 shows the TEM micrographs of the sisal whiskers at different magnifications. The acid hydrolysis process and the subsequent steps successfully led to the separation of the crystalline parts of the cellulose (rod-like fragments). At a higher magnification (Figure 5.1b), it was possible to clearly see the individual whiskers. The whiskers possessed an average length of approximately 195 nm and a diameter of approximately 15 nm.

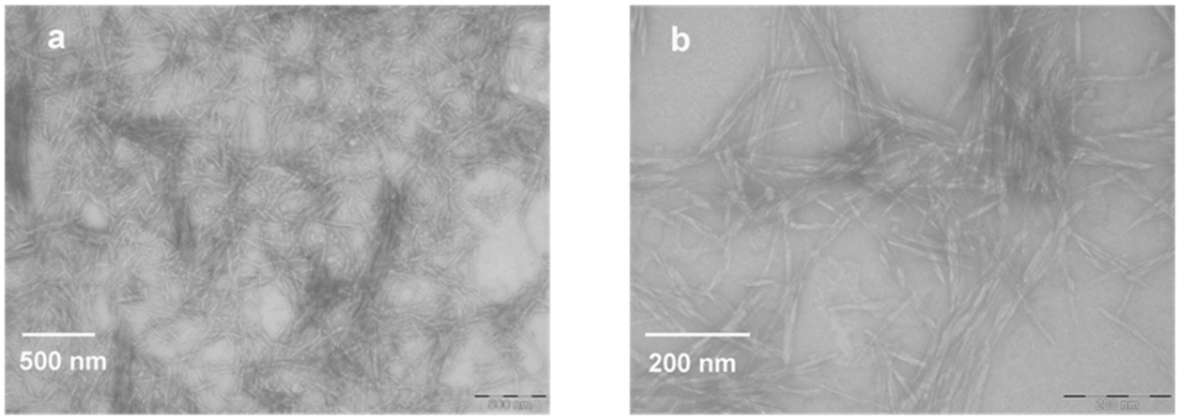

Figure 5.1 TEM images of sisal whiskers

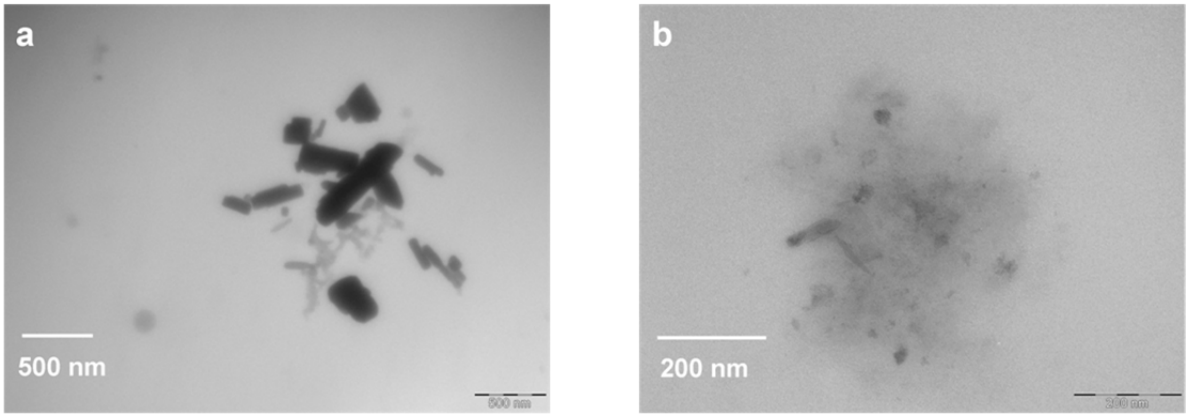

Figure 5.2 TEM images of the untreated 98/2 w/w PLA/sisal whiskers nanocomposite at two different magnifications

The dispersion of the sisal whiskers within the PLA matrix was examined using TEM. Figure 5.2 shows the TEM images of the untreated nanocomposite sample (98/2 w/w PLA/sisal whiskers) at different magnifications. It is possible to conclude from Figure 5.2 that even for the untreated sample, although not completely dispersed, a number of the sisal whiskers were

separated to some extent. A similar morphology was observed for the treated nanocomposites (micrographs not shown) and the treatment did not seem to significantly improve the dispersion.

FTIR analyses were carried out to examine the possible interactions between the different components of the untreated as well as the MA/DCP and DCP treated nanocomposites. Figure 5.3 represents the FTIR spectra of the sisal whiskers, the neat PLA, and the untreated as well as the treated nanocomposites. It is obvious from Figure 5.3 that the spectrum of the sisal whiskers is a typical cellulose spectrum [37-39]. All the characteristic absorption peaks of the neat PLA at 2997 cm^{-1} and 2946 cm^{-1} (-CH_3 asymmetric and symmetric stretching vibrations), 1749 cm^{-1} (-C═O), 1452, 1382, and 1360 cm^{-1} (-CH_3 and -CH bending vibrations), 1266 cm^{-1} (stretching vibration of -COC), 1181, 1127, and 1044 cm^{-1} (asymmetric and symmetric bending vibrations of -COC as well as -CH_3 rocking), 956 cm^{-1} (C-C stretching vibration), and 867 cm^{-1} (C-COO) are obvious in Figure 5.3 [40]. The FTIR spectra of the untreated and the treated nanocomposites were almost identical and no changes in the peaks intensities or a shift in the peak positions could be noticed. The only difference from the spectrum of the neat PLA is the presence of the absorption peak around 3340 cm^{-1}, which is the stretching vibration of –OH originally present in the spectrum of the sisal whiskers. No distinctive absorption peaks, indicative of grafted MA, could be seen in the spectrum of the MA treated samples. This is possibly due to the low percentage of the added MA, which was 1 wt% based on the weight of PLA.

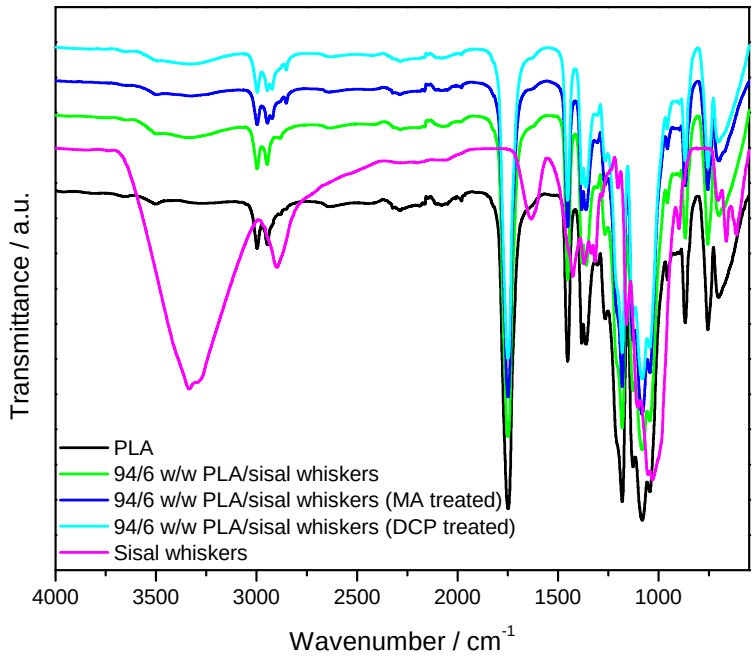

Figure 5.3 ATR-FTIR spectra of the sisal whiskers, neat PLA, the untreated as well as MA/DCP and DCP treated nanocomposites (94/6 w/w PLA/sisal whiskers)

DSC measurements were conducted to investigate the effect of sisal whiskers loadings and the addition of MA/DCP or DCP on the thermal behaviour of the PLA. The DSC curves of the neat PLA and its nanocomposites are shown in Figure 5.4. Table 5.1 summarizes the values of the glass transition, cold crystallization, and melting temperatures, which were obtained from the DSC curves. The observed and the calculated melting and cold crystallization enthalpies are shown in Table 5.2. Table 5.3 shows the crystallinity values of the PLA and its nanocomposite samples. It is clear from Figure 5.4 and Table 5.1 that all the samples show well-defined glass transition (T_g), cold crystallization (T_{cc}), and melting (T_m) transitions. Concerning the untreated nanocomposites, the incorporation of sisal whiskers did not affect the values of T_g, T_{cc}, and T_m significantly (Table 5.1). However, a slight increase in the percent crystallinity (X_m) with the incorporation of the whiskers is observed (Table 5.3). The observed and calculated melting enthalpies were almost the same for PLA and the untreated nanocomposites, but the observed cold crystallization enthalpies were lower than the calculated ones for the untreated composites (Table 5.2). Fewer crystals were therefore formed during cold crystallization, indicating that the initial crystallinity was higher for the

nanocomposites. The reason for this is probably that the nanowhiskers to some extent acted as nucleating sites for the PLA chains during the nanocomposite preparation.

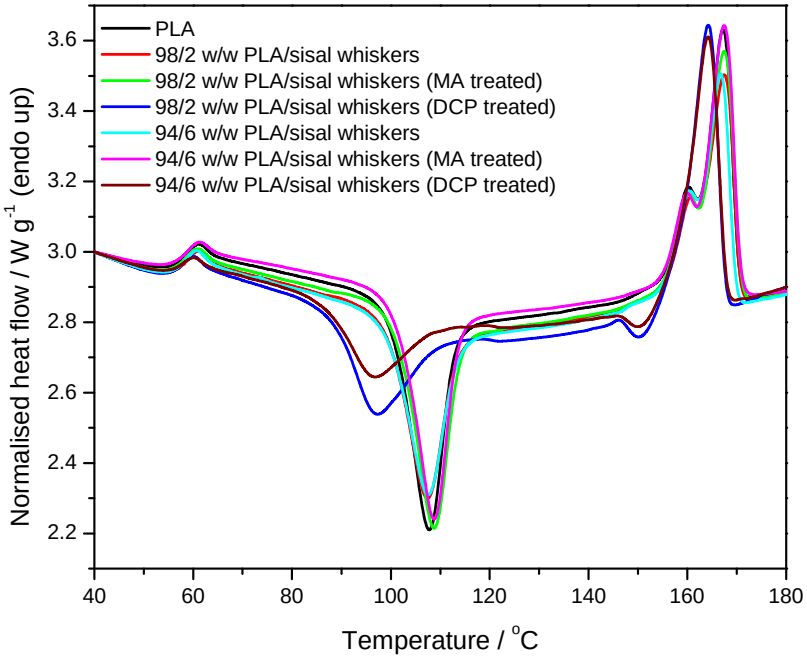

Figure 5.4 DSC curves of the neat PLA and its untreated and treated nanocomposites

Table 5.1 DSC second heating results for PLA and its sisal whiskers nanocomposites

PLA/sisal whiskers (w/w)	T_g / °C	T_{cc} / °C	T_m / °C
100/0	60.5 ± 0.1	107.5 ± 0.4	167.0 ± 0.5
98/2	60.6 ± 0.2	107.2 ± 0.2	167.1 ± 0.5
94/6	60.9 ± 0.5	108.0 ± 0.5	167.5 ± 0.7
Maleic anhydride grafted samples			
98/2	60.5 ± 0.1	108.7 ± 0.5	167.2 ± 0.3
94/6	60.4 ± 0.5	108.4 ± 0.5	166.7 ± 0.8
DCP treated samples			
98/2	59.8 ± 0.5	97.3 ± 0.6	164.7 ± 0.6
94/6	59.8 ± 0.6	96.6 ± 0.8	164.8 ± 1.0

The MA/DCP treated samples were found to have almost the same values of T_g, T_{cc}, and T_m than PLA and the untreated samples. Although the cold crystallization and melting enthalpies of the MA/DCP treated composites are higher than those of the untreated samples, their initial crystallinities (calculated as X_m - X_{cc}) were of the same order as those of the untreated nanocomposites. It seems as if the MA/DCP treatment did not really change the influence of the nanowhiskers on the crystallization behaviour of the PLA.

Table 5.2 The observed and the calculated melting and cold crystallization enthalpies of the pure PLA and its sisal whiskers nanocomposites

PLA/sisal whiskers (w/w)	ΔH_m / J g^{-1}	ΔH_{cc} / J g^{-1}	ΔH_m^{calc} / J g^{-1}	ΔH_{cc}^{calc} / J g^{-1}
100/0	34.9 ± 0.4	-28.7 ± 0.2	34.9	-28.7
98/2	32.9 ± 0.6	-24.3 ± 0.5	34.2	-28.1
94/6	31.2 ± 0.5	-23.0 ± 0.8	32.8	-27.0
Maleic anhydride grafted samples				
98/2	35.2 ± 0.7	-27.5 ± 0.9	34.2	-28.1
94/6	35.3 ± 0.7	-27.4 ± 1.0	32.8	-27.0
DCP treated samples				
98/2	31.5 ± 0.5	-18.0 ± 1.5	34.2	-28.1
94/6	30.6 ± 0.6	-13.0 ± 0.6	32.8	-27.0

The treatment of the nanocomposites with DCP, on the contrary, gave rise to significantly lower T_{cc} and ΔH_{cc}, while the T_m and ΔH_m were slightly lower. The initial crystallinities (calculated as X_m - X_{cc}) of the nanocomposites were, however, appreciably higher. These results indicate that the number of crystallites increased, while the lamellar thickness decreased. This can be attributed to grafting between the PLA chains and the sisal whiskers, giving rise to increased effectiveness of the sisal whiskers as nucleating agents. This resulted in the formation of more, but smaller and more imperfect crystallites. This could also explain the disappearance and the shift of the first melting peak (Figure 5.4) in the peroxide treated samples, which appears as a small shoulder in the DSC curves of the other samples.

Table 5.3 Crystallinity values of PLA and its nanocomposites samples

PLA/sisal whiskers (w/w)	X_m / %	X_{cc} / %	$X_m - X_{cc}$ / %
100/0	37.5	30.8	6.7
98/2	36.1	26.7	9.4
94/6	35.7	26.3	9.4
Maleic anhydride grafted samples			
98/2	38.6	30.2	8.4
94/6	40.3	31.3	9.0
DCP treated samples			
98/2	34.5	19.7	14.8
94/6	35.0	14.9	20.1

Figure 5.5 shows the residual mass % as a function of temperature for the sisal whiskers, neat PLA, as well as the untreated and treated nanocomposites. The TG analyses were carried out in the temperature range 30 °C to 550 °C, but only the temperature range where significant degradation takes place is shown in Figure 5.5. The TGA curve of the sisal whiskers shows a multistep degradation behaviour. The first small mass loss step at temperatures lower than 200 °C is due to moisture loss. The second degradation step starts at about 250 °C and almost 10 wt% of the whiskers was degraded at this temperature. Most of the degradation took place between 290 and 350 °C. There is also a third degradation step accompanied by a slow mass loss that was incomplete at the end of the analysis. These degradation steps are corresponding to the thermal degradation of glycosidic links and α-cellulose [42,43].

For neat PLA the TGA curve shows only one degradation step between 300 and 360 °C. The TGA curves of the nanocomposites (untreated and treated) also show one degradation step (Figure 5.5), but their thermal stabilities differ slightly. The thermal stabilities of the untreated and the MA/DCP treated nanocomposites were found to be lower than that of the neat PLA and there were no significant differences between their thermal stabilities. The DCP treated nanocomposites show slightly higher thermal stabilities than the neat PLA and the other nanocomposite. This could be attributed to the formation of crosslinked structures, which reduce the chains mobility and inhibits the chain unzipping during the propagation of the degradation process. All the nanocomposites displayed lower thermal stabilities at higher

whiskers loadings, which could be due to the lower thermal stability of the cellulosic whiskers [44].

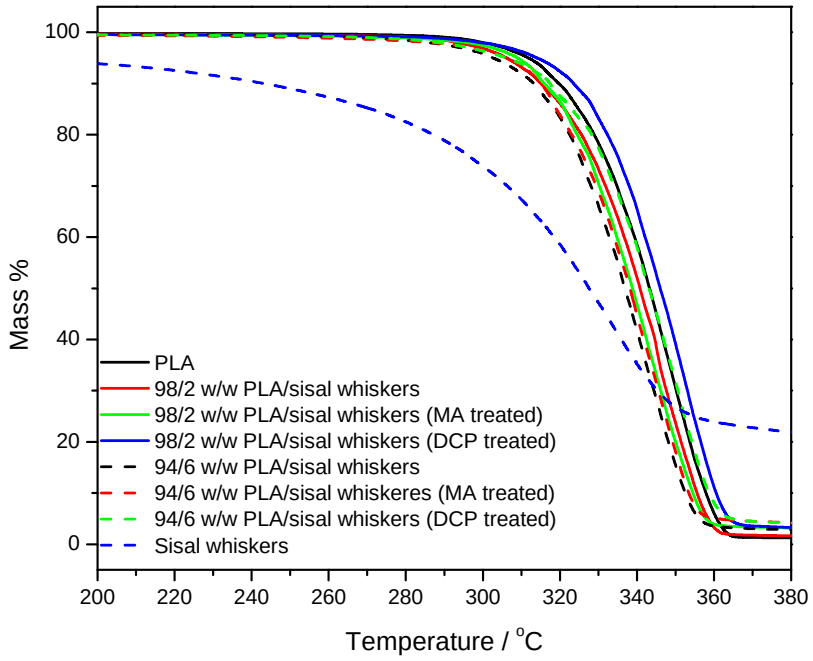

Figure 5.5 TGA curves of the sisal whiskers, pure PLA, and its untreated and treated nanocomposites

Dynamic mechanical analysis was carried out to investigate the effect of the sisal whiskers loadings and different treatments on the viscoelastic properties of the PLA nanocomposites. Figures 5.6 and 5.7 show the storage modulus and the mechanical loss factor (tan δ) as a function of temperature. In general, the storage moduli of the nanocomposites were higher than that of the neat PLA over the temperature range used in this study. Moreover, with increasing whiskers content the storage moduli of the nanocomposites were further increased. This could be attributed to the reinforcing effect of the sisal whiskers and to the higher modulus of the whiskers themselves. It does not seem as if the treatments had much influence on the storage modulus values. In the case of the DCP treated PLA the storage modulus values are higher than those of the neat PLA and similar to the untreated and the maleic anhydride treated (98/2 w/w PLA/sisal whiskers) samples. This could be ascribed to the presence of the crosslinks brought about by DCP treatment, which should impart more

rigidity and stiffen the PLA matrix. Although the presence of crosslinking is expected to reduce the crystallinity of the PLA and in turn its modulus, the crosslinks seem to play a bigger role than the crystallinity. Above the glass transition temperature (67 °C), the curves of the storage modulus show the evolution of the cold crystallization process where the PLA chain segments acquired some translational mobility and crystallization occurred. In general, it can be observed from Figure 5.6 that all the nanocomposites had higher storage modulus values in this temperature range compared to neat PLA, which could be due to restriction of the polymer chain mobility by the presence of the more rigid whiskers.

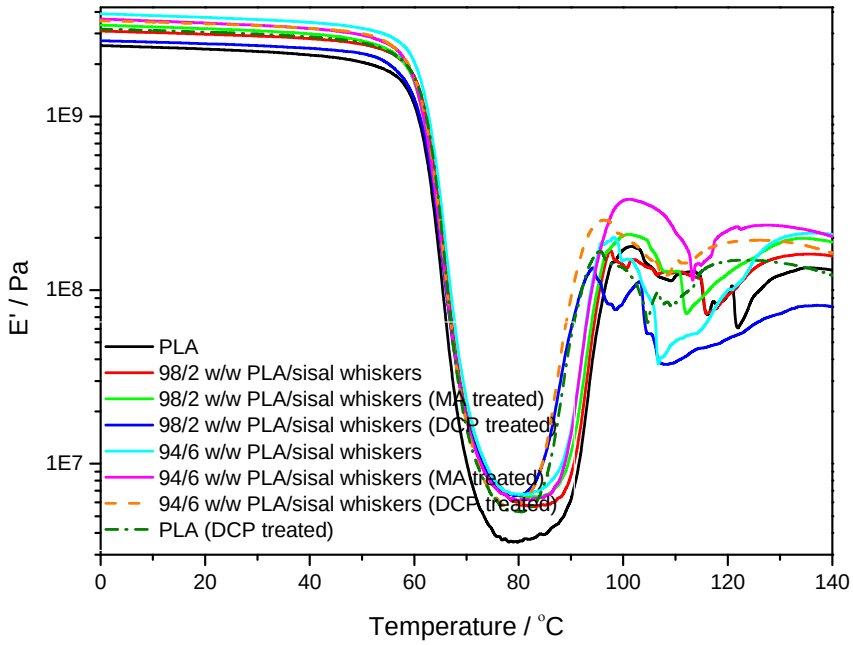

Figure 5.6 DMA storage modulus curves for pure PLA and its untreated and treated nanocomposites

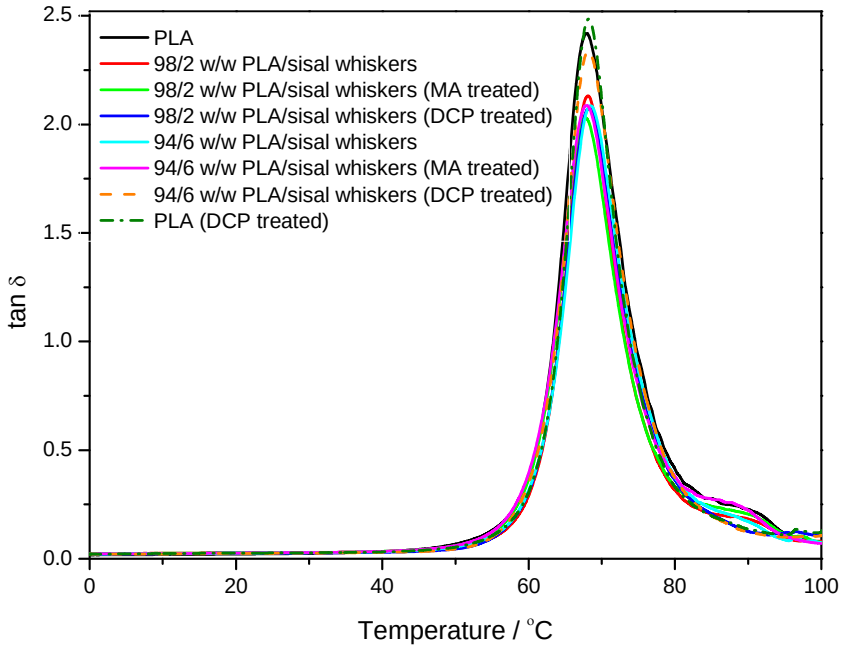

Figure 5.7 DMA tan δ curves for pure PLA and its untreated and treated nanocomposites

5.4 Conclusions

Biobased nanocomposites of sisal whiskers reinforced PLA were successfully prepared by melt mixing and hot melt pressing. The morphology, thermal, and dynamic mechanical properties of the untreated and (MA/DCP and DCP) treated nanocomposites were investigated. It was found that the treatments of the samples did not significantly change the dispersion of the whiskers within the PLA matrix. However, the freezing of the whiskers and the premixing of the components before melt mixing was a relatively effective approach to overcome the difficulties of the dispersion of the cellulose whiskers within the non-polar polymer. The incorporation of sisal whiskers altered the crystallization and the melting behaviour of the PLA depending on whether the samples were treated or not, and on the type of treatment. The thermal stabilities of the nanocomposites depended on the presence and amount of sisal whiskers, and on the type of compatibilizing treatment used. The presence of the whiskers increased the stiffness of the nanocomposites, but reduced the intensity of the glass transition relaxation. However, no trend was observed in terms of the influence of the compatibilizing treatment on the viscoelastic properties of the nanocomposites.

5.5 References

1. P. Wambua, J. Ivens, I. Verpoest. Natural fibres: Can they replace glass in fibre reinforced plastics? Composites Science and Technology 2003; 63:1259-1264.
   DOI: 10.1016/S0266-3538(03)00096-4
2. A.K. Bledzki, J. Gassan. Composites reinforced with cellulose based fibres. Progress in Polymer Science 1999; 24:221-274.
   DOI: 10.1016/S0079-6700(98)00018-5
3. A.K. Mohanty, M. Mishra, G. Hinrichsen. Biofibres, biodegradable polymers and biocomposites: An overview. Macromolecular Materials and Engineering 2000; 276/277:1-24.
   DOI: 10.1002/(SICI)1439-2054(20000301)276
4. J.M. John, S. Thomas. Biofibres and biocomposites. Carbohydrate Polymers 2008; 71:343-364.
   DOI: 10.1016/j.carbpol.2007.05.040
5. N.D. Saheb, P.J. Jog. Natural fibre polymer composites: A review. Advances in Polymer Technology 1999; 18:351-363.
   DOI: 10.1002/(SICI)1098-2329(199924)18
6. P.A. Fowler, J.M. Hughes, R.M. Elias. Biocomposites: Technology, environmental credentials, and market forces. Journal of the Science of Food and Agriculture 2006; 86:1781-1789.
   DOI: 10.1002/jsfa.2558
7. Y. Li, Y-M. Mai, L. Ye. Sisal fibre and its composites: A review of recent developments. Composites Science and Technology 2000; 60:2037-2055.
   DOI: 10.1016/S0266-3538(00)00101-9
8. S. Kamel. Nanotechnology and its application in lignocellulosic composites, a mini review. eXPRESS Polymer Letters 2007; 1:546-575.
   DOI: 10.3144/expresspolymlett.2007.78
9. S.J. Eichhorn, A. Dufresne, M. Aranguren, N.E. Marcovich, J.R. Capadona, S.J. Rowan, C. Weder, W. Thielemans, M. Roman, S. Renneckar, W. Gindl, S. Veigel, J. Keckes, H. Yano, K. Abe, M. Nogi, A.N. Nakagaito, A. Mangalam, J. Simonsen, A.S. Benight, A. Bismarck, L.A. Berglund, T. Peijs. Review: Current international research

into cellulose nanofibres and nanocomposites. Journal of Materials of Science 2010; 45:1-33.
DOI: 10.1007/s10853-009-3874-0

10. M.A.S. Aziz Samir, F. Alloin, A. Dufresne. Review of recent research into cellulosic whiskers, their properties, and their application in nanocomposites field. Biomacromolecules 2005; 6:612-626.
DOI: 10.1021/bm0493685

11. Y. Habibi, L.A. Lucia, O.J. Rojas. Cellulose nanocrystals: Chemistry, self-assembly, and application. Chemical Reviews 2010; 110:3479-3500.
DOI: 10.1021/cr900339w

12. H. Håkansson, P. Ahlgren. Acid hydrolysis of some industrial pulps: Effect of hydrolysis conditions and raw material. Cellulose 2005; 12:177-183.
DOI: 10.1007/s10570-004-1038-6

13. M.M. de Souza Lima, R. Borsali. Rodlike cellulose microcrystals: Structure, properties, and applications. Macromolecular Rapid Communications 2004; 25:771-787.
DOI: 10.1002/marc.200300268

14. S. Beck-Candanedo, M. Roman, D.G. Gray. Effect of reaction conditions on the properties and behavior of wood cellulose nanocrystals suspensions. Biomacromolecules 2005; 6:1048-1054.
DOI: 10.1021/bm049300p

15. I. Kvien, B.S. Tanem, K. Oksman. Characterization of cellulose whiskers and their nanocomposites by atomic force and electron microscopy. Biomacromolecules 2005; 6:3160-3165.
DOI: 10.1021/bm050479t

16. D. Bondeson, A. Mathew, K. Oksman. Optimization of the isolation of nanocrystals from microcrystalline cellulose by acid hydrolysis. Cellulose 2006; 13:171-180.
DOI: 10.1007/s10570-006-9061-4

17. A.K. Mohanty, M. Misra, L.T. Drzal, E. Selke, B.R. Harte, G. Hinrichsen. Natural fibres, biopolymers, and biocomposites: An introduction. In: A.K. Mohanty, M. Misra, L.T. Drzal (Eds.). Natural Fibres, Biopolymers, and Biocomposites. Taylor & Francis Group: Boca Raton (2005) p.1-6.

18. M. Mitrus, A. Wojtowicz, L. Moscicki. Biodegradable polymers and their utility. In: P.B.M. Leon, L. Moscicki. Thermoplastic starch: A Green Material for Various Industries. WILEY-VCH Verlag GmbH & CO. KGaA: Weinheim (2009) p.1-3.
19. D.E. Henton, P. Gruber, J. Lunt, J. Randall. Polylactic acid technology. In: A.K. Mohanty, M. Misra, L.T. Drzal (Eds.). Natural Fibres, Biopolymers, and Biocomposites. Taylor & Francis Group: Boca Raton (2005) p.1-37.
20. S. Inkinen, M. Hakkarainen, A-C. Albertsson, A. Södergård. From lactic acid to poly(lactic acid) (PLA): Characterization and analysis of PLA and its precursors. Biomacromolecules 2011; 12:523-532.
DOI: 10.1021/bm101302t
21. Y. Cheng, S. Deng, P. Chen, R. Ruan. Polylactic acid (PLA) synthesis and modifications: A review. Frontiers of Chemistry in China 2009; 4:259-264.
DOI: 10.1007/s11458-009-0092-x,
22. R.M. Rasal. A.V. Janorkar, D.E. Hirt. Poly(lactic acid) modifications. Progress in Polymer Science 2010; 35:338-356.
DOI: 10.1016/j.progpolymsci.2009.12.003
23. L. Avérous. Polylactic acid: Synthesis, properties and applications. In: M.N. Belgacem, A. Gandini (Eds.). Monomers, Polymers and Composites from Renewable Resources. Elsevier Ltd.: Amsterdam (2008) p.433-442.
24. L-T. Lim, R. Auras, M. Rubino. Processing technologies for poly(lactic acid). Progress in Polymer Science 2008; 33:820-852.
DOI: 10.1016/j.progpolymsci.2008.05.004
25. N.L. Garcia de Rodriguez, W. Thielemans, A. Dufresne. Sisal cellulose whiskers reinforced polyvinyl acetate nanocomposites. Cellulose 2006; 13:261-270.
DOI: 10.1007/s10570-005-9039-7
26. A.J. Uddin, J. Araki, Y. Gotoh. Characterization of the poly(vinyl alcohol)/cellulose whisker gel spun fibers. Composites Part A 2011; 42:741-747.
DOI: 10.1016/j.compositesa.2011.02.012
27. N. Ljungberg, C. Bonini, F. Bortolussi, C. Boisson, L. Heux, J.Y. Cavaillé. New nanocomposites materials reinforced with cellulose whiskers in atactic polypropylene: Effect of surface and dispersion characteristics. Biomacromolecules 2005; 6:2732-2739.
DOI: 10.1021/bm050222v

28. H. Yuan, Y. Nishiyama, M. Wada, S. Kuga. Surface acylation of cellulose whiskers by drying aqueous emulsion. Biomacromolecules 2006; 7:696-700.
DOI: 10.1021/bm050828j

29. G. Siqueira, J. Bras, A. Dufresne. New process of chemical grafting of cellulose nanoparticles with a long chain isocyanate. Langmuir 2010; 26:402-411.
DOI: 10.1021/la9028595

30. N. Ljungberg, C. Bonini, F. Bortolussi, C. Boisson, L. Heux, J.Y. Cavaillé. New nanocomposites materials reinforced with cellulose whiskers in atactic polypropylene: Effect of surface and dispersion characteristics. Biomacromolecules 2005; 6:2732-2739.
DOI: 10.1021/bm050222v

31. L. Petersson, I. Kvien, K. Oksman. Structure and thermal properties of poly(lactic acid)/cellulose whiskers nanocomposite materials. Composites Science and Technology 2007; 67:2535-2544.
DOI: 10.1016/j.compscitech.2006.12.012

32. D. Bondeson, K. Oksman. Polylactic acid/cellulose whiskers nanocomposites modified by polyvinyl alcohol. Composites: Part A 2007; 38:2486-2492.
DOI: 10.1016/j.compositesa.2007.08.001

33. K. Oksman, A.P. Mathew, D. Bondeson, I. Kvien. Manufacturing process of cellulose whiskers/polylactic acid nanocomposites. Composites Science and Technology 2006; 66:2776-2784.
DOI: 10.1016/j.compscitech.2006.03.002

34. A.N. Frone, S. Berlioz, J-F. Chailan, D.M. Panaitescu, D. Donescu. Cellulose fiber-reinforced polylactic acid. Polymer Composites 2011; 32:976-985.
DOI: 10.1002/pc.21116

35. D. Bondeson, K. Oksman. Dispersion and characteristics of surfactant modified cellulose whiskers nanocomposites. Composite Interfaces 2007; 14:617-630.
DOI: 10.1163/156855407782106519

36. D.E. Henton, P. Gruber, J. Lunt, J. Randall. Polylactic acid technology. In: A.K. Mohanty, M. Misra, L.T. Drzal. Natural Fibres, Biopolymers, and Biocomposites. Taylor and Francis Group: Boca Raton (2005) p.24-26.

37. X.F. Sun, R.C. Sun, Y. Su, J.X. Sun. Comparative study of crude and purified cellulose from wheat straw. Journal of Agricultural and Food Chemistry 2004; 52:839-847.
DOI: 10.1021/jf0349230

38. H. Yang, R. Yang, H. Chen, D.H. Lee, C. Zheng. Characteristics of hemicellulose, cellulose and lignin pyrolysis. Fuel 2007; 86:1781-1788.
DOI: 10.1016/j.fuel.2006.12.013

39. J.I. Morán, V.A. Alvarez, V.P. Cyras, A. Vázquez. Extraction of cellulose and preparation of nano-cellulose from sisal fibers. Cellulose 2008; 15:149-159.
DOI: 10.1007/s10570-007-9145-9

40. V. Krikorian, D.J. Pochan. Crystallization behaviour of poly(L-lactic acid) nanocomposites: Nucleation and growth probed by infrared spectroscopy. Macromolecules 2005; 38:6520-6527.
DOI: 10.1021/ma050739z

41. S.K. Majhi, S.K. Nayak, S. Mohanty, L. Unnikrishnan. Mechanical and fracture behaviour of banana fibre reinforced polylactic acid biocomposites. International Journal of Plastics Technology 2010; 14:57-75.
DOI: 10.1007/s12588-010-0010-6

42. H. Yang, R. Yan, H. Chen, D.H. Lee, C. Zheng. Characteristics of hemicellulose, cellulose and lignin pyrolysis. Fuel 2007; 86:1781-1788.
DOI: 10.1016/j.fuel.2006.12.013

43. N.Chand, S. Sood, D.K. Singh, P.K. Rohatgi. Structural and thermal studies on sisal fibre. Journal of Thermal Analysis 1987; 32:595-599.
DOI: 10.1007/BF01912712

44. M. Roman, W.T. Winker. Effect of sulfate groups from sulfuric acid hydrolysis on the thermal degradation behavior of bacterial cellulose. Biomacromolecules 2004; 5:1671-1677.
DOI: 10.1021/bm034519

45. L.M. Lim, R. Auras, M. Rubino. Processing technologies for poly(lactic acid). Progress in Polymer Science 2008; 33:820-852.
DOI: 10.1016/j.progpolymsci.2008.05.004

Chapter 6

Thermal and dynamic mechanical properties of biobased poly(furfuryl alcohol)/sisal whiskers nanocomposites

Abstract

In the present study, bio-based nanocomposites of sisal whiskers reinforced poly(furfuryl alcohol) (PFA) were prepared by using an *in situ* polymerization method. Furfuryl alcohol (FA), which is a derived renewable monomer, was used to serve first as a solvent to disperse the whiskers and later as a monomeric precursor to produce PFA. Sisal whiskers were prepared *via* acid hydrolysis, which was followed by freeze-drying and redispersion of the dried whiskers in FA by sonication for 20 min. The polymerization process was catalyzed using citric acid, which is also a renewable carboxylic acid found in citrus fruits. The effect of increased sisal whiskers loading on the thermal and dynamic mechanical properties of the nanocomposites was investigated using thermogravimetric and dynamic mechanical analyses. The TGA results showed slightly higher thermal stability for the nanocomposite samples compared to neat PFA. The DMA results showed that the incorporation of sisal whiskers imparts significant enhancement in the storage modulus of the PFA matrix. Moreover, the intensity of the tan δ peak at 75 °C for the nanocomposites was remarkably reduced compared to that of neat PFA.

Keywords: poly(furfuryl alcohol); sisal whiskers; *in situ* polymerization; biopolymer; nanocomposites; TGA; DMA

6.1 Introduction

The dwindling of fossil resources, the growing concerns about the environment, and the ever-increasing prices of petroleum-based materials are some of the driving forces toward exploitation of renewable and eco-friendly materials. In recent years, bio-based polymer nanocomposites have attracted increasing attention as potential candidates to replace their existing petroleum based counterparts. Possible applications of polymers from renewable

resources and the perspectives for the future research have recently been reviewed in the featured article in Macromolecules by Alessandro Gandini [1].

Owing to the advancement in technology, modifications of the naturally existing polymers and syntheses of novel new polymers from renewable monomers have been increasingly expanding. Poly(furfuryl alcohol) (PFA) is a crosslinked thermosetting polymer, which is produced *via* acid catalyzed polymerization of furfuryl alcohol (FA). Furfuryl alcohol is directly obtainable from the reduction of furfural, which is a renewable chemical produced from agricultural and forestry wastes [1,2]. PFA has found successful applications and usage in different fields include metal-casting cores and moulds, corrosion resistant coatings, polymer concrete, wood adhesives and binders, sand consolidation and well plugging, materials processing low flammability and low smoke release, modifier for natural fibre surfaces, and precursor for glassy carbons and carbon nanocomposites [2-4].

Cellulose whiskers (CW) are bio-based nanofillers, which are produced from various agricultural, wood, and animal resources through an acid hydrolysis method [5-7]. They have a lot of potential as reinforcing materials in polymer matrices due to their high surface area coupled with their good mechanical properties as well as their availability, renewability, recyclability, and biodegradability [5-9].

Very few works [9,10] have been published so far on composites comprising poly(furfuryl alcohol) and bio-based nanofillers. Generally, the incorporation of these nanofillers was found to enhance the thermal stability of the PFA. However, to our best knowledge, the possible influence of cellulose whiskers on the viscoelastic properties of a PFA matrix has not been reported yet. In the present study, completely bio-based nanocomposites of sisal whiskers reinforced PFA were prepared *via* an *in situ* polymerization method. Furfuryl alcohol, which is a derived renewable monomer, was used to serve first as a solvent to disperse the whiskers and later as a monomeric precursor for the polymerization of PFA. Citric acid, which is naturally found in citrus fruits, was used to catalyze the polymerization process. The effect of increased sisal whiskers content on the thermal and dynamic mechanical properties of a PFA matrix was investigated.

6.2 Experimental

6.2.1 Materials

Sisal fibres were obtained from the National Sisal Marketing Committee in Pietermaritzburg, South Africa. Sulphuric acid (assay 95-99 %) was supplied by Merck Chemicals (Pty) Ltd. Sodium hydroxide pellets (assay 97 %) was supplied by Associated Chemical Enterprises (Pty) Ltd. Sodium hypochlorite was obtained from the local markets (JIK-household bleach, which contains sodium hypochlorite as an active ingredient with a concentration of 3.5 % (w/v), Reckitte Benckiser (Pty) Ltd., South Africa). Furfuryl alcohol (minimum assay 98 %) was purchased from Illovo sugar Ltd., South Africa. Citric acid monohydrate (assay 99.5 %) was supplied by Saarchem (Pty) Ltd., South Africa.

6.2.2 Preparation of sisal whiskers (nanofibres)

Sisal fibres were cut with a Tecator sample grinder (Cyclotec-1093 sample mill, made in Sweden) until fine particulate fibres were obtained. The fibres were then treated with a 4 wt% sodium hydroxide solution at 80 ºC in a water bath for 2 h under mechanical stirring. This treatment was done three times to remove other constituents than cellulose from the fibres. After each treatment, the fibres were filtered and washed with distilled water until all the akali was removed. A subsequent bleaching treatment was carried out to bleach the fibres. The solution used in this treatment consisted of equal parts of an acetate buffer (27 g of NaOH and 75 mL glacial acetic acid, diluted to 1 L using distilled water) and aqueous chlorite (1.7 wt % $NaClO_2$ in water). The bleaching treatment was performed at 80 ºC for 4 h under mechanical stirring and was repeated four times. After each treatment, the fibres were filtered and washed with distilled water. The fibres were subsequently dried in an oven at 60 ºC for 24 h. The dried fibres were ground to a fine powder using a Philips grinder (HR2021-400 W). Acid hydrolysis of the fine fibre powder was performed at 50 ºC in a water bath, for about 50 min by using a 65 wt% sulphuric acid, under mechanical stirring. The fibre content during all these chemical treatments was in the range 5-6 wt%. The suspension was diluted with ice cubes to stop the reaction. Successive washings in a centrifuge (HARRIER 18/80 Refrigerated Centrifuge, Model MSB080.CR1.K, made in the UK) at 10 ºC and 5000 rpm for 30 min were then performed. Dialysis (SnakeSkin® Pleated Dialysis Tubing-3,500 MWCO)

against distilled water was done to remove the free acid in the dispersion. This was verified by determining the neutrality of the dialysis effluent. Complete dispersion of nano-whiskers was obtained by a sonication step using a Cole-Parmer Ultrasonic Processor (Model CP 505, 500 Watts). The dispersion was then filtered through a No. 1 fritted glass filter to remove residual aggregates, and then freeze-dried using a Freeze Dryer (Flex-Dry^{TM} µP-Microprocessor Control, FTS Systems, Inc., USA).

6.2.3 Preparation of poly(furfuryl alcohol)/sisal whiskers nanocomposites

PFA nanocomposites were prepared by adding the freeze-dried nanowhiskers (1 and 2 wt %) to FA (40 g sample), as they are both hydrophilic, followed by a sonication step for 20 min. 5 phr citric acid monohydrate was then added to the mixture to catalyze the polymerization process of FA. The mixture was heated at 85 °C under strong stirring for 8 hours and then the resultant thick dark-brown material was transferred to the mould and subsequently heated in an oven, first at 70 °C for 2.30 hours, and then the temperature was raised to 100 °C and the heating was continued for an additional 3 hours. The final curing step was done by raising the temperature of the oven to 150 °C and the end of the curing was confirmed by using differential scanning calorimetry (no residual exothermic process was observed in the DSC curve). For comparison, pure PFA samples were prepared under the same conditions.

6.2.4 Characterization methods

The sisal whiskers suspension was examined using a transmission electron microscope, Philips (FEI) CM100 (The Netherlands), to confirm the separation of the nanofibres and to determine their dimensions. A drop of the diluted suspension was allowed to dry on a carbon coated grid at ambient conditions and then the sample was stained using a uranyl acetate solution (2 wt%). The stained sample was observed using an accelerating voltage of 60 kV.
The nanocomposites were examined by cutting very thin sections from the samples using ultramicrotomy and viewed under TEM.

ATR-FTIR spectra of FA, pure PFA, and its nanocomposite sample were obtained using a Perkin Elmer Spectrum 100 FTIR spectrometer. The samples were analyzed over a range of 550-4000 cm^{-1} with a resolution of 4 cm^{-1}. All the spectra were averaged over 8 scans.

Thermogravimetric analysis was used to study the thermal stabilities of the sisal whiskers, neat PFA, and its nanocomposite samples in a Perkin Elmer TGA7 thermogravimetric analyzer. Samples with weights in the range of 5 to 10 mg were heated under a flowing nitrogen atmosphere (20 mL min^{-1}) from 30 to 800 ºC at a heating rate of 10 ºC min^{-1}, and the corresponding mass loss was recorded.

The dynamic mechanical properties (storage and loss modulus, as well as dissipation factor) of the samples were determined in a Perkin Elmer Diamond DMA dynamic mechanical analyzer. The measurements were carried out in the dual cantilever-bending mode and the corresponding viscoelastic properties were determined as a function of temperature. The samples were heated under nitrogen flow (30 mL min^{-1}) from 25 ºC to 190 ºC at a heating rate of 3 ºC min^{-1}, and at a frequency of 1 Hz.

6.3 Results and discussion

TEM was used to study the morphology of the obtained sisal whiskers and to determine their dimensions (length and diameter). Figure 6.1 shows the TEM micrographs of the sisal whiskers at different magnifications. It can be concluded that the process of acid hydrolysis coupled with sonication and filtration have successfully led to breakdown of the microfibres to produce the rod-like particles (whiskers). At higher magnification (Figure 6.1b), it is possible to see the individual whiskers. The whiskers possessed an average length of approximately 195 nm and a diameter of approximately 15 nm.

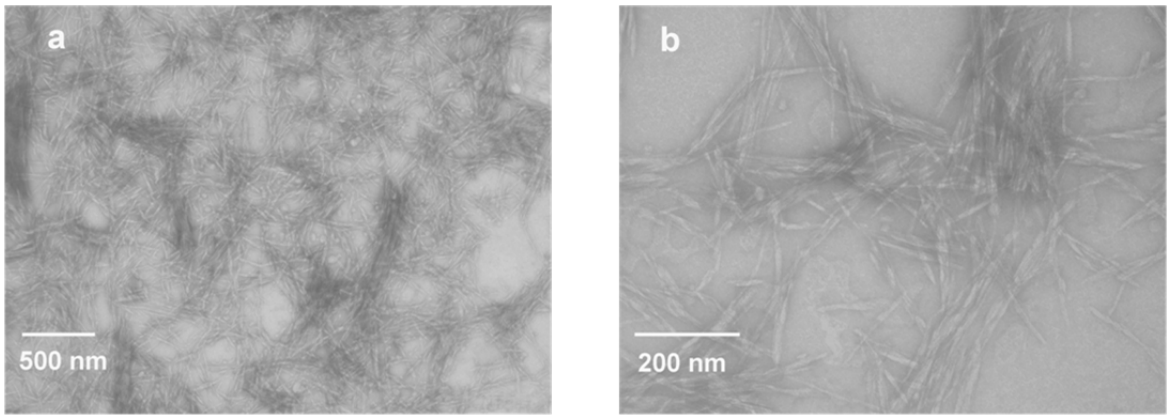

Figure 6.1 TEM images of sisal whiskers

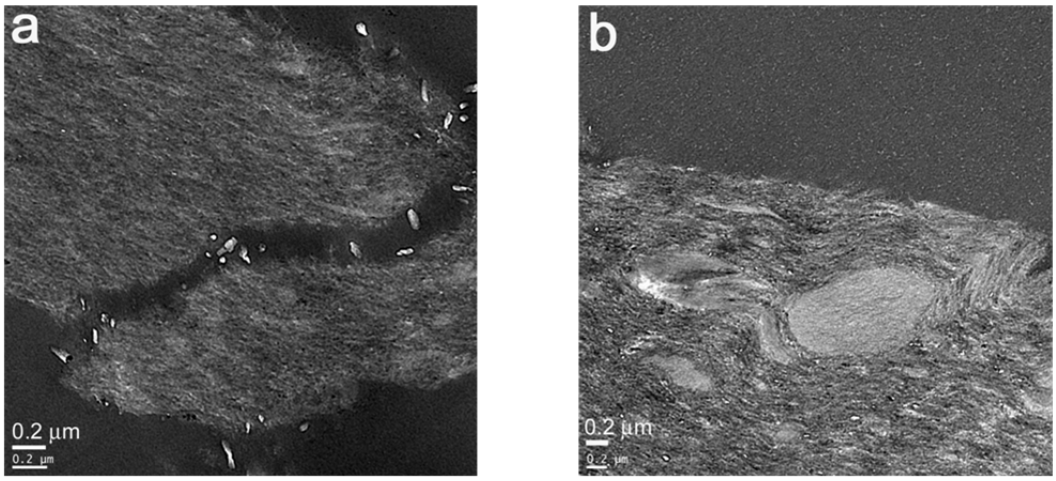

Figure 6.2 TEM images of (a) 99/1 w/w PFA/sisal whiskers (b) 98/2 w/w PFA/sisal whiskers

Figure 6.2 shows the TEM images of the nanocomposite samples. It is clear that the nanowhiskers were significantly agglomerated and no individual whiskers could be seen.

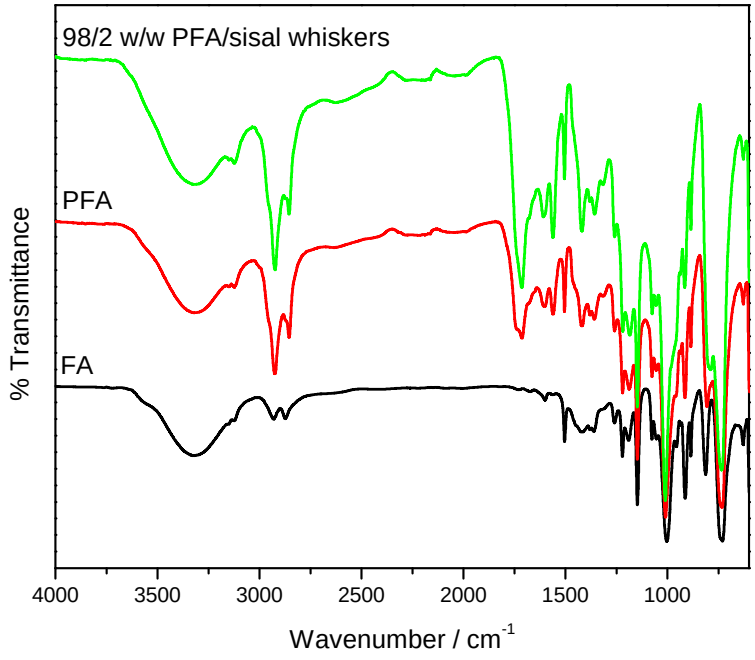

Figure 6.3 ATR-FTIR spectra of the FA, neat PFA, and PFA reinforced sisal whiskers nanocomposite (98/2 w/w PFA/sisal whiskers)

The polymerization of FA to produce PFA was confirmed by using FTIR analysis. In addition, FTIR analyses of PFA and its nanocomposite sample (98/2 w/w PFA/sisal whiskers) were also carried out to examine the possible interactions between PFA and sisal whiskers. The FTIR spectra of the three materials are shown in Figure 6.3. The presence of the furan rings in all three spectra is proved by the absorption peaks at 3125, 1600, 1505, 1148, 1075, 1016, 885, 780, 730, and 600 cm^{-1} [11-13]. The aliphatic functional groups give rise to the bands at 2930, 1420, and 1377 cm^{-1}. The broad band at 3322 cm^{-1} is assigned to the stretching vibration of both –OH end groups in PFA and to –OH groups in the monomeric FA. In the spectrum of PFA and PFA-whiskers nanocomposite one can also notice two bands positioned at 1713 and 1560 cm^{-1} that are not present in the spectrum of the monomer. These bands, respectively assigned to the carbonyl group stretching vibration of γ-diketones formed from hydrolytic ring opening of the furan rings and the skeletal vibration of 2,5-disubstituted furan rings, also indicate the resinification of FA [9,11,13]. No significant changes between the absorption bands in the spectra of neat PFA and its nanocomposite sample could be noticed. This indicates that the curing process was successfully completed in the presence of sisal nanowhiskers, and that there was no chemical interaction between the matrix and the filler.

Thermal degradation of neat PFA and its nanocomposite samples was studied using TGA. Figure 6.4 shows the mass loss of these samples as a function of temperature. In general, the incorporation of sisal whiskers slightly improves the thermal stability of the PFA in the temperature range studied here. It can also be noticed from Figure 6.3 that the TGA curves show several degradation steps for all the samples. The first step starts above 200 °C and involves scission of the weaker chemical bonds [14]. The second degradation step occurs in the temperature range 320 to 400 °C, while from 400 °C, the mass gradually decreases. At the end of the measurement (800 °C), the observed mass losses for all the samples were about 50 %. Guigo *et al*. [14] identified the volatile compounds during thermal degradation of neat PFA using TGA-GC-MS. Their results showed a multi-step degradation pathway for the neat PFA. At lower temperatures, formation of alkylfurans (e.g., 2-methyl furan and 2-furfuryl-5-methylfuran) due to scission of both methylene and methyne links was observed. At higher temperatures, scission of furanic links form ketonic volatile compounds (e.g., acetone, 2-butanone, and 2-pentanone) occurs. It is also important to mention that the thermal degradation of sisal whiskers starts above 200 °C (curve not shown) and the maximum rate of

degradation appears around 350 °C. Since the TGA curves of the pure PFA and the nanocomposites are almost identical (Figure 6.4), it can be concluded that the sisal whiskers do not influence the degradation route of the matrix.

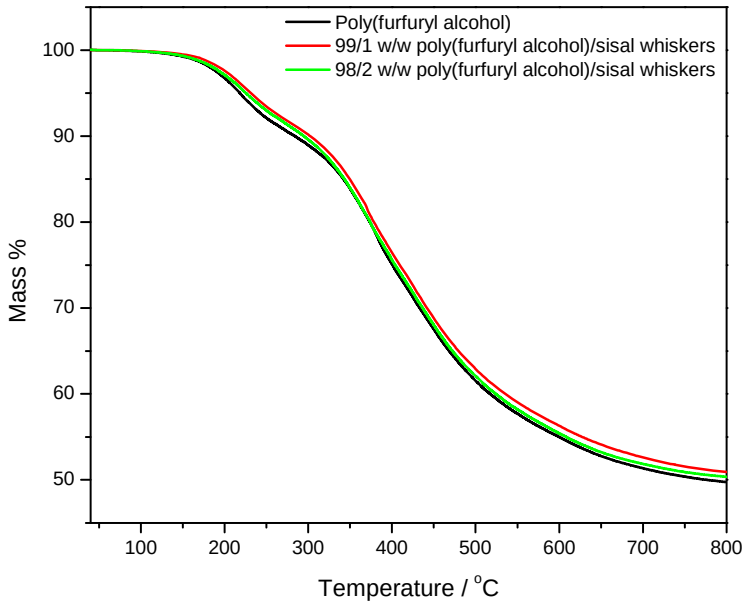

Figure 6.4 TGA curves of the neat PFA and its nanocomposites

The effect of incorporation of sisal whiskers on the viscoelastic properties of PFA was investigated in the temperature range from 25 to 180 °C. The variation of the storage modulus (*E'*) and loss tangent (tan δ) of the pure PFA and the PFA-nanocomposites are shown in Figures 6.5 and 6.6. As can be seen from Figure 6.5, although the whiskers content is relatively low, the storage modulus of the nanocomposites is significantly increased after introduction of the filler in the whole temperature range. The storage modulus of the nanocomposite sample with 2 wt % of sisal whiskers is almost three times higher than that of the neat PFA. This implies a strong reinforcement effect of the high specific surface nanofiller, which was well dispersed in the FA during the sonication step. Later, during the polymerization of FA, the whiskers tended to agglomerate due to the formation of the hydrophobic PFA matrix. However, it is possible that some of the well dispersed whiskers were trapped by the PFA matrix during the polymerization process and hence maintained their good dispersion in the PFA matrix. This should lead to good reinforcement and better stress transfer between the PFA and the whiskers. Figure 6.5 shows a slight increase in the

storage modulus (hardening) of the neat PFA and the nanocomposites at temperatures above 130 °C, and above 140 °C, respectively. The former effect could be attributed to desorption of the bound water formed during the polycondensation of FA [15] or to release of the water incorporated in the citric acid crystal structure. The observed temperature difference at which hardening takes place might be a consequence of retardation in water desorption in the presence of whiskers.

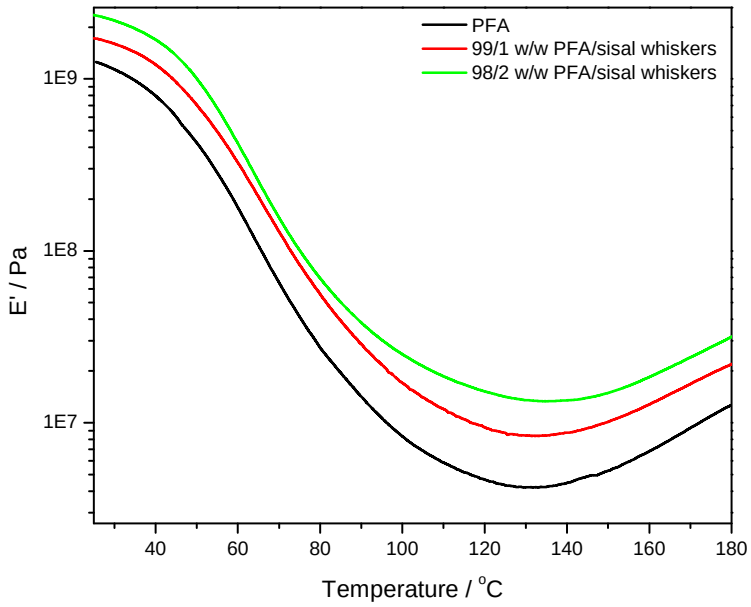

Figure 6.5 DMA storage modulus curves for pure PFA and its nanocomposites

The variation of tan δ of the PFA and its nanocomposites as a function of temperature is presented in Figure 6.6. Both nanocomposite samples show lower values of tan δ in the temperature interval studied here. The sisal whiskers obviously improve the elasticity of the matrix and reduce the energy losses. On the other hand, the position of the tan δ relaxation peak (glass transition temperature of PFA) was slightly shifted towards lower temperature after introduction of the filler (Figure 6.6). The observed shift is probably the result of an increase of the average matrix free volume in the presence of whiskers. In this sense, the whiskers induce different effects on the PFA matrix: they increase storage modulus due to higher stiffness with respect to the matrix, but at the same time they increase the mobility of the chains (observed via reduced glass transition temperature). Still, taking into account their strong influence on the overall elasticity, they can be considered good reinforcement for the PFA.

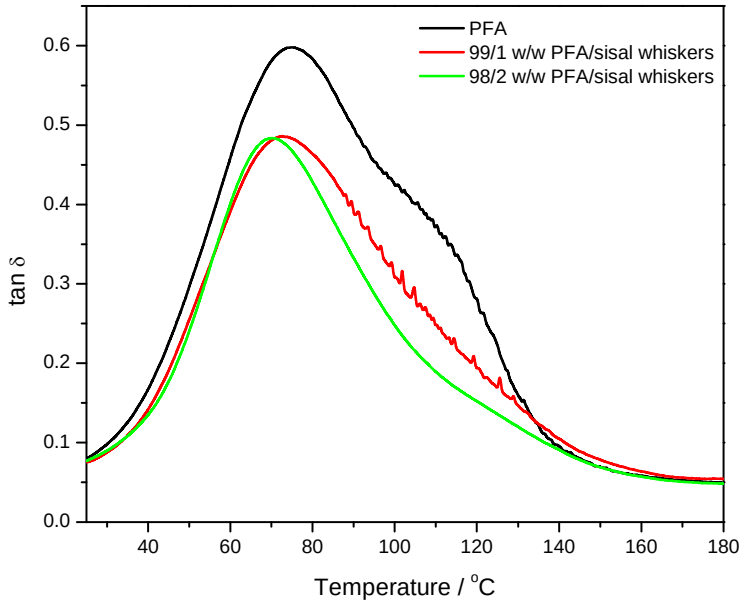

Figure 6.6 DMA tan δ curves for pure PFA and its nanocomposites

6.4 Conclusions

Biobased nanocomposites of poly(furfuryl alcohol) and sisal whiskers were prepared by an *in situ* polymerization method and their thermal and dynamic mechanical properties were investigated. The resinification of FA was followed by using FTIR spectroscopy. No chemical interaction between PFA and sisal whiskers could be noticed from the IR spectrum of the nanocomposite. TGA analysis showed multistep degradation behaviour for all the samples and the thermal stabilities of the nanocomposite samples were very slightly higher than that of the neat PFA. The effect of the sisal whiskers on the viscoelastic properties of PFA was examined by using DMA. In comparison to neat PFA, all the nanocomposite samples showed significantly higher storage moduli and lower intensities of the glass transition peaks in the tan δ curves. At the same time the glass transition temperature was slightly reduced after introduction of the filler.

6.5 References

1. A. Gandini. Polymers from renewable resources: A challenge for the future of macromolecular materials. Macromolecules 2008; 41:9491-9504.
   DOI: 10.1021/ma801735u
2. A. Gandini, M.N. Belgacem. Furans in polymer chemistry. Progress in Polymer Science 1997; 22:1203-1379.
   DOI: 10.1016/S0079-6700(97)00004-X
3. H. Wang, J. Yao. Use of poly(furfuryl alcohol) in fabrication of nanostructured carbons and nanocomposites. Industrial and Engineering Chemistry Research 2006; 45:6393-6404.
   DOI: 10.1021/ie0602660
4. W.G. Trindade, W. Hoareau, I.A.T. Razera, R. Ruggiera, E. Frollini, A. Castellan. Phenolic thermoset matrix reinforced with sugar cane bagasse fibres: Attempt to develop a new fibre surface modification involving formation of quinines followed by reaction with furfuryl alcohol. Macromolecular Materials and Engineering 2004; 289:728-736. DOI: 10.1002/mame.200300320
5. M.A.S. Aziz Samir, F. Alloin, A. Dufresne. Review of recent research into cellulosic whiskers, their properties, and their application in nanocomposites field. Biomacromolecules 2005; 6:612-626.
   DOI: 10.1021/bm0493685
6. Y. Habibi, L.A. Lucia, O.J. Rojas. Cellulose nanocrystals: Chemistry, self-assembly, and application. Chemical Reviews 2010; 110:3479-3500.
   DOI: 10.1021/cr900339w
7. M.M. de Souza Lima, R. Borsali. Rodlike cellulose microcrystals: Structure, properties, and applications. Macromolecular Rapid Communications 2004; 25:771-787.
   DOI: 10.1002/marc.200300268
8. J.P. de Mesquita, C.L. Donnici, F.V. Pereira. Biobased nanocomposites from layer-by-layer assembly of cellulose nanowhiskers with chitosan. Biomacromolecules 2010; 11:473-480.
   DOI: 10.1021/bm9011985

9. L. Pranger, R. Tannenbaum. Biobased nanocomposites prepared by in situ polymerization of furfuryl alcohol with cellulose whiskers or montmorillonite clay. Macromolecules 2008; 41:8682-8687.
DOI: 10.1021/ma8020213

10. L. Pranger, G.A. Nunnery, R. Tannenbaum. Mechanism of the nanoparticle-catalyzed polymerization of furfuryl alcohol and the thermal and mechanical properties of the resulting nanocomposites. Composites: Part B (In press).
DOI: 10.1016/j.compositesb.2011.08.010

11. R. González, J.M. Figueroa, H. González. Furfuryl alcohol polymerization by iodine in methylene chloride. European Polymer Journal 2002; 38:287-297.
DOI: 10.1016/S0014-3057(01)00090-8

12. A. Gok, L. Oksuz. Atmospheric pressure plasma deposition of polyfuran. Journal of Macromolecular Science, Part A: Pure and Applied Chemistry 2007; 44:1095-1099.
DOI: 10.1080/10601320701524021

13. Z. Wang, Z. Lu, X. Huang, R. Xue, L. Chen. Chemical and crystalline structure characterizations of polyfurfuryl alcohol pyrolyzed at 600 °C. Carbon 1998; 36:51-59.
DOI: 10.1016/S0008-6223(97)00150-4

14. N. Guigo, A. Mija, R. Zavaglia, L. Vincent, N. Sbirrazzuoli. New insights on the thermal degradation pathways of neat poly(furfuryl alcohol) and poly(furfuryl alcohol)/SiO_2 hybrid materials. Polymer Degradation and Stability 2009; 94:908-913.
DOI: 10.1016/j.polymdegradstab.2009.03.008

15. N. Guigo, A. Mija, L. Vincent, N. Sbirrazzuoli. Eco-friendly composite resins based on renewable biomass resources: Polyfurfuryl alcohol/lignin thermosets. European Polymer Journal 2010; 46:1016-1023.
DOI: 10.1016/j.eurpolymj.2010.02.010

Chapter 7

Conclusions

The first objective of this thesis was to find convincing evidence for peroxide initiated grafting between the cellulose (sisal) fibres and polyethylene matrices, as well as to investigate the influence of the polyethylene molecular characteristics on the grafting efficiency. Three types of polyethylene, low-density (LDPE), linear low-density (LLDPE), and high-density (HDPE) polyethylenes were chosen as polymer matrices. To address this objective, treated PE/sisal fibre composites with different fibre loadings were prepared by adding DCP to the mixture during compounding. For comparison, untreated composites and neat matrices were also prepared under the same conditions. The morphologies as well as the thermal, mechanical, and dynamic mechanical properties of these samples were investigated. The findings of the gel content, the SEM micrographs of the cryofractured surfaces of both the as-prepared and xylene-extracted samples, DSC, and the tensile testing and dynamic mechanical analysis results of the treated composites strongly suggested the presence of grafting between the polyethylene matrices and sisal fibre. However, the grafting efficiency was found to vary significantly with respect to the polyethylene molecular characteristics. Polyethylenes with higher number average molecular weight, higher vinyl group content, relatively lower molecular weight distribution, and higher branching content were found to have the highest grafting efficiency. In the present study the LLDPE was found to have the highest grafting efficiency followed by LDPE and then HDPE, for which no grafting was detected.

The second objective was to investigate whether the grafting efficiency significantly influenced the thermal and mechanical properties of each of the investigated polymers. It was found that the crystallization behaviour of the treated LLDPE composites was observably influenced. The melting temperatures and the calculated percent crystallinity of these composites decreased in the presence of sisal fibre and with increasing fibre loading. The measured melting enthalpies were also lower than the calculated ones. The tensile strength and Young's modulus of the treated LLDPE samples, on the other hand, were significantly improved. The tensile results correlated well with the dynamic mechanical measurements,

which showed increased stiffness of the treated composites. Their glass transition temperatures also increased. The grafting efficiency did not significantly affect the thermal stabilities of all the polyethylene composites. For the treated LDPE composites, the results showed that the crystallization behaviour was only slightly affected. Both the tensile and viscoelastic properties of these composites were considerably enhanced, similar to the treated LLDPE samples. The glass transition temperature also increased. The treated HDPE composites, however, did not show significant changes in the crystallization behaviour, and their stiffness was noticeably decreased. There were only marginal differences between the tensile strength of the treated and the untreated composites. It is therefore clear that the grafting efficiency of the polyethylene matrices was reflected in their crystallization behaviour and in their tensile and dynamic mechanical properties.

The third objective was to investigate the influence of the incorporation of sisal whiskers on the properties of two biopolymers, poly(lactic acid) and poly(furfuryl alcohol), as well as to study the effect of addition of MA/DCP and DCP on the properties of the resultant PLA nanocomposites. Untreated and the treated PLA nanocomposites were prepared by melt mixing and hot melt pressing. Two approaches were tried to achieve better dispersion of the whiskers in the PLA matrix. First, the aqueous suspensions of the sisal whiskers were freeze-dried to reduce the hydrogen bonding between the whiskers and then the powdered PLA and the dried whiskers were thoroughly mechanically mixed before the melt mixing step. Second, the nanocomposites were treated with MA/DCP and with DCP to enhance the interfacial bonding between the whiskers and the PLA matrix in order to further improve the dispersion of the whiskers. The morphology as well as the thermal and the dynamic mechanical properties of the nanocomposites were characterized. It was found that the dispersion of the whiskers in the PLA matrix was similar, whether the samples were treated or not. The crystallization and the melting behaviour of the PLA matrix was affected to some extent by the presence and the content of the whiskers as well as by the type of treatment used. The presence of sisal whiskers and the type of treatment did not significantly change the thermal stability of the nanocomposites. All the nanocomposites had higher storage modulus values than PLA and the incorporation of sisal whiskers reduced the intensity of the tan δ relaxation. Finally, it could be concluded that the approaches used to prepare the samples and the different treatments did not significantly enhance the properties of the resulting PLA nanocomposites, which could be attributed to the formation of agglomerates, to the lack of

good interfacial adhesion between the whiskers and the PLA matrix, and to a certain extent to the small amounts of whiskers mixed into the PLA.

Poly(furfuryl alcohol) nanocomposites were prepared by *in situ* polymerization of the FA monomer in the presence of the freeze-dried sisal whiskers and citric acid as a catalyst. The effect of increased sisal whiskers content on the thermal and the dynamic mechanical properties of the PFA was investigated. The presence of the sisal whiskers was found to increase the stiffness of the PFA matrix quite significantly and to remarkably reduce the intensity of the glass transition peaks in the tan δ curves. Compared to the neat PFA, the thermal stabilities of the nanocomposites were slightly improved, although there was a decrease in thermal stability at higher sisal whiskers loadings. It can be concluded that the presence of sisal whiskers imparted significant reinforcement to the PFA matrix. For future work, it would be interesting to characterize the tensile and the impact properties for these nanocomposites.

Acknowledgements

First of all I would like to thank **Allah** (God) who gave me strength, blessing, and courage during this study and during all of my life.

I would like to express my deepest and profound gratitude to my supervisor **Prof. Adriaan Stephanus Luyt** for his guidance, encouragement, and endless support during my Ph.D. study. I learned a lot throughout your supervision. I really feel that words will not express my appreciation to whatever you have done for me.

Many thanks to **Prof. Luyt's family** for their generosity and hospitality. It was a wonderful holiday (Drakensberg – Cayley lodge, December 2010) to be with you. Thank you for treating me as a family member.

I would also like to thank:

- ♥ All my former and present colleagues in Prof. AS Luyt's research group (Mr. Mfiso Mngomezulu, Mr. Thabang Mokhothu, Mr. Sibusiso Ndlovu, Mr. Mokgaotsa Mochane, Mr. Teboho Mokhena, Dr Stephen Ochigbo, Miss Motshabi Sibeko, Dr Spirit Molefi, Mr. Teboho Motsoeneng, Dr. Nagi Greesh, Mr. Tankiso Mokoena, Miss Cheryl-Ann Clarke, Dr. He Wei, Mr. Bongane Msibi, Mr. Lucky Dlamini, Mr. Tladi Mofokeng, Mrs. Moipone Mokoena, Mr. Tshwafo Motaung, Mrs. Doreen Mosiangaoko, Mr. S. Jeremia Sefadi).
- ♥ Julia Puseletso Mofokeng for her help, support, and kindness (Juliano thank you).
- ♥ Dr. Vladimir Djokovic, Dr. Daniel Bem, Mrs. Marlize Jackson, and Miss Makhosazana Mthembu for their kindness and support.
- ♥ The University of the Free State, the National Research Foundation, and Sudan University of Science and Technology for their financial support.
- ♥ All my brothers and friends especially, Mr. Zein Alabdeen Ahmad Alsheikh and Dr. Malik Abdellah for their good friendship and brotherhood.
- ♥ All my colleagues, friends, and former lecturers at Department of Chemistry, Faculty of Science, SUST, Sudan.

Appendix

Below are the results that were initially included in the papers, but which the reviewers requested to be removed.

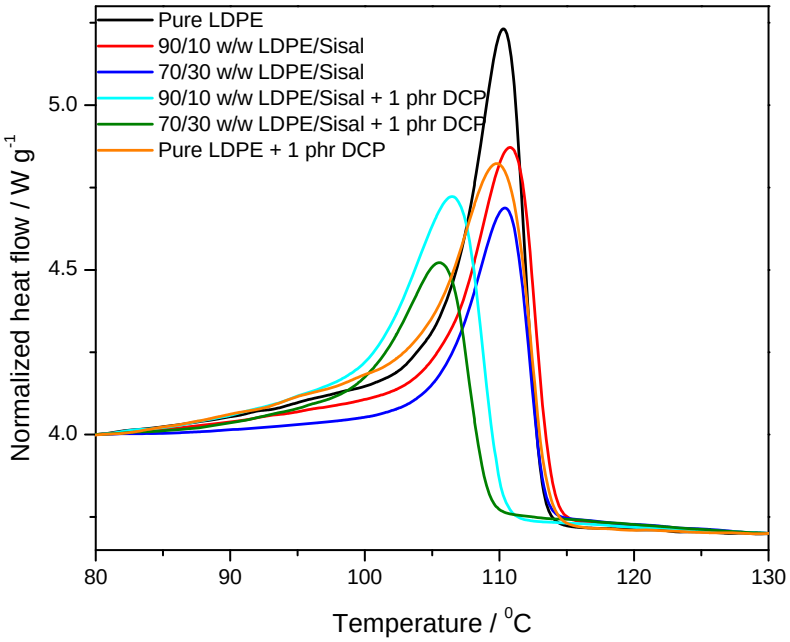

Figure A.1 DSC heating curves of LDPE, DCP treated LDPE, as well as untreated and DCP treated composites

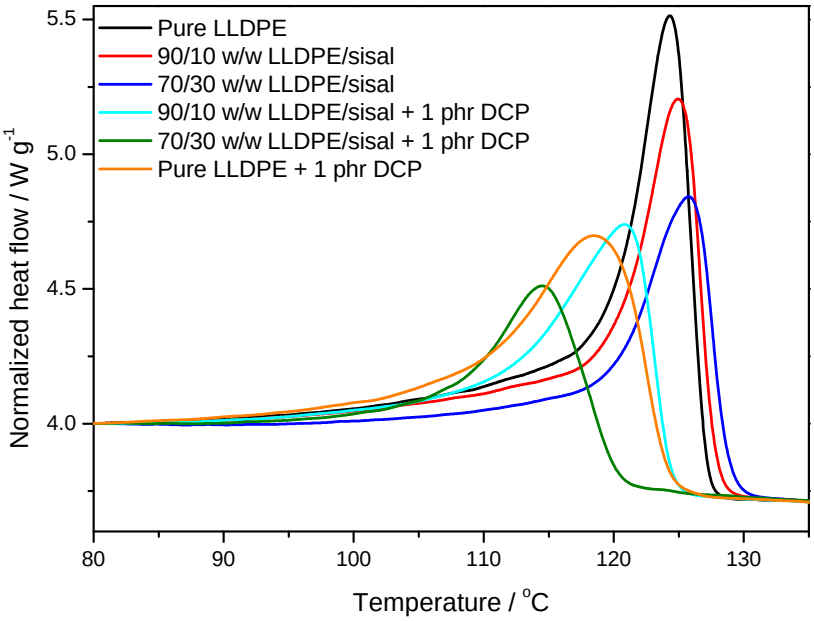

Figure A.2 DSC heating curves of LLDPE, DCP treated LLDPE, as well as untreated and DCP treated composites

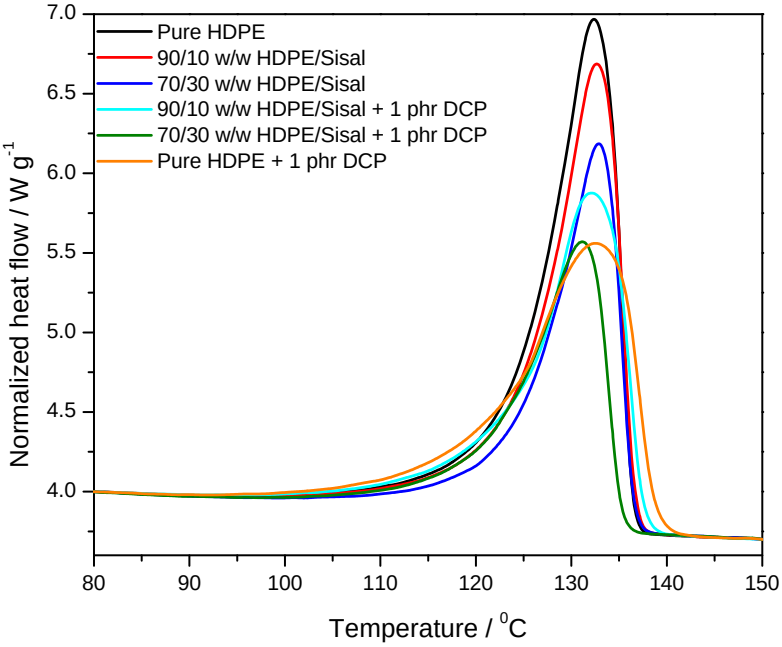

Figure A.3 DSC heating curves of HDPE, DCP treated HDPE, as well as untreated and DCP treated composites

Table A.1 Tensile properties of neat LDPE, as well as its untreated and treated composites

LDPE/sisal (w/w)	Elongation at break / %	Tensile strength / MPa	E-modulus / MPa
Untreated composites			
100/0	510 ± 34	10.0 ± 0.9	82.0 ± 6.0
90/10	45.0 ± 8.9	7.6 ± 0.4	102 ± 7
80/20	21.0 ± 4.0	6.0 ± 0.3	111 ± 7
70/30	11.9 ± 1.9	6.5 ± 0.7	147 ± 15
Treated composites			
90/10	54.0 ± 8.0	8.0 ± 0.5	108 ± 8
80/20	20.8 ± 3.7	9.0 ± 1.0	129 ± 10
70/30	13.0 ± 2.0	12.0 ± 1.0	189 ± 18

Table A.2 Tensile properties of neat LLDPE, as well as its untreated and treated composites

LLDPE/sisal (w/w)	Elongation at break / %	Tensile strength / MPa	E-modulus / MPa
Untreated composites			
100/0	880 ± 133	20.0 ± 4.0	114 ± 7
90/10	61.0 ± 4.8	7.0 ± 0.6	114 ± 10
80/20	35.8 ± 9.8	7.0 ± 0.5	153 ± 12
70/30	19.7 ± 3.0	7.0 ± 0.4	171 ± 13
Treated composites			
90/10	99.0 ± 27.7	10.0 ± 0.8	110 ± 5
80/20	25.9 ± 7.8	10.5 ± 0.4	167 ± 11
70/30	15.0 ± 3.0	12.6 ± 2.0	213 ± 18

Table A.3 Tensile properties of neat HDPE, as well as its untreated and treated composites

HDPE/sisal (w/w)	Elongation at break / %	Tensile strength / MPa	E-modulus / MPa
Untreated composites			
100/0	471 ± 190	16.0 ± 1.9	304 ± 19
90/10	13.0 ± 1.7	20.9 ± 1.5	353 ± 19
80/20	9.6 ± 1.0	17.0 ± 0.8	346 ± 13
70/30	7.9 ± 1.6	15.0 ± 1.9	313 ± 30
Treated composites			
90/10	24.6 ± 7.0	20.5 ± 1.0	291 ± 31
80/20	13.0 ± 5.0	18.0 ± 3.0	312 ± 36
70/30	7.0 ± 1.6	12.7 ± 2.0	287 ± 21